ABSTRACT

HEAT CONDUCTIVITY MEASUREMENTS AT LOW TEMPERATURES

A thesis submitted for the
Degree of Doctor of Philosophy
in the University of Oxford

December, 1969.

Rasiah Ratnalingam
Wadham College

ABSTRACT

The transport properties of the rare earth elements exhibit many interesting features, especially around the magnetic transition temperatures. The little data available on the thermal conductivity of the heavy rare earth metals cover mostly the high temperature range (5 - 300°K)[1-3]. The results reported at the lower end of this temperature range are unexpected, the thermal conductivity largely exceeding the value derived from the electrical conductivity via the Wiedemann-Franz law. For example, the Lorenz numbers given varied from 3 to 12 x 10^{-8} watts- ohms- K^{-2} (theoretical value 2.45 x 10^{-8} watts- ohms-K^{-2}). These authors concluded that mechanisms of heat transport other than the usual dominant electronic term must also be present. Recently some anomalous results were reported for some of the heavy rare earths in the He^4 temperature range and the results did not extrapolate to the origin at 0°K[4].

These discrepancies and the hope that at sufficiently low temperatures a predominantly electronic thermal conductivity obeying Widemann-Franz law would emerge were good reasons for a detailed investigation down to a lower limit of temperature. In this thesis we present a systematic thermal conductivity study of the heavy rare earth metals

in the temperature range 0.4 to 4.2°K. covered by two different cryostats - a He^3 and a He^4 cryostat. The specimens studied were gadolinium (2 samples), dysprosium (2 samples), holmium (2 samples), erbium (2 samples), terbium (1 sample) and ytterbium (1 sample).

The results obtained by us show no anomaly and are very consistent. The thermal conductivity of all the specimens can be separated into a linear and a small quadratic term in temperature. Furthermore our results do not confirm the anomalously high Lorenz numbers previously referred to in the literature but when we relate the linear temperature dependence of the thermal conductivity to the residual electrical resistivity using Wiedemann-Franz law we obtain, for all the specimens, Lorenz numbers which are remarkably close to the theoretical value. We therefore conclude that the linear term represents an electronic contribution, with the electron mean free path limited by 'impurity' scattering.

To account for the small quadratic contribution, we have invoked other carriers - phonons and magnons. We have observed this term in specimens which have spin waves and also in those which have no spin waves below 4°K. Further measurements were done to see the effects of dislocations on this small quadratic contribution. The results of these experiments lead us to believe that the major contribution

to this quadratic term in thermal conductivity is due to phonon conduction limited by electron scattering. We may have not reached the upper limit, for there may be a little additional scattering of the phonons due to dislocations, which has the same temperature dependence.

The thesis is divided into three chapters. In chapter one a brief account of the theory of thermal conduction in metals at low temperatures is presented. We have also given some magnetic properties of the rare earth ferromagnets in this chapter.

The second chapter describes the He^3 cryostat, which we designed and built for measuring the thermal conductivity below $1^{\circ}K$. Also discussed are the techniques used.

Finally in the third chapter the results are discussed.

1. Aliev, N.G., and Volkenshtein,N.V. (1966) Soviet Phys. - Solid State, 7, 2068.

Aliev, N.G. and Volkenshtein,N.V. (1966) Soviet Phys. - JETP, 22, 17.

2. Arajs, S. and Colvin, R.V. (1964) J. App. Phys. 35, 1043.

Arajs, S. and Dunmyre (1965) Physica 31, 1466.

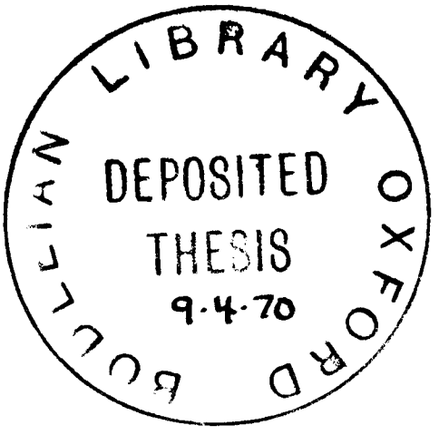
3. Nellis, W.J. and Legvold, S. (1968) Phys. Rev. 180, 581.

4. Rao, K.V. (1967) Phys. Letters, 24A, 39.

Rao, K.V. and Karagyozyan, A.G. (1967) Phys. Letters 25A, 235.

HEAT CONDUCTIVITY MEASUREMENTS AT LOW TEMPERATURES

A thesis submitted for the
Degree of Doctor of Philosophy
in the University of Oxford



December , 1969.

Rasiah Ratnalingam,
Wadham College.

CONTENTS

ABSTRACT i

CHAPTER ONE

THEORY

Introduction 1.1

Section 1A

Formal theory (the Boltzmann transport equation) 1.4

Section 1B

1. Phonons 1.8
2. Formal Theory of Phonons Conduction 1.9
3. Phonon-Phonon Interaction 1.11
4. Boundary Scattering 1.14
5. Defect Scattering 1.16

Section 1C

1. Thermal Conduction by Electrons 1.18
2. Wiedemann-Franz law 1.21
3. Impurity Resistivity 1.24
4. Resistivity due to Phonon Scattering 1.25
5. The Electronic Thermal Conductivity 1.28
6. Lattice Conduction in a Metal 1.29

Section 1D

Rare Earth Metals

Introduction 1.31

1. Rare Earth Ferromagnets 1.33

2. Magnetic Structure of the Rare Earth Ferromagnets 1.35

3. Spin Waves 1.37

4. Indirect Exchange Interaction 1.40

5. Conduction Processes in Rare Earth Ferromagnets 1.42

References to Chapter One 1.45

CHAPTER TWO

APPARATUS AND EXPERIMENTAL TECHNIQUES

Introduction 2.1

Section 2A

Cryogenic apparatus 2.3

1. The He^3 cryostat

2. Storage and Handling of $Helium^3$ 2.6

3. The $Helium^4$ Bath 2.7

Section 2B

The Experimental Arrangement

1. The Specimen Holder 2.9

2. The Heat Supplied $\dot{Q}$ and the Power Supply 2.10

3. Specimen Mounting and Contacts 2.11

4. Thermal Anchor and Leads 2.11

Section 2C

Thermometry

Introduction 2.12

1. Carbon Resistor Thermometers 2.12

2. Vapour Pressure Thermometry 2.16

3. Thermomolecular Pressure Correction 2.18

4. Purity of He^3 2.19

5. The Temperature Regulator 2.21

Section 2D

Experimental Procedure

1. Pre-cooling 2.22

2. Resistivity Measurements 2.23

Section 2E

1. Errors 2.25

2. Performance of the He^3 cryostat 2.27

References to Chapter Two 2.28

CHAPTER THREE

RESULTS AND DISCUSSION

Introduction 3.1

Section 3A Samples 3.3

Section 3B Gadolinium 3.5

Section 3C Dysprosium 3.10

Section 3D Holmium 3.15

Section 3E Erbium 3.21

Section 3F Ytterbium 3.25

Section 3G Terbium 3.29

Section 3H General analysis 3.33

Conclusion 3.48

References to Chapter Three 3.50

Appendix A

Acknowledgements

CHAPTER ONE

THE THERMAL CONDUCTIVITY OF METALS

Introduction

There are two well established mechanisms by which heat may be transported through a solid. First due to the strong coupling between the atoms in a crystal lattice; conduction can take place by means of the lattice vibrations (or phonons). This is the mechanism in dielectrics. In metals the 'free' electrons are additional heat carriers and in fairly pure metals nearly all the heat is in fact carried by the electrons and very little by the lattice vibrations. In semi-conductors, impure metals and in alloys the lattice contribution is comparable to the electronic term.

The total thermal conductivity K of a metal will be given by

$$K = K_e + K_g \qquad (1.1)$$

where K_e and K_g are the electronic and phonon conduction respectively. Both the conductivities are limited by various scattering mechanisms. The calculation of the two thermal conductivities requires the solution of the Boltzmann equation (separately) to give the velocity distribution of the electrons (or phonons) in the presence of an external field.

There are other excitations in solids than the two mentioned above. If the excitations in solids are treated as gas particles (e.g. phonon gas, free electron gas) then the kinetic formulation of thermal conduction

$$K = \frac{1}{3} Cvl \qquad (1.2)$$

can be used. C is the heat capacity per unit volume, v is the average particle velocity, l the mean free path of the particle between collisions. Though the kinetic approach has a basic flaw in the fact that in an ideal gas there is not a net flow of particles, while in transport phenomena this is not so (e.g. in a phonon gas, while the energy is conserved, the phonon number is not), it provides a useful insight into the main features of thermal conductivity observations.

In rare earth metals (the group of metals on which we have measured the total thermal conductivity and presented in a later chapter) there are further excitations than those mentioned above. Specific heat studies of most heavy rare earth metals at low temperatures show that magnons can contribute significantly to the total specific heat (the magnetic specific heat is caused by the interatomic exchange interaction between the 4f electronic spins) and it would correspondingly not be improbable that magnons could carry a significant amount of heat. There seems to be no detail theoretical investigation on the thermal conductivity of

the rare earth metals allowing for their particular electronic structure and magnetic properties.

In this chapter we shall briefly review the theory of thermal conduction in metals with special reference to low temperatures. Only those aspects of the theory will be given which have some bearing on the experimental results, which will be discussed in later chapters.

First of all, we shall give a simple account of the transport equation; and this is followed by the behaviour of phonon conductivity, with particular reference to heat transport in non-metals. The next section is devoted to the electronic contribution to the thermal conduction. Finally, a short review of the useful information (especially magnetic) of the rare earth metals is given.

Section 1A

Formal Theory (The Boltzmann Transport Equation)

In the method of Boltzmann, a distribution function $f(\underline{k},\underline{r},t)$ is assumed for an assembly of quasi-particles, to study the irreversible processes by which equilibrium is established and maintained. The distribution function, which is the density of particles at any point in phase space at any particular time, depends explicitly upon the mechanism of interaction between the particles, and the fields cannot, as in equilibrium problems, be determined once and for all. The distribution function f has the "equilibrium value" f_0, say for a rod of conductor in equilibrium at a constant temperature T and with no external field acting on it. For free electrons in a metal this is usually taken to be the Fermi-Dirac distribution function in the form

$$f_0 = 2\left(\frac{m}{h}\right)^3 \left[e^{(E-\xi)/k_0T}+1\right] \quad \ldots\ldots\ldots\ldots \quad (1.3)$$

where E is the energy of an electron with velocity v; ξ, the chemical potential of the electrons, is a function of the temperature and the density of electrons in co-ordinate space.

When external fields are applied, or there exist temperature gradients, this distribution will be disturbed and the electrons (or phonons) tend to diffuse from one point to another. With $\underline{C}$ as a six dimensional velocity

composed of $d\underline{k}/dt$ and $d\underline{r}/dt$, one can write for the rate of change of the distribution

$$\frac{df(\underline{k},\underline{r},t)}{dt} = -\nabla.(f\underline{C})$$

$$= -f\nabla\underline{C} - \underline{C}.\nabla f \ldots\ldots \quad (1.4)$$

In a uniform metal C is divergence free when the forces depend on velocities only. Since, when there are no collisions $d\underline{k}/dt = \underline{F}/h$, and $d\underline{r}/dt = \underline{v}$, equation (1.4) can be written as

$$\frac{df}{dt} + \frac{1}{\hbar}\underline{F}.\nabla_k f + \underline{v}.\nabla_r f = 0 \quad \ldots\ldots \quad (1.5)$$

If there are collisions, scattering the particles in a way not described by the force system F, the equation then becomes,

$$\frac{df}{dt} + \frac{1}{\hbar}\underline{F}.\nabla_k f + \underline{v}.\nabla_r f = \left.\frac{df}{dt}\right]_{colln.} \quad (1.6)$$

This most general form is known as the Landau-Boltzmann transport equation[1]. When there is no explicit time dependence i.e., assuming a steady state process, for the changes brought about by collision processes only, we have the well known Boltzmann Transport equation,

$$\frac{1}{\hbar}\underline{F}.\nabla_k f(\underline{k},\underline{r}) + \underline{v}.\nabla_r f(\underline{k},\underline{r}) = \left.\frac{df}{dt}\right]_{colln.} \quad (1.7)$$

The evaluation of the collision term on the right of equation (1.7) for all conditions represents a very

formidable problem. When the deviation from equilibrium is small however, it is customary to assume that, in the absence of external forces the rate of change of f due to collisions is proportional to the deviation, i.e. we have

$$\left.\frac{df}{dt}\right]_{coll^n.} = \frac{f - f_0}{\tau} \qquad \ldots\ldots \quad (1.8)$$

where τ is the relaxation time so defined that if the external field is removed any change in f from its equilibrium value will relax exponentially with the time constant τ towards the equilibrium value f_0.

If several scattering processes act together, we would expect the inverse of the relaxation rates to be additive, i.e. the transition probabilities to be additive and can be written as

$$\tau^{-1}(q) = \tau_1^{-1}(q) + \tau_2^{-1}(q) + \tau_3^{-1}(q) + \cdots \qquad (1.9)$$

In the case of electrical (and thermal) resistives this amounts to the empirical statement of Matthiessen.

In calculating the phonon and electron contributions to thermal conductivities of a metal, a separate Boltzmann equation is set up for the steady state of electron and phonon distributions. It is assumed[2-4] that in calculating the electronic thermal conductivity the distribution function of the lattice vibrations may be replaced by its value of thermal equilibrium of the

lattice, i.e. any possible non-equilibrium of the lattice in the presence of a temperature gradient may be ignored in deriving the non-equilibrium electron distribution and vice versa. This procedure is not strictly correct. Sondheimer (1957)[5] discusses a more sophisticated approach to this problem, in which the coupled Boltzmann equations for phonons and electrons in metals are solved simultaneously.

Section 1B

(1) Phonons

In the simple approach of Boltzmann to the aspect of internal energy of solid bodies, every atom in the body had a position of rest, about which it executed thermo-kinetic oscillations. However, the atoms are not bound to their equilibrium sites, but to their neighbouring atoms. These vibrations can be thought of as wave motions passing through the materials with energy being transferred from atom to atom, (coupled through inter atomic forces) and heat is conducted by the transfer of vibrational energy of the atoms. These thermal motions can be resolved into a set of travelling plane waves and for a perfect lattice with harmonic interactions these are the normal modes of vibrations.

These normal modes of vibrations in an ideal crystal may be quantised in the same way as other forms of oscillatory energy, and for a wave number q and energy $E(q)$ we can write

$$E(q) = (n+\tfrac{1}{2})\hbar\omega \qquad (1.10)$$

where ω is the frequency of vibrations. Each quanta of vibrational energy $\hbar$ is called a 'phonon'. Phonons obey Bose-Einstein statistics and there is no limit to the number of phonons in a normal mode. The energy states are equally spaced and so the average number of phonons in

a normal mode, in thermal equilibrium at temperature T, is given by

$$N(q) = \frac{1}{\left[e^{\frac{\hbar\omega}{k_0 T}} - 1\right]} \qquad (1.11)$$

(2) Formal Theory of Phonon Conduction

In non-metals heat transport is through the lattice - the phonons. When discussing heat conductivity, each normal mode is regarded as consisting of two waves travelling in opposite directions. We consider wave packets composed of groups of phonons with a small spread in angular frequency $\omega (= 2\pi\nu)$ and wave number q. If there are N(q) phonons in the mode q the heat current (the sum of the current carried by normal modes) is :-

$$Q = \sum_q N(q)\,\hbar\omega\,\frac{d\omega}{dq} \qquad \ldots\ldots \quad (1.12)$$

where the velocity of the wave packets v(q) is given by $\frac{d\omega}{dq}$. In thermal equilibrium, in the absence of a temperature gradient, there are the same number of phonons propagating in opposite directions, so that N(q) = N(-q), and the net heat flow is zero.

There is a gradient in the density of phonons of any particular wave vector q at every point in the crystal when a temperature gradient exists, and a net flow of phonons results. The flow of phonons into and out of each region tends to change the values of N(q) there from $N_0(q)$,

a normal mode, in thermal equilibrium at temperature T, is given by

$$N(q) = \frac{1}{\left[e^{\frac{\hbar\omega}{k_0 T}} - 1\right]} \qquad (1.11)$$

(2) Formal Theory of Phonon Conduction

In non-metals heat transport is through the lattice - the phonons. When discussing heat conductivity, each normal mode is regarded as consisting of two waves travelling in opposite directions. We consider wave packets composed of groups of phonons with a small spread in angular frequency $\omega (= 2\pi\nu)$ and wave number q. If there are N(q) phonons in the mode q the heat current (the sum of the current carried by normal modes) is :-

$$Q = \sum_q N(q)\,\hbar\omega\,\frac{d\omega}{dq} \qquad \ldots\ldots \quad (1.12)$$

where the velocity of the wave packets v(q) is given by $\frac{d\omega}{dq}$. In thermal equilibrium, in the absence of a temperature gradient, there are the same number of phonons propagating in opposite directions, so that N(q) = N(-q), and the net heat flow is zero.

There is a gradient in the density of phonons of any particular wave vector q at every point in the crystal when a temperature gradient exists, and a net flow of phonons results. The flow of phonons into and out of each region tends to change the values of N(q) there from $N_0(q)$,

the density in thermal equilibrium at the same temperature. This flow is opposed by the collision processes and the Boltzmann equation for phonons in the notation of equation (1.8)

$$\frac{\partial N(q)}{\partial t}\Big]_{coll.} = \frac{N(q) - N_0(q)}{\tau(q)} \quad \ldots\ldots \quad (1.13)$$

or

$$\frac{\partial N}{\partial t}\Big]_{coll} = -\left[v(q).\,grad.\,T\right]\frac{\partial N(q)}{\partial T} = -\frac{N_0(q) - N(q)}{\tau(q)}$$

$$= -\frac{n(q)}{\tau(q)} \quad \ldots\ldots \quad (1.14)$$

where $\tau(q)$ is the relaxation time defined in equation (1.8) and n(q) is the measure of deviation of asymmetry from the equilibrium distribution of phonons. The solution of such an equation is of the form

$$K = \tfrac{1}{3}\int C_j(q)\; V_j^2(q)\; \tau_j(q)\, dq \quad \ldots\ldots \quad (1.15)$$

where Cj(q)dq is the contribution to the specific heat from the phonons of wave vector q with polarization j and v(q). τ (q) is equal to 1 the effective mean free paths of the phonons. This relation has a formal similarity to that obtained for the conductivity of gas from kinetic theory considerations

$$K = \tfrac{1}{3}\, Clv \quad \ldots\ldots \quad (1.16)$$

Having summarised the formal theory of conduction, we shall consider various scattering mechanisms responsible

for the finite phonon conductivity. As there are several such mechanisms it follows from equation (1.9) that in order to calculate the total thermal conductivity one uses the Matthiesson's rule, which assumes that the resulting resistivities is the sum of resistivities due to each type of scattering separately. Thus

$$W = \frac{1}{K} = \sum_a W_a = \sum_a \frac{1}{K_a} \quad \ldots\ldots \quad (1.17)$$

While deviations from Matthiessen's rule do exist[6] the complete assumption of his rule never involves great errors and certainly with pure metals it may be used quite freely.

(3) Phonon-Phonon Interaction

A scattering which occurs in real crystals is the interaction of phonons with one another. There would be no exchange of energy between phonons in a crystal for which the forces between the atoms were perfectly harmonic, but in real crystals an harmonicity always occurs. This interaction at low temperatures in general, results in three phonon processes (neglecting higher processes).

$$\text{phonon (1)} + \text{phonon (2)} \rightleftharpoons \text{phonon (3)}$$

A phonon with wave vector q_1 and angular frequency w_1, combines with a phonon with q_2 and w_2 to form a third phonon.

The conservation condition may then be written

$$\hbar\omega_1 + \hbar\omega_2 = \hbar\omega_3 \quad \ldots\ldots \quad (1.18)$$

and

$$\underline{q}_1 + \underline{q}_2 = \underline{q}_3 + \underline{g} \quad \ldots\ldots \quad (1.19)$$

If $\underline{g} = 0$ the interaction is a Normal process, while if $\underline{g}$ is a reciprocal lattice vector we have an Umklapp process. In N-processes the sum $\sum N(q)q$ is conserved and as a heat flow corresponds to a non-zero value of this term, if only N-processes were operative, a heat flow once set up would continue without dissipation. We cannot, however, ignore the effect of N-processes; they are a means by which energy is exchanged among the modes, and thereby influence the action of other scattering processes(7)

As N-processes cannot by themselves lead to finite thermal conductivity so we consider those interactions in equations (1.19) where $g \neq 0$. g is a reciprocal lattice vector, which is determined by the structure and periodicity of the actual space lattice involved. The vector g has a magnitude of $2\pi/a_0$, where a_0 is the interatomic spacing of the actual lattice. In Umklapp collisions not only do the phonons collide but the direction of energy is also changed (giving rise to resistance) i.e. one of the phonons involved has undergone a Bragg reflection by the crystal lattice itself, as a result there is a dramatic change in net momentum of these three phonons. A U-process can therefore be considered as an interference effect in which

phonons are reflected by the crystal lattice as a whole. Peierls argued that these particular collisions are vitally important in limiting a heat flow, because we now have a mechanism which disrupts effectively the overall flow of momentum carried by the stream of phonons.

At high temperatures ($T \gg \Theta$ Debye) most of the phonons would have wave numbers which will be large enough to enable U-processes to occur, and there would be no difficulty generally, in providing the required U-processes to limit the momentum and the corresponding heat flow of phonons. The probability of a U-process will be proportional to the phonon density and therefore to the absolute temperature.

Only low frequency phonons are generally excited at low temperatures ($T \ll \Theta$), i.e. the vast majority of phonons will be those with small wave vector q. For U-process to occur, at least one of the colliding phonons in equation (1.19) must have a wave vector at least greater than one half of the maximum vibrational frequency of the lattice i.e. $1/2\ \nu$ max = $1/2\ k\Theta/h$ (from Deby's model). The probability of such phonon is proportional to $(e^{\Theta/2T} - 1)^{-1}$ which will tend to $e^{-\Theta/2T}$ for small values of T. Klemens (1958)[8] has given for $T \ll \Theta$

$$W_u = \text{Const. } T^n e^{-\Theta/2T} \qquad (1.20)$$

The constant contains terms which are a measure of lattice anharmonicity. Thus at sufficiently low temperatures

we must expect the rate of occurance of U-process to decay exponentially, and consequently the thermal resistivity would also decay exponentially. The measurements of Berman et al (1951)[9] are in agreement with the above predictions except at low temperatures where the above model would give a rapid rise of conductivity to infinite values at zero temperatures. This is impossible, as the mean free path of phonons then becomes infinite, so further scattering mechanism to limit the conductivity has to be considered.

(4) Boundary Scattering

It was pointed out by Pierls that his theory was applicable only to infinite crystal lattice and that for crystals of finite size, there will always be a temperature below which the mean free path (of elastic waves) between Umklapp collisions becomes comparable to the dimensions of the crystal and there will be scattering of elastic waves by the boundaries of the crystal, which will give rise to an additional resistance.

At low temperatures, the time of relaxation for Umklapp collisions increases with decreasing temperature as the number of phonons taking part in such collisions decreases exponentially and the U-collisions become rare. The relaxation times τ eventually become comparable with the time taken by phonons to cross the crystal from side to

side and scattering at the (discontinuity in structure, i.e. internal grain boundaries in the case of poly-crystalline crystals) external boundaries become the dominant scattering mechanism. One can then write $\tau = \frac{L}{v}$ (v being constant) L being the diameter of the crystal, and the conductivity should be proportional to specific heat C_v, (equation 1.16)). At such low temperatures K will be proportional to T^3, as the specific heat varies as T^3. Casimir (1938)[10] worked out the theory to show that the thermal conductivity becomes size dependent and is no longer an intrinsic property of the material and according to him

$$K = 2.31 \times 10^3 \, \mathbf{R} p A^{\frac{2}{3}} T^3 \text{ watts/cm.deg.} \qquad (1.21)$$

where R is the radius of the crystal, p is a dimensionless quantity and is about 1.4 for most crystals. A is the constant in the expression $C_v = AT^3$ for the specific heat per unit volume at low temperature on the Debye theory.

A more detailed investigation by Berman et al (1955)[11], has shown that this type of conductivity would not only depend upon the diameter of the crystals, (though the T^3 variation of dielectric crystals and superconductors has been observed for most of the crystals) but also on the state of crystal surfaces (which determines the degree of diffuse reflections), and in the overall length of

the specimen employed. These are all the simplifications in the derivation of Casimir's formula, where he treated a perfectly rough surface as it absorbed all phonons incident upon it and re-emitted them at a rate depending on the absolute temperature of the surface, according to the theory of Black-Body radiation.

In the presence of specular reflections on the walls of the crystal (scattering of phonons inside the bulk of the material), K would vary more slowly than T^3 (12).

(5) Defect Scattering

The only resistivities in ideal crystals would be from Umklapp-collisions (W_u) and boundary scattering (W_g). But scattering of phonons by point defects, isotopes and dislocations are also observed in practice. In metals and semi-metals the electrons act as further scattering mechanism to the phonons.

A static imperfection can be expected to perturb the lattice potential on account of (i) the difference between the masses of the solvent and solute atoms, (ii) the difference between the elastic properties of the solvent-solvent and solvent-solute atomic linkages.

Klemens (1958(8) neglects dispersion and calculates the scattering probability using the terms in the perturbation energy, which are quadratic in the phonon amplitudes (this is because only these terms describe

elastic scattering). The heat resistivity arising on this account is W_A, where $W_A = AT$, the coefficient A is the phonon defect scattering coefficient. Callaway (1959)[7] by a rigourous treatment gives W_A = Const.x $T^{3/2}$. Klemens finds also no essential difference between the scattering powers of vacancies and substitutional impurities.

For single dislocation Klemens obtains

$$W_D = D\,T^{-2} \qquad \ldots\ldots \qquad (1.22)$$

where D is the phonon-dislocation scattering coefficient.

For the overall lattice thermal resistivity of a dielectric solid we can write

$$\frac{1}{Kg} = Wg = W_u + W_B + W_A + W_D \qquad (1.23)$$

SECTION 1C

(1) Thermal Conduction by Electrons

In a metal the valence electrons are regarded as free to move through the crystal under the self consistent field of all other electrons; otherwise they are influenced only by the attractive forces of the ions. These ions are persumed to form a geometrically perfect lattice with no faults throughout the crystal. Bloch[2,3] showed that the wave function moving in the periodic potential V(r) of a crystal lattice has the form

$$\psi_k(\underline{r}) = \phi_k(\underline{r})\, e^{i\underline{k}.\underline{r}} \qquad (1.24)$$

where $\phi_k(\underline{r})$ is a function periodic in the lattice spacing. Thus the Bloch function $\psi_k(\underline{r})$ represents plane waves modulated with the lattice periodicity and having a wavelength $2\pi/k$ travelling in the direction $\underline{k}$. The energy $E(\underline{k})$ of the electron is a function of $\underline{k}$, however, the form of the function depends upon the details of the lattice potential V(r) in a unit cell, as does the form $\phi_k(\underline{r})$. The principal features of these solutions is the presence of broad energy bands separated by energy gaps. These gaps are values of the energy which are forbidden because they do not yield well behaved solutions.

Electrons obey Fermi-Dirac statistics and in equilibrium the distribution function of an electron is

given by

$$f_o(\mathcal{E}) = \left[e^{(\mathcal{E}-\xi)/k_oT} + 1 \right]^{-1} \tag{1.25}$$

where ξ is the chemical potential given by the condition

$$\int f_o\ (\mathcal{E}, \xi\ )\ n(\mathcal{E})\ d\mathcal{E} = N \tag{1.26}$$

Here $n(\mathcal{E})\ d\mathcal{E}$ is the number of states in the energy interval $\mathcal{E}$, $d\mathcal{E}$. The chemical potential ξ is temperature dependent, although this dependence is small in most metals, since $k_oT \ll \xi$ (k_o is the Boltzmann constant). At absolute zero $\xi = E_F$, the Fermi energy.

If the lattice potential is truly periodic, the electron wave will be propagated through the lattice without loss of energy i.e. there will be zero resistance to the motion of conduction electrons. This is contrary to experience, and the observed finite resistance to the transport of heat and electricity is due to lattice sources, which upset the regularity and periodicity of the lattice potential, i.e. which would tend to restore any non-equilibrium[1]. The deviations of the potential from perfect periodicity originates partly in thermal vibrations (which are there at any finite temperature even in a perfect crystal) and partly in the static imperfections. The thermal vibrations of the ions provide

a major source of scattering of electrons, except at very low temperatures ($T \ll \theta_{Debye}$), where scattering due to static lattice imperfections predominates and leads to a strongly temperature dependent thermal resistance.

An electric field $\underline{F}$ or a temperature gradient tend to disturb the equilibrium. The actual probability of occupation $f(\underline{k})$ in the steady state, under these conditions, are governed by the Boltzmann equation

$$\frac{e}{\hbar}\underline{F}.\frac{\partial f}{\partial \underline{k}} + \frac{1}{\hbar}\frac{\partial E}{\partial \underline{k}}.\text{grad}\,T\,\frac{df}{dT} = \left.\frac{df}{dt}\right]_{coll.} \qquad (1.27)$$

Where $v = \hbar^{-1}\frac{\partial E}{\partial k}$ is the velocity of the electrons in state $\underline{k}$ and the right hand side denotes the rate of change of $f(\underline{k})$ arising from the interaction processes.

In the notation of equation (1.8), we can write

$$\frac{f-f_o}{\tau} = \frac{df}{dt} = -\frac{g(\underline{k})}{\tau(\underline{k})} \qquad (1.28)$$

In this way deviation from equilibrium $g(\underline{k})$ can be obtained in terms of $\tau(\underline{k})$. In the case of an isotropic medium in which $E(\underline{k})$ is a function of k only and in which F and grad T are in the same direction we can write

$$g(\underline{k}) = -\mu\tau(\underline{k})\frac{df}{dE}\frac{1}{\hbar}\frac{dE}{dk}\left[eF - \text{grad}\,T\left(\frac{E}{T} + \frac{d\xi}{dT}\right)\right] \qquad (1.29)$$

where μ is the direction cosine of $\underline{k}$ relative to $\underline{F}$ and grad T is positive. The electrical and thermal currents are then given by

$$J = \int e \frac{1}{\hbar} \frac{\partial E}{\partial k} g(k) \frac{2}{(2\pi)^3} dk \qquad (1.30)$$

and

$$Q = \int E \frac{1}{\hbar} \frac{\partial E}{\partial k} g(k) \frac{2}{(2\pi)^3} dk \qquad (1.31)$$

The electric conductivity σ is given by $\sigma = J/F$ when grad T = 0, the thermal conductivity $K = \frac{-Q}{\text{grad } T}$ with the condition J = 0, and we can obtain

$$\sigma = \frac{e^2}{12\pi^3} \int \frac{\tau v^2}{|\text{grad}_k E|} dS \qquad (1.32)$$

$$K = \frac{k_o^2 T}{36\pi} \int \frac{\tau v^2}{|\text{grad}_k E|} dS \qquad (1.33)$$

where k_o is the Boltzmann constant. The integration extends over the Fermi surface ($E = \xi$) and dS is an element of that surface. Thus only the area of the Fermi surface, the velocity distribution and the relaxation time $\tau(\underline{k})$ at this surface enter into the values of the conductivities.

(2) Wiedemann-Franz Law

If $\tau(k)$ is independent of the function g(k), one obtains for the ratio of the conductivities

$$\frac{K}{\sigma T} = \frac{\pi^2}{3}\left(\frac{k_0}{e}\right)^2 = L_0 \text{ a universal constant}$$

$$= 2.45 \times 10^{-8} \text{ watts-ohm/deg}^2 \qquad (1.34)$$

This is the Widemann-Franz law and L_0 is the Lorentz number. From the above equation it is clear the above law would be valid no matter how complicated the shape of the Fermi surfaces. As long as the time of relaxation $\tau(k)$ is independent of the form of the asymmetry of the electron distribution function, equation (1.34) holds. However, the value of L is a consequence of the strong degenercy of the electron gas i.e. $k_0 T \ll \xi$.

The Wiedemann-Franz law is obeyed to within few percent by many metals at such low temperatures that the resistance is entirely due to impurity scattering of electrons and at high temperatures ($T \gg \theta$) it is also reasonably well obeyed. When the temperature is raised to such a point that the electrical resistance begins to rise from its residual value at something like T^5, while T/K rises something like T^3 so that the Wiedemann-Franz law cannot be maintained. The reason for this is the invalidity of the relaxation time assumption.

A useful physical insight is gained by dividing electron scattering processes into two classes; "horizontal" processes in which the direction of the electron is

changed but not its energy, and "vertical" processes in which the electron energy is changed but not its direction. The electrical conductivity is limited by the horizontal processes only. The thermal resistivity on the other hand can be due (i) elastic collision processes (keeping the electron energy unchanged), which ar e due to collisions with imperfections and impurity atoms and causes the horizontal movement and (ii) inelastic collision processes (which change the energy by an amount of the order of $k_o T$), which are due to electron-phonon collisions and causes the so called vertical movement on the Fermi surface.

We thus see that the electrical resistance mechanism and the horizontal thermal resistance mechanism are processes giving identical relaxation times and we expect in the case of elastic scattering the Lorentz number to be constant. For inelastic scattering processes, we may expect a shorter relaxation time for thermal conduction than for electrical conduction at low temperatures. This will of course lead to a deviation from the Wiedemann-Franz law and the Lorentz number L will sink below the value L_o in equation (1.34).

(It can be shown at high temperatures ($T \gg \theta$) the scattering by lattice waves is essentially an

elastic process. The change in electron energy due to impact with a phonon will be $k_o\Theta$, which is small compared to k_oT and for such temperatures the Wiedemann-Franz law can be expected to be obeyed).

We can divide the electron scattering and hence resistivities into two sources, namely static imperfections and lattice vibrations. To a first approximation, their contribution to the scattering of electrons is additive. By Matthiessen's rule we find

$$\frac{1}{\sigma} = \rho = \rho_o + \rho_i \qquad (1.35)$$

$$\frac{1}{K} = W = W_o + W_i \qquad (1.36)$$

in which the subscript i denotes the ideal (or intrinsic) resistivities and o the imperfection (or residual) resistivities. Below we consider how the two types of scattering depend upon the temperature.

(3) The Impurity Resistivity

At the lowest temperatures the lattice vibrations are largely unexcited and the only irregularities in the lattice potential are caused by lattice imperfections due to impurities and to various defects such as vacancies, grain boundaries, stacking faults and dislocations. An impurity can scatter an electron through almost any

angle as it being small of dimensions comparable to the wavelength of a Fermi electron and so can also grain boundaries, stacking faults etc. The change in energy is very small as all these imperfections are massive and locked to the lattice.

Bloch (1930)[3], introduced the idea of a temperature independent mean free path for the case of randomly distributed impurity atoms for this type of elastic scattering and the mean free path l will be of the order of the mean distance between the impurities. Putting $l \simeq \tau v_F$ we find from equation (1.32) σ to be independent of temperature and from equation (1.34) that the thermal conductivity is linearly proportional to the temperature. This type of scattering gives rise to a constant residual resistivity ρ_0 . The Wiedemann-Franz law is valid in this region

$$W_0 T = \beta = \rho_0 / L \qquad (1.37)$$

The β is the measure of the imperfection in the crystal whether by the addition of chemical impurities or by upsetting of the crystal lattice.

(4) Resistivity due to Phonon Scattering

Electron-phonon interaction is responsible for the ideal resistivity in the electrical and thermal conduction. This may be described in terms of individual processes in

which an electron with wave vector $\underline{k}$ and phonon $\underline{q}$ combine to give an electron $\underline{k}'$or vice-versa. Energy is conserved.

$$E(\underline{k}) + E(q) = E(\underline{k}') \qquad (1.38)$$

$$\underline{k} - \underline{k}' \pm \underline{q} = \begin{cases} 0 \\ n\underline{G} \end{cases} \qquad (1.39)$$

giving two energetically possible types of scattering processes. $\underline{G}$ is a vector in the resiprocal lattice. The collision with $\underline{G} = 0$ are known as Normal processes and for which $\underline{G} \neq 0$ are called Umklapp processes. Identical processes occur in the study of phonon-phonon scattering which we have discussed in an earlier section.

In metals at low temperatures ($T \ll \theta$), the fact that most of the phonons have a very long wavelength has a marked effect on the scattering of electrons. It turns that there is very little change of momentum of an electron when it collides with a phonon, so that the electrical resistivity falls very rapidly as the temperature is lowered ($\rho_i \propto T^5$). The transfer of energy when an electron collides with a long wavelength phonon, is rather more effective than the transfer of momentum. The energy gain is comparable to the Fermi energy $k_o T$. Thus the electronic thermal conductivity does not fall so rapidly as the electrical resistivity with decreasing temperatures, since its energy transfer that is important in the heat conduction processes.

If one considers the interaction between lattice waves and electrons, a complicated integral equation is obtained in the Boltzmann equation (1.8) for the function $\left(\frac{\partial f}{\partial t}\right)$ collisions. The solution of this is quite difficult and has only been solved for quasi-free electrons (12-14)

Bloch calculated the transition probability in terms of a quantity C (which has the dimensions of an energy and characterises the strength of electron phonon coupling), and for spherical Fermi surface the order of magnitude C_D is the Fermi energy ξ . He assumed in his calculation Debye's vibrational spectrum, ignored Umklapp processes and that phonon distribution is unaffected either by electric field or temperature gradient. The transition probability would be zero, unless the lattice wave is longitudinally polarised.

The general result of these calculations shows that at low temperatures ($T < \theta/10$), the thermal resistance W_i is of the form

$$W_i = a T^2 \qquad (1.40)$$

where

$$a = \frac{A}{K_\infty \theta^2} N_a^{2/3} \qquad (1.41)$$

N_a is the number of conduction electrons per atom, K_∞ is the limiting constant thermal conductivity at high temperatures and A is a dimensionless constant. It has

different values depending on the kind of approximation used in the solutions.

A = 95.3	According to Wilson's first approximation of the variational method.[14]
A = 71.6	According to Sondheimer's third approximation[6].
A = 64.0	According to Klemen's numerical solution[15].

Equation (1.41) is not satisfied experimentally[16] and the discrepancy is due to over simplifications of Bloch's assumption in the solution of the Boltzmann equation for electron-phonon coupling. Later work, with some of Bloch's assumption modified by Ziman (1954)[17], Bailyn (1960)[18], etc. show that a maximum in W_i which the earlier theories had suggested ought to exist at about $\Theta/5$ and which had never been observed was now almost entirely removed. The T^2 dependence of W_i still holds at low temperatures but a reduced α in expression (1.41) to be in accordance with experiments on many metals.

(5) The Electronic Thermal Conductivity

By applying Matthiessen's rule, we see that the total electronic thermal resistivity W_e is of the form (Sondheimer (1950)[6] has shown that the above rule can be applied to the thermal resistivities within an

accuracy of 1%)

$$We = Wi + Wo$$
$$= \alpha T^2 + \beta/T \qquad (1.42)$$

This expression will apply in the region where W_i is proportional to T^2 and this will be at temperatures of $\Theta/50$ to $\Theta/100$[19], instead of the expected temperatures of $\Theta/10$. The overall experimental picture of the variation of the thermal conductivity with temperature is well explained by the theory. A detailed comparison with experiment is discussed in Rosenberg (1962)[20].

(6) Lattice Conduction in a Metal

In alloys, annealed metals and superconductors well below the transition temperature phonon conduction can be significant. The lattice conductivity in a metal is influenced by all the factors which determine it in a non-conductor and in addition the presence of free electrons play an important role in reducing its magnitude, The main contribution to the total phonon resistivity arises from the scattering by the electrons, which is reverse of the process described in an earlier section and the interference condition (1.38) and (1.39) also apply in this case. Mackinson (1938)[4] and Klemens (1954)[15] give expressions for the scattering of phonons by the electrons (for $T \ll \Theta_{Debye}$) of the form

$$W_{ge} = ET^{-2} \qquad (1.43)$$

In determining the constant of proportionality E,

Makinson assumes that the longitudinal and transverse waves interact equally with the electrons (this is contrary to the simple Bloch theory) in determining the interaction constant between the electrons and the phonons. Makinson's expression for the lattice conductivity at low temperatures, when limited by electron scattering is given by

$$Wge = \frac{\Theta^2 N_a^2 T^{-2}}{C K_{e\infty}} \qquad (1.44)$$

where C is a constant with the value of 4.93. Makinson used the limiting high temperature value of the electronic thermal conductivity $K_{e\infty}$. Klemens used the low temperature electronic thermal resistivity ($W_i = a T^2$ equation (1.40)) and his expression for Wge is

$$Wge = 3.2 \times 10^{-3} a \Theta^4 N_a^{4/3} T^{-2} \qquad (1.45)$$

The other contribution to the phonon resistivity which can become important in metals is that produced by dislocations. This is directly proportional to the dislocation density and varies as T^{-2}, the same temperature dependence as Wge.

For highly resistive alloys ($\rho > 10^{-5}$ ohm. cm. at few degrees absolute) when the electron mean free path becomes sufficiently small, Pippard (1957)[21] has shown that the lattice conductivity is proportional to T instead of T^2 and the lattice thermal conductivity represented by

$$K_g = A T + B T^2 \qquad (1.46)$$

Section 1D

RARE EARTH METALS

(1) Introduction

The fourteen elements of the rare earth group are characterized by the presence of 4f electrons in their normal electronic configurations. The number varies from element to element and depends on the valency. With lanthanum they form a category of chemically-similar elements, and this series represented by $4f^n5d^16s^2$ is known as 'Lanthanides'. They oxidize readily, exhibit medium strength and hardness, and have pronounced magnetic properties due to the f electrons. They all (except Eu and Yb) have three valence electrons and their closely resembling physical and chemical properties make them difficult and costly to separate.

The 4f electrons are closely bound inside the outer closed shells on the atoms and therefore play a small role in the chemical bonding. Since the 4f electrons are 'isolated' from the neighbouring atoms - behaving as they would in a free ion - the 4f shell fills according to Hund's rule. Hund's principle of maximum multiplicity suggests that the unpaired 4f electrons should increase regularly in number from one with cerium to seven with gadolinium, and then decrease regularly to one with

ytterbium. It is these electrons, carrying with them the magnetic moment, that are responsible for the interesting magnetic properties in these metals.

To summarise, for the series of rare earth metals, lanthanum to lutetium, there are three electron groups performing three separate functions:

$4f^n$ - magnetic electrons

$5p^6$ - closed shell, providing repulsive energy

$5d^16s^2$ - bonding electrons providing attractive energy.
(5d 6s for Eu and Yb)

Most of the metals conform to the picture outlined above of tripositive ions embedded in a sea of conduction electrons formed from the three, 5d and 6s, valence electrons. However, even the valence properties differ a little, and the crystal structure of the elements in the second half of the series differs slightly from that common in the first half. Furthermore as Eu and Yb come immediately before the middle and the end of the series and, in the tripositive form, would have configurations $4f^6$ and $4f^{13}$ they evidently prefer to gain the extra correlation energy for a half-filled or completed shell and take a divalent form and this is borne out by their properties.

At normal temperatures each of the rare earth metals exhibits an effective highly localised moment in the

paramagnetic state (both spin and orbital motions of unpaired electrons are sources of magnetic effect). Ytterbium has only a small paramagnetism as is expected from a closed shell. Europium shows large moments as expected from $4f^7$. As the temperature is reduced there is in general at a certain critical temperature a transition from the pramagnetic state, in which the atomic moments are randomly oriented, to an ordered state of anti-ferromagnetic configuration. This is the case with rare-earth metals of the first half of the series - cerium, praseodymium, neodymium, samarium and europium - known as the 'light Lanthanides'. The second half known as the 'heavy Lanthanides' - gadolinium, dysprosium, terbium, erbium, holmium and thulium - takes on a further order-order transformation and become ferromagnetic at lower temperatures.

(2) Rare Earth Ferromagnets

The rare earth ferromagnets (the heavier lanthanides) have very characteristic properties differing from those of the ferromagnets of the iron group. The most remarkable property of the rare earth ferromagnets is the fact that five of them (Tb, Dy, Er, Ho, and Tm) exhibit antiferromagnetism in a certain range of temperature. This antiferromagnetism is of special type: spiral or helicoidal. The majority of the rare earth metals of

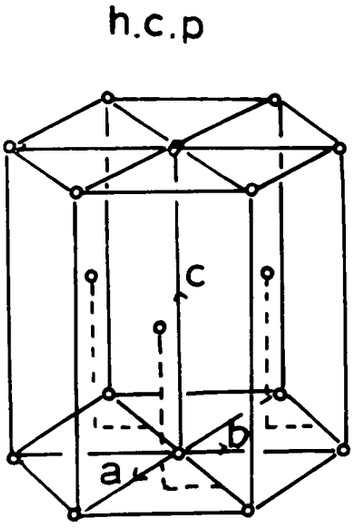


FIGURE 1.1

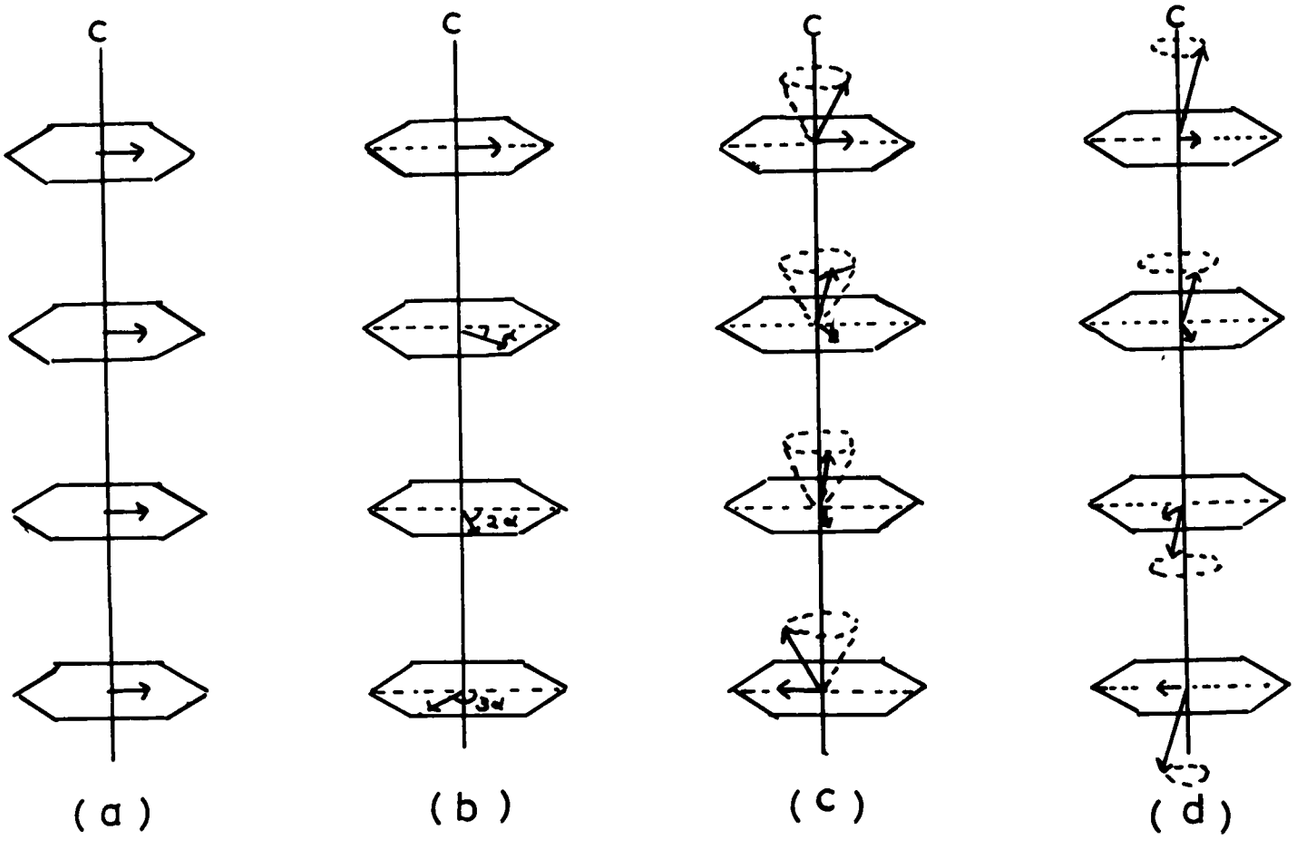


FIGURE 1.2

the cerium group exhibit antiferromagnetism at very low temperatures. For most of the heavy rare earths there are two magnetic transition temperatures, Tc, the Curie temperature (when ferro to antiferromagnetism occurs) and T_N the Neel temperature (antiferro to paramagnetic) where $T_c < T_N$.

All the heavierrare earth metals with the exception of yetterbium crystalize in a close packed hexagonal form (fig. 1.1) with c/a ratio from 1.57 to 1.59 a little different from the ideal value of 1.63. Ytterbium has a cubic closest packed structure. Their density increases monotonically from 7.868 gm./cm. for gadolinium to 7.849 gm./cm. for lutetium.

The electronic properties of a metal tend to be very dependent on the details of the electron energy spectrum. Very little is known of the detail band structure of the three conduction electrons in these materials. Based on crude assumption of nearly free electrons the rare earth ferromagnets have two atoms per cell and the vectors of the resiprocal lattice also form a hexagonal lattice. The first Brillouin zone is shown to be a hexagonal prism of side $4\pi/3a$ and height $2\pi/c$. The free electron Fermi surface is a sphere with radius

$$k_f = 2\sqrt{3\pi}/(2\pi a^2 c)^{1/3}$$

and this Fermi surface stretches out over five zones.

Table 1.1

* The ordered magnetic phases of rare earth metals.

Element	At.no.	Patterns of order	
Gadolinium	64	Ferromagnetic in c- axis	$T_c = 290^{\circ}K$
Terbium	65	Ferromagnetism in basal plane	$T_c = 218^{\circ}K$
		Helical antiferromagnetism	$T_N = 230^{\circ}K$
Dysprosium	66	Ferromagnetic in basal plane	$T_c = 85^{\circ}K$
		Helical antiferromagnetism	$T_N = 179^{\circ}K$
Holmium	67	Helical ferromagnetism with resultant moment in c- axis	$T_c = 19^{\circ}K$
		Helical antiferromagnetism	$T_N = 133^{\circ}K$
Erbium	68	Helical ferromagnetism with resultant moment in c- axis	$T_c = 20^{\circ}K$
		Modulated antiferro-magnetism	$T_N = 80^{\circ}K$
Thulium	69	4,3,4,3 ferromagnetism at changing to sinusoidal antiferro.	$4^{\circ}K$
			$T_N = 56^{\circ}K$
Europium	63	Antiferromagnetic	$T_N = 87^{\circ}K$

* Martin, D.H., 'Magnetism in Solids' - London Iliffe Books Ltd.

The energy bands and hence the Fermi surface are discontinuous across various planes according to Bragg conditions.

(3) Magnetic Structure of the Rare Earth Ferromagnets

It is found in the rare earth ferromagnets the atomic moments are directed in patterns which depend on the temperature and on the element (see table 1.1). Dysprosium and terbium have the simplest magnetic structure. In the ferromagnetic region the magnetic moments lie in the basal plane and are parallel to one another (fig. $1.2^{(a)}$). Gadolinium below $290^{\circ}K$ has the same moment parallel to the hexagonal axis.

In the antiferromagnetic state for dysprosium and terbium the resultant magnetic moment of each basal plane is rotated by a certain angle α_o with respect to the direction of the moment in the next basal plane (fig. 2.2(b)). Looking through the c- axis one then observes a simple spiral structure. The c- axis in this case will be perpendicular to the magnetic moments and $360^{\circ}/\alpha_o$ the turn angle gives the pitch before the magnetic structure repeats itself - thus giving an idea of the magnetic super lattice.

The magnetic structure of holmium is more complex. Below T_c in the ferromagnetic state the magnetic component along the hexagonal axis of holmium (at 4.2 K) is $2\mu B$

per atom and at the same temperature the component of the moment in the basal plane is 9.5μ_B per atom; the magnetic field component in the basal plane are helicoidaly ordered and do not have a resultant magnetic moment (fig. 1.2(c)). Thus the ferromagnetic moment of holmium is due only to the component parallel to the hexagonal axis. It has a strong distorted helicoidal structure in the antiferromagnetic state.

Erbium has a structure similar to holmium below T_c but in the antiferromagnetic region the magnitude and direction of the magnetic moment component along the c-axis vary periodically from layer to layer in accordance with a sine law (fig. 1.2(d)).

For thulium at 4.2°K the resultant magnetic moment is directed along the c-axis. In this temperature region, the spins alternate in four neighbouring plans the magnetic moments are directed in one way and in the next three planes they are directed in the opposite way. The several structures described above were all deduced directly from the neutron diffraction patterns[22-23].

At present there is no complete theory, which would explain these magnetic structures and transitions in them with temperature, though many theoretical attempts have been done[24]. Belov et al (1964)[25] gives an excellent review of these partially correct theories

and comparison with experimental observations on temperature dependence on magnetization, specific heat, resistivity etc. are made.

(4) Spin Waves

A ferromagnetic system behaves as if every magnetic moment were alligned parallel and even in the absence of a magnetic field we observe a large spontaneous magnetization. This spontaneous magnetization decreases as we warm the crystal and vanishes at a well defined temperature, the Curie temperature T_c. Weiss postulated a 'molecular field' that could make the ionic and atomic magnetic moment in a paramagnetic substance line up in the same way. From the measurement of the Curie temperature the Weiss internal field is very large - much larger than that produced by the magnetic moments of the other ions in the crystal.

The strong interaction responsible for spontaneous magnetization was recognised by Heisenberg in 1926 as being exchange interaction between electrons. This interaction tends to order the spin moments of two close electrons either in parallel or antiparallel allignment depending on the details of their states of motion. Following Heisenberg and Dirac it can be shown[26] on certain assumptions that the energy of interaction of atoms i, j bearing spins S_i, S_j contains a term

$$E_{ex} = - 2J_{ij}S_i . S_j . \qquad (1.47)$$

where J_{ij} is the average integral and is related to the overlap of the charge distributions i,j. This exchange energy, basically of electrostatic origin, is without a classical analogue and expresses the difference in Coulomb interaction energy of the systems when the spins are parallel or antiparallel. The average value of J is about 10^{-4}eV in gadolinium and in general falls off rapidly as the neighbour distance increases.

The interaction $-2JS_iS_j$ coupling the spins, all parallel (at $T = 0^oK$) in the simple ferromagnet, classically amounts to a torque exerted by one spin on another. Spin deviations will not then stay localised in the crystal but will travel through the lattice as spin waves. The simple spin wave theory[27] assumes a purely isotropic Hamiltonian for the magnetic spin system, which is approximated formally by an assembly of harmonic oscillators. A magnon or spin wave frequency spectrum $\hbar\omega(q)$ is then obtained and from this one can calculate the various statistical properties. Spin wave energies are quantised and for a ferromagnet at small wave vectors for a simple cubic lattice, the energy of a magnon is proportional to the square of its wave vector

$$Eq = \hbar w(q) = A\, a^2q^2 \qquad (1.48)$$

where a is the lattice constant. One can then define an 'effective mass' m^* such that

$$\hbar\omega(q) = \frac{\hbar^2q^2}{2m^*} \qquad (1.49)$$

For a typical ferromagnet with a Curie temperature of a few hundred degrees K, m^* is found to be 10 times the mass of a free electron. Cooper et al (1962)[28], have calculated the spin wave spectrum from a Hamiltonian including anistropic exchange, axial and hexagonal anistropy for the various types of magnetic order to occur in the heavy rare earth metals.

Any excited state is made up of many independent waves of spin disorder, each with frequency W_q and wave vector q and each excited to a quantised amplitude such that its energy is $n_q \hbar \omega_q$. The permissible values of q are finite in number for a finite crystal. The energy of the i^{th} state is

$$E_i = \sum_q n_q^i \hbar \omega_q \qquad (1.50)$$

The excitation of one quantum of spin wave i.e. one magnon, reduces the magnetic moment of the system by $g\mu_B$ regardless of the value of q. Magnons obey Bose-Einstein statistics and so the average occupation number can be written as

$$\bar{n}_q = \left[\exp(\hbar\omega_q/k_oT) - 1\right]^{-1} \qquad (1.51)$$

The simple spin wave theory predicts

(Magnetization) $$M = M_o \left[1 - A(k_oT)^{3/2}\right] \qquad (1.52)$$

(Specific heat) $$C_M = B\,(k_oT)^{3/2} \qquad (1.53)$$

(Ele.Resistivity) $$\rho_M = D\,(k_oT)^2 \qquad (1.54)$$

where A, B and D are constants.

(5) Indirect Exchange Interaction

In the rare earth metals it is clear that the spontaneous magnetization comes mainly from electrons which are well localised at individual ions and which move in 4f states closely resembling those in isolated ions. In these metals the magnetic shells are so well localised that the overlap between atoms must be negligibly small and the direct exchange interaction is much too small to account for the strong ordering in the rare earth metals. Electrons other than the 4f electrons must therefore take part in the interaction leading to the magnetic ordering even though they may make only a small contribution to the spontaneous moment.

Considering Zener's model, the indirect exchange interaction gives an effective spin Hamiltonian

$$H = -2\sum_{ij} J_{ij}\, S_i . S_j - 2\sum_{im} J_{im}\, S_i . s_m - 2\sum_{mn} J_{mn}\, s_m . s_n \qquad (1.55)$$

where i, j ... label ions and m, n ... label itinerant electrons and where J's are exchange constants. In the resultant interaction each ion polarises the gas of itinerant electrons which then couples to the spin of other atoms to produce an effective exchange with long range. This type of exchange and its effects were first examined in metals by Rudermann and Kittel (1954)[29] for

the coupling of nuclei. Kasuya (1956)[30] proposed that it was the important interaction in the rare earths and Yosida (1957)[31] used it for electron spin coupling in other systems.

If a coupling of the form described above exists, any ordering of the local magnetic moments will produce an effect on the conduction electrons. Mackintosh (1962)[32] Elliot and Wedgewood (1963)[33] and Miwa (1963)[34] point out that at the onset of antiferromagnetism ordering (at T_c) a magnetic periodicity differing from the ionic lattice periodicity introduced in the c- axis direction and this magnetic periodicity introduces planes of energy discontinuity called magnetic superzones. These superzones destroy parts of the Fermi surface normal to the c- axis, but leave components of the Fermi surface in the basal plane unchanged. Both the electrical and the thermal conductivities depend on integrals over the Fermi surfaces.

In rare earth metals there is the additional factor that the orbital momentum of an ion is not quenched and since the orbital moments are strongly coupled to the crystal lattice by the crystal fields, there is normally a large anistropy in a rare earth metal, which is reflected on the energy of the spin systems through the spin orbit coupling.

(6) Conduction Processes in Rare Earth Ferromagnets

The appearance of the new superzone boundaries mentioned in the earlier section has important effects on the properties associated with conduction electrons. The most important is the electrical resistivity, which shows marked anomalies at the transition temperatures.

Mannari (1958)[35] has shown that the magnetic contribution to the electrical resistivity of a simple ferromagnet at low temperatures can be written

$$\rho_M = \text{Const.} \times T^2 \qquad (1.56)$$

The other contribution to the resistivity are due to temperature independent impurity scattering and phonon scattering, which contributes a term proportional to T^5 at low temperatures. Therefore in the low temperature region, considering only the temperature dependent terms, the decrease of conductivity with increasing temperature is due to increasing scattering of the conduction electrons by phonons and spin waves.

The abrupt decrease in conductivity at T_c can be explained by the appearance of new magnetic planes of energy discontinuity, together with perhaps a change in spin disorder scattering. We note that in the integral (equation 1.32) there is a strong reduction as the Fermi surface is lost.

As we move up in temperature towards T_N, the ordering

in the plane disappears, causing a change in the electronic structure, which, together with rapid change of magnetic disorder scattering leads to a decrease of conductivity with temperatures.

Above T_N the decrease in conductivity with temperature is due just to increased lattice scattering. In the pramagetic region we can write

$$\rho = \rho_0 + \rho_s + aT \qquad (1.57)$$

The spin-disorder scattering ρ_s has been shown to be temperature independent in this region[36] and it is appreciably larger than ρ_0 . A characteristic feature of the high temperature electrical resistivity of the magnetic rare earths is the constant spin-disorder contribution. The corresponding characteristic of the high temperature thermal conductivity is the positive slope above the ordering temperature[37].

From the theory of Niira (1960)[38], ρ_M for a anistropic ferromagnet at low temperatures we get

$$\rho_M = CT^2 e^{-\Delta/k_0 T} \qquad (1.58)$$

Δ represents the minimum energy required to excite a spin wave. Niira has shown that a hexagonal close packed ferromagnet with magnetic anistropy both between the hexagonal axis and the basal plane has preferred

direction of magnetization and for dysprosium and terbium his model applies. From experiments on specific heat[39-40] the magnetic contribution to the specific heat for terbium and dysprosium is negligible below 4.2°K and these results can be understood in terms of non excitation of spin waves at low temperatures. This energy gap for dysprosium is Δ/k_o = 30°K.

Other transport properties[37] also show anomalies at the magnetic transitions which arise from the same effect that cause the electrical resistivity anomalies, but they have not been interpreted in detail.

References to Chapter One

1. Prange, R.N., and Sachs, A. (1967) — Phys. Rev. 158, 678.
2. Bloch, F. (1928) — Z. Phys. 52, 555) See 13.
3. Bloch, F. (1930) — Z. Phys. 59, 208)
4. Makinson, R.E.C. (1938) — Proc. Camb. Phil. Soc. 34, 474.
5. Sondheimer, E.H.(1957) — Corter, Prog. in Low Temperature. Vol.II. Published by North Holland Publishing Co.Ltd.
6. Sondheimer, E.H.(1950) — Proc. Camb. Phil. Soc. 34,474.
7. Callaway, J. (1959) — Phys. Rev. 113, 1046.
8. Klemens, P.G. (1958) — Solid State Phys. 7, 1.
9. Berman, R., Simon,F.F., and Wilks, J. (1951) — Nature, 168, 277.
10. Casimir, H.B.G. (1938) — Physica 5, 495.
11. Berman, R., Foster, E.L., and Ziman, J.M. (1955) — Proc. Roy. Soc. A231,130.
12. Klemens, P.G.(1956) — Handbuch der Physick XIV Berlin Springer-Verlag.
13. Olsen, J.L.(1962) — Electron Transport in Metals. Inter Science Publishers.
14. Wilson A.H. (1937) — Proc. Camb. Phil. Soc. 33,371.
15. Klemens, P.G. (1954) — Austral. J. Physics 7, 57.
16. Mendelssohn, K., and Rosenberg, H.M. (1961) — Solid State Phys. Vol 12,223.
17. Ziman, J.M. (1954) — Proc. Roy. Soc. A226, 436.

References to Chapter One cont'd.

18. Bailyn, M.(1960) Phys. Rev. 120, 381.

19. Rosenberg, H.M.(1955) Phil. Tran. Roy. Soc. A247, 441.

20. Rosenberg,H.M. (1962) Low Temp. Solid State Physics., Section (5.7) Clarendon Press.

21. Pippard, A.B.(1957) J. Phys. Chem. Solids, 3, 175.

22. Koehler et al (1962) J. App. Phys. 33, suppl.1124.

23. Koehler et al (1963) J. App. Phys. 32, 485, 495.

24. Yosida, K., and Miwa, H. (1961) Progr. Theoret. Phys. (Kyoto) 26, 693.

25. Belov et al (1964) Sov. Phys. Uspekhi 7, 179.

26. Van Vleck, J.H.(1945) Revs. Mod. Phys. 17, 27.

27. Van Kranendonk, J., and Van Vleck, J.H.(1958) Rev. Mod. Phys. 30, 1.

28. Cooper et al (1962) Phys. Rev. 127, 57.

29. Ruddermann, M.A., and Kittel, C. (1954) Phys. Rev. 96, 99.

30. Kasuya, T. (1956) Progr. Theoret. Phys. (Kyoto) 16, 45.

31. Yosida, K. (1957) Phys. Rev. 106, 893.

32. Mackintosh, A.R.(1962) Phys. Rev. Letters 9, 90.

33. Elliot, R.J., and Wedgewood, F.A. (1963) Proc. Phys. Soc. (London), 81, 846.

34. Miwa, H. (1962) Progr. Theoret. Phys. (Kyoto) 28, 208.

35. Mannari, I. (1958) Progr. Theoret. Phys. (Kyoto) 22, 335.

36. Dekker, A.J. (1965) J. App. Phys. 36, 906.

37. Boys, D.W., and Legvold, S. (1968) Phys. Rev. 174, 377.

References to Chapter One cont'd.

38. Miira, K. (1960) Phys. Rev. 117, 129.

39. Lounasmaa, O.V., and Roach, P.R. Phys. Rev. 128, 622.

40. Lounasmaa, O.V., and Guenther, R.A.(1962) Phys. Rev. 126, 1357.

CHAPTER TWO

APPARATUS AND EXPERIMENTAL TECHNIQUES

Introduction

Thermal conductivity can be measured by the static and dynamic methods. Most of the really accurate measurements of thermal conductivity at and below room temperature make use of the static, absolute method. This was the method we used, in which our specimens in the form of a rod or drawn out wire about five to six centimeters long and a few millimeters in diameter was mounted in vacuum, with one end in good thermal contact to the heat sink at temperature T, and heat was supplied to the other end by an electric heater. In between, at two convenient points, the temperature gradient was measured using carbon thermometers by a differential method. By the use of an electronic regulator the temperature of the sink (He^3 cryostat) was maintained to better than $10^{-4}{}^{o}K$ and the temperature was determined by measuring the vapour pressure of the cryogenic liquid used (He^3 and He^4 in our case). In the $helium^4$ cryostat the pumped bath was maintained steady using a diaphram type manostat.

In this chapter we shall describe the apparatus and the experimental techniques used to measure the thermal

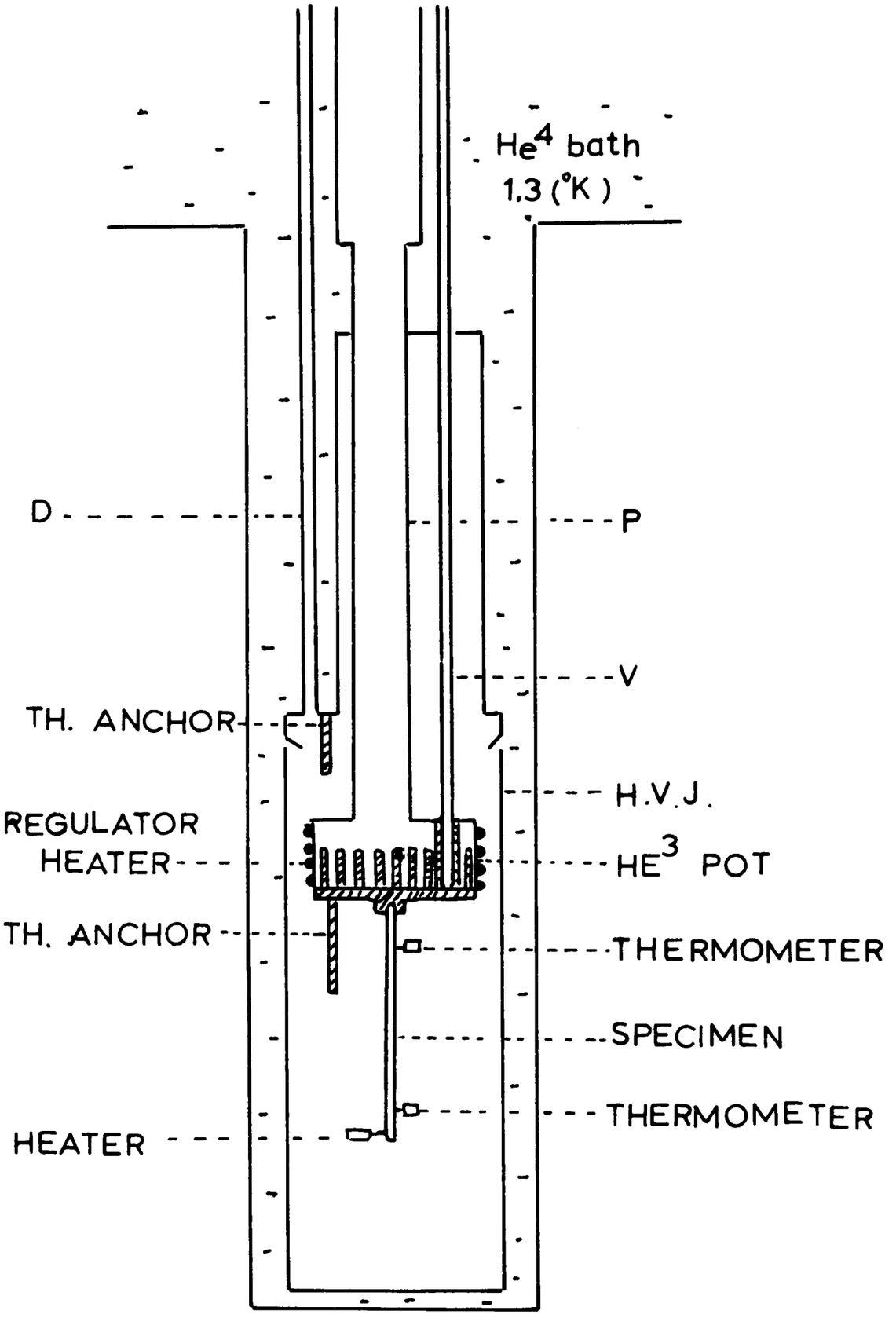
conductivity. The measurement below 1.4°K was done on a specially designed helium^3 cryostat, which is described in section 2A. Temperatures down to 0.4°K were obtained by pumping on liquid helium three.

The measurement between 4.2° and 1.2°K was done on a typical helium^4 cryostat. As the helium^4 apparatus and techniques used are the same as those used by Sousa (1968)[1], no attempt will be made to give the details of the apparatus.

The vapour pressure of the liquid helium three in the helium^3 pot was measured using Mcleod gauges and after corrections the temperature was determined using the published vapour pressure temperature relation (1962 Helium^3 scale of temperature[2]). The vapour pressure of the helium^4 bath was measured with mercury and oil manometers.

A great care is necessary to maintain and measure the temperature of the sink, the power into the heater and the temperature gradient. It is important to see that there is no heat input into the specimen along the leads etc. because, while this is very small it can cause appreciable error if the specimen has low thermal conductivity and if there is poor thermal contact at the heat sink. We shall describe later in this chapter how these problems have been confronted.

FIGURE 2.1


He4 bath
1.3 (°K)
D
P
V
TH. ANCHOR
H.V.J.
REGULATOR
HEATER
HE3 POT
TH. ANCHOR
THERMOMETER
SPECIMEN
THERMOMETER
HEATER

Section 2A:

APPARATUS

(1) The He^3 Cryostat

To measure thermal conductivity below 1^oK, we designed and built a typical helium three cryostat. In the design of our apparatus, we had to take into consideration that helium three is a rather rare isotope and that it is not lost or contaminated. The helium three gas is condensed directly into a chamber (the He^3 pot) in the cryostat, which has been cooled below the critical point (3.35^oK) by thermal contact with a bath of ordinary liquid $helium^4$ - in our cryostat the $helium^4$ bath is maintained at 1.3^oK. The helium three chamber is further cooled by pumping on the helium three bath. We have ensured that the heat leaks to the $helium^3$ bath are low so as a small quantity of liquid $helium^3$ would last for several hours.

In figure 2.1 is shown the He^3 bath (capacity 3.0 c.c.) made out of copper. A spiral of copper strip is soldered to the bottom of the container, so that heat transfer to the liquid He^3 is improved as these fins increase the area of contact. The He^3 pot at its base carries a specimen holder, which can be screwed on to the pot.

The bath is suspended on a thin walled, 8 mm. diameter german silver tube P , which is also used forpumping He^3.

A 3 mm. diameter german silver tube V was used for the vapour pressure line. This line ended in a separate bulb in the copper pot. A little helium three is condensed in the vapour pressure bulb. Hence the temperature we now measure, by means of vapour pressure, will not be that at the surface of the main He^3 bath but the vapour pressure in the thermometer bulb.

The He^3 bath is surrounded by a copper vacuum jacket and surrounding the vacuum jacket, H.V.J., is a liquid He^4 dewar. in which a temperature of $1.3^{\circ}K$ is maintained by a separate pumping unit. The copper vacuum jacket is suspended on a thick copper tube. Tubes P and V meet this copper tube about 13 cms. above the H.V.J. through a brass bush. Three cm. above this point, tube P is increased to 1 cm. diameter german silver tube for a length of 12 cms. and then to a diameter of 2.5 cms. for a length of 45 cms. till it reaches the top of the cryostat. The couplings used at the joints are designed to block the flow of radiation from higher temperatures. Tube V , the vapour pressure tube was joined to a 1/8 inch Yorkshire tubing outside the cryostat through a coupling (at room temperatures). The Yorkshire tubing led to manometers and macleod gauges and also to a side arm through which He^3 gas could be introduced. D is a 4 mm. german silver tube which is used

as a pumping line for the internal high vacuum jacket (H.V.J.). At about 26 cms. above where it meets the H.V.J., the diameter of tube D is increased to 8 mm. till the top of the cryostat. This tubing also carries the electrical leads down (15,42 s.w.g., constantan leads) from the top of the cryostat. These electrical leads are thermally anchored to the lower end of tube D inside the vacuum space, with G.E. 7031 varnish, at 1.3°K and finally anchored at the specimen holder which is at the temperature of the He^3 bath (see figure 2.1).

A cupro-nickel tube (4 mm. diameter) enters the cryostat from the top, spirals down around the other tubes and opens into tube P at the point where the diameter of tube P is increased from 1 cm. to 2.5 cms. This cupro-nickel tube serves the purpose of admitting He^3 gas into the cryostat.

Incoming He^3 is cooled on its way to the cryostat by cooled evaporated He^4, then by contact with the He^4 bath at 1.3°K. The He^3 condenses on the walls in contact with the He^4 bath. The liquid runs down into the pot (which is still at temperatures of 4.2°K). In this way the pot cools down by transferring heat through He^3 to He^4. Eventually the bath cools down sufficient to condense He^3. Now the valve is closed.

STORAGE AND HANDLING OF HELIUM THREE

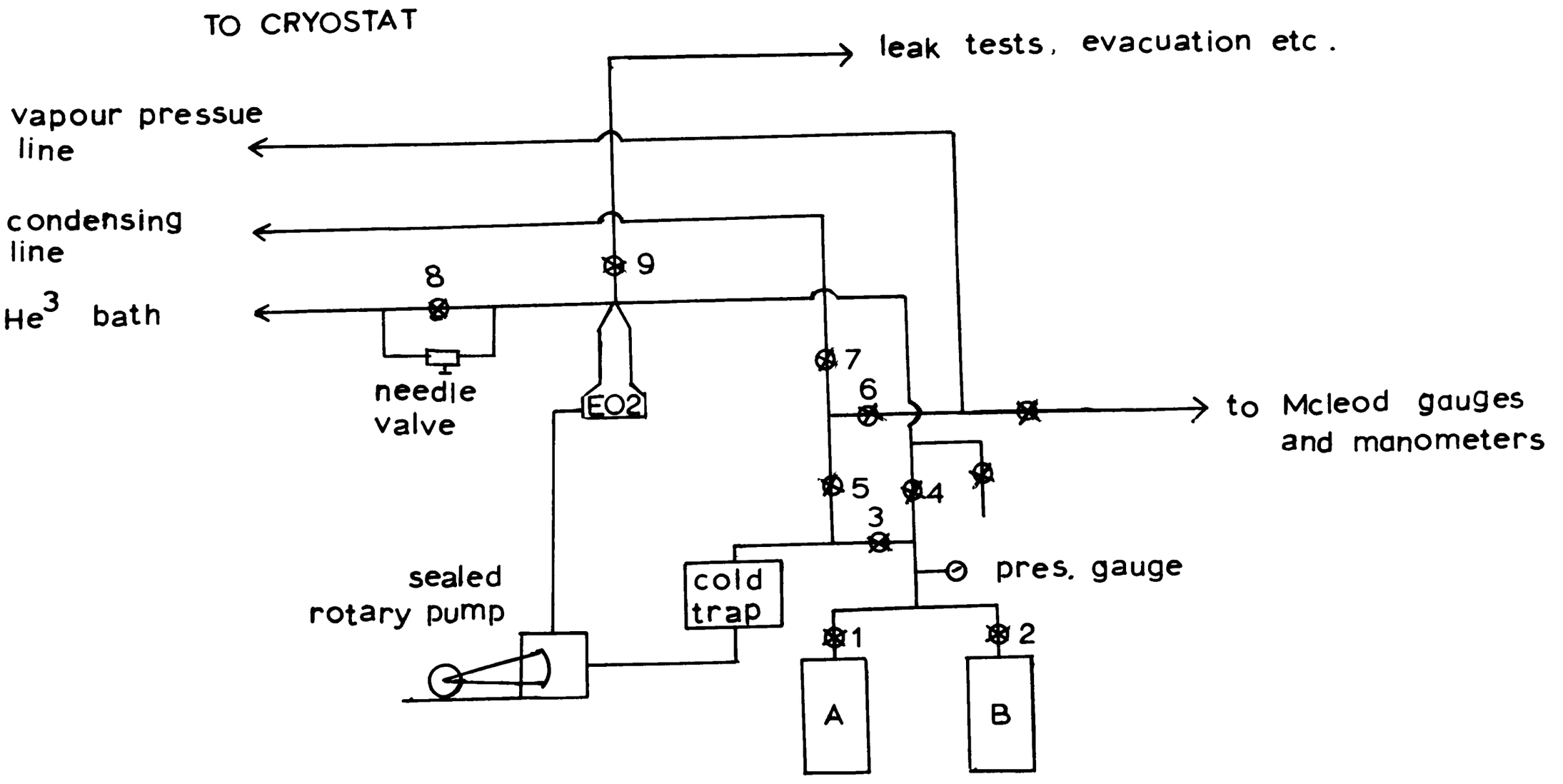


FIGURE 2.2

The pressure over the condensed He^3 in the cryostat can now be reduced with the diffusion pump E02 and the sealed rotary pump (ED 35), pumping He^3 into container A through carefully controlled Needle valve and valve 8. (fig. 2.2)

The heat leaks due to conduction down the tubes to the He^3 pot were less than 2×10^{-5} watts, and so, during a normal experiment most of the heat input to the helium three came from sources connected with the equipment.

(2) Storage and Handling of $Helium^3$

Figure 2.2 shows the distribution and storage assembly for the helium three of our cryostat. Three litres of He^3 gas at S.T.P. are stored in a brass container A of 6 litres capacity. B is also a similar container, but empty. Our system has a sealed rotary pump (ED 35) (speed 47 lit./min.) and an oil vapour diffusion pump (E02 speed 150 lit./sec.). The sealed rotary pump is a modified mechanical rotary pump to ensure that there is no leak where the rotating shaft enters the casing. The whole system including the pumps, the He^3 bath, manometers and the Mcleod gauges are evacuated through another diff. pump, backed by a rotary pump via valve 9. A very high vacuum (10^{-6} mm. Hg.) is produced in the system.

The whole assembly is thoroughly leak tested. Normally

all the valves are closed, container B is empty and the gas is stored in the metal container A. When the temperature of 1.3°K is reached in the outer He^4 bath the whole system is vacuum tested again via valve 9. The pumps are switched on and they pump the He^3 from A and admit it into the cryostat by way of the condensing line through valves 1,4,5 and 7 via the cold carbon trap. The pressure over the condensed He^3 in the cryostat can now be reduced with the diffusion and rotary pumps through the wide pumping tube and valve 8. The output of the rotary pump is fed via valve 3, with now valves 4 and 5 shut, into the vessel A.

At the end of the experiment all the He^3 must be pumped out of the cryostat. The system now contains most of the gas in container A and some in the pipework from the output of the rotary pump to the containers. We now shut valve 1 and open valve 2 (container B is empty). The volume of B is very much larger to that of the pipework and so most of the remaining He^3 in the pipework will be collected in B and very little left behind in the pipework and hence only extremely little He^3 would be lost.

(3) <u>The Helium^4 Bath</u>

Most helium^3 systems have a 4.2°K helium^4 bath and a pumped helium^4 bath at about 1.1°K to precool and condense the helium^3 gas. We had instead just one main bath kept

HELIUM^4 DEWAR

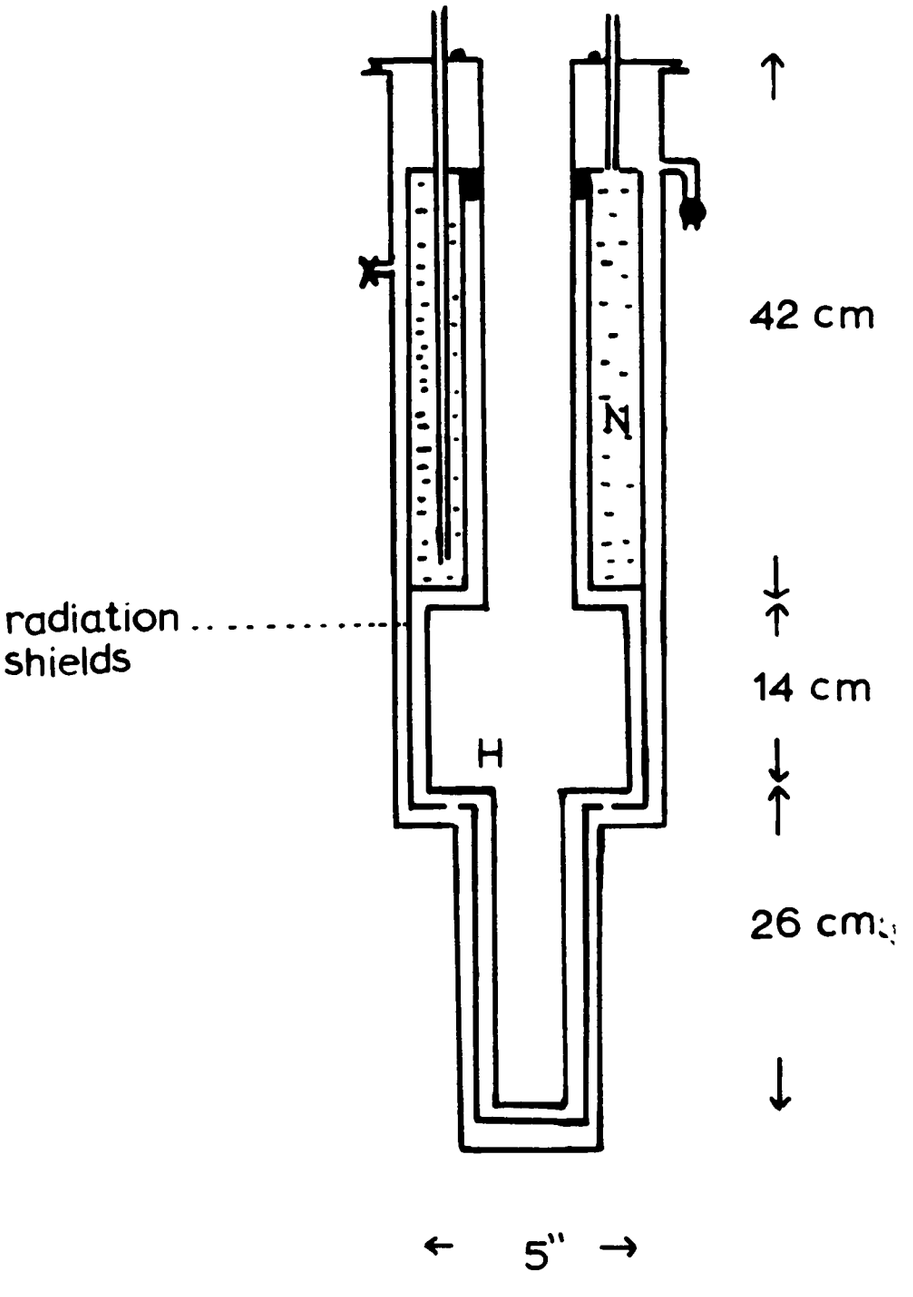


FIGURE 2.3

at 1.3°K and the helium^3 system being 'immersed' in it. This makes the design and construction very much simpler but exposing it to λ leaks, which was prevented by having well soldered joints, Moreover these joints had to be done only once except for the wood's metal joint of the H.V.J., which had to be done when we changed specimens etc.

The outer dewar which contained the liquid helium^4 is of metal (figure 2.3) ending in a tailpiece 26 cms. long. The helium^4 container has a silver plating on the outside and protected by radiation shields maintained at liquid nitrogen temperatures. The neck of the dewar (42 cms. long) was of stainless steel.

There were baffles at intervals of 6 cms. down the neck and the fins of the baffles about 2 mm. apart from the neck of the dewar so to ensure a good heat exchange with the cold outflowing gas and the heat conducted into the storage vessel[1].

The helium^4 bath was pumped down to temperatures of 1.3°K using a speedivac single stage rotary ISC 450 B (510 litres per minute) pump. At these temperatures the boil off rate was about 40 c.c. of liquid helium^4 an hour.

Section 2B:

THE EXPERIMENTAL ARRANGEMENT

The main experimental arrangement inside the H.V.J. can be classified as

1. the specimen holder
2. the heater and power supply
3. specimen mounting and contacts
4. the thermal anchor and leads
5. thermometers
6. the temperature regulator

We shall describe below the various aspects of our experimental arrangement in the helium^3 cryostat. Thermometry and temperature regulation will be described in more detail in a separate section as they play a very important part in accurate determination of thermal conductivity.

(1) The Specimen holder

The specimen holder consists of a copper disc 1 inch in diameter and 1 millimmeter thick, with a machined recess (1 m.m. thick with 2 m.m. internal diameter and 3 m.m. deep) for attaching the specimen. The holder could be attached to the sink by 3 8 BA screws. The thermal contact is further improved by applying a thin layer of vacuum grease between the two metallic contacts.

(2) Heat supplied $\dot{Q}$ and the power supply

The heater consists of a silk insulated 48 s.w.g. constantan wire of total resistance about 1000 ohms, non-inductively wound on a light brass rod about 1.6 cms. long and a mm. diameter with one end reduced so that it can be soldered directly on to the specimen contact. To the other end of this rod is screwed a fibre ring with two terminals on it for connection to the ends of the heater wire. Any heat flow into the sink through the connecting leads from the main body of the heater is virtually eliminated, by connecting insulated constantan leads of length 15 cms. from the terminals to the anchor. The windings are further insulated and glued in position to the specimen holder using GE7031 varnish.

The heat supplied to the specimen was measured through a standard potentiometric arrangement. The heater was in series with a standard resistor (1000 ohms), a small current was passed through the circuit and the voltage across the heater and 1 K ohm standard resistor measured separately with a Tinsley potentiometer (Type 3387B). The heater current was obtained from a variable direct power supply, which was specially designed and built with a current stabilization ratio of 2000, at a load of 1K (the resistance of the heater).

(3) Specimen Mounting and Contacts

The rare earth metals do not take solder on to them directly, hence at two ends of the specimen, two close turns of 0.25 mm. diameter platinium wire are spot-welded on to the metal. One end of the specimen could now be placed tightly inside the recess in the specimen holder and Wood's metal soldered. The heater is soldered to the platinium contact at the other end of the specimen.

The thermal contacts to measure the temperature gradient were made as follows. A turn of platinium wire are spot welded at two convenient points along the specimen. Two carbon thermometers were attached to these points by means of soldering the platinium wire end to the ends of the copper wire, which were wrapped around the thermometers (we have described this in more detail in a later section).

(4) Thermal Anchor and Leads

The leads are made of constantan (42 s.w.g.) and they come down into the chamber along the H.V.J. pumping line. These leads are first anchored at the lower end of the pumping line on a projection of a copper bush with G.E.7031 varnish at the temperature of the pumped helium^4 bath (1.3°K). They are then anchored on a copper rod on the specimen holder (figure 2.1), which is at the temperature of the helium^3 bath.

Section 2C:

THERMOMETRY

Introduction

The measurements of temperature below 1°K are a problem, and primary standards cannot be used. The most important characteristics for secondary thermometers are sensitivity, reproducibility and convenience. In the region below 20°K mettalic resistance thermometers and thermocouples become quite insensitive and resistance thermometers made of semiconductors and of carbon become the most useful secondary thermometers. They can be extremely sensitive and are very convenient to use. Reproducible temperature determinations can be made in the low temperature range by measuring the susceptibilities of magnetic salts (primarily below 1°K), the equilibrium vapour pressure of helium^3 or helium^4 or the pressure of helium gas in a constant volume. The apparatus for all three kinds of measurement is bulky and, particularly for accurate pressure measurements, the procedure is clumsy and tedious. The available precision is, however, considerable.

(1) Carbon Resistor Thermometers

After the pioneering work of Clement and Quinnell,

commercial carbon composition resistors came into general use as low temperature thermometers. Their desirable properties are well known and include high sensitivity, low heat capacity, low sensitivity to magnetic fields and low cost.

The accuracy of low temperature thermal conductivity measurements depends on the accurate measurement of small differences of temperature. The temperature gradient along the specimen was measured using two Allen Bradley 10 ohms, one-tenth watt, carbon resistors and 470 ohms $\frac{1}{2}$ watt, carbon resistors on different runs. The resistance of the two thermometers used in our experiments varied from 500 ohms at 1.1^{o}K to 50,000 ohms at 0.35^{o}K (Allen Bradley) and in the case of Speers it was 1200 ohms at 1^{o}K and 10,000 ohms at 0.3^{o}K.

The thermometers were prepared in the usual way. The resistors were cleaned of paint, wrapped around with bare copper wire and were covered in araldite and baked. One end of the copper wire was used to attach the thermometer to the platinium contact, spot welded on the specimen.

The method of measuring the resistances of the thermometers was quite standard[1]. With the use of carbon resistors, the main problem is in having a well defined calibration for the thermometers, since no exact

EXPERIMENTAL ARRANGEMENT FOR THE MEASUREMENT OF THERMAL CONDUCTIVITY

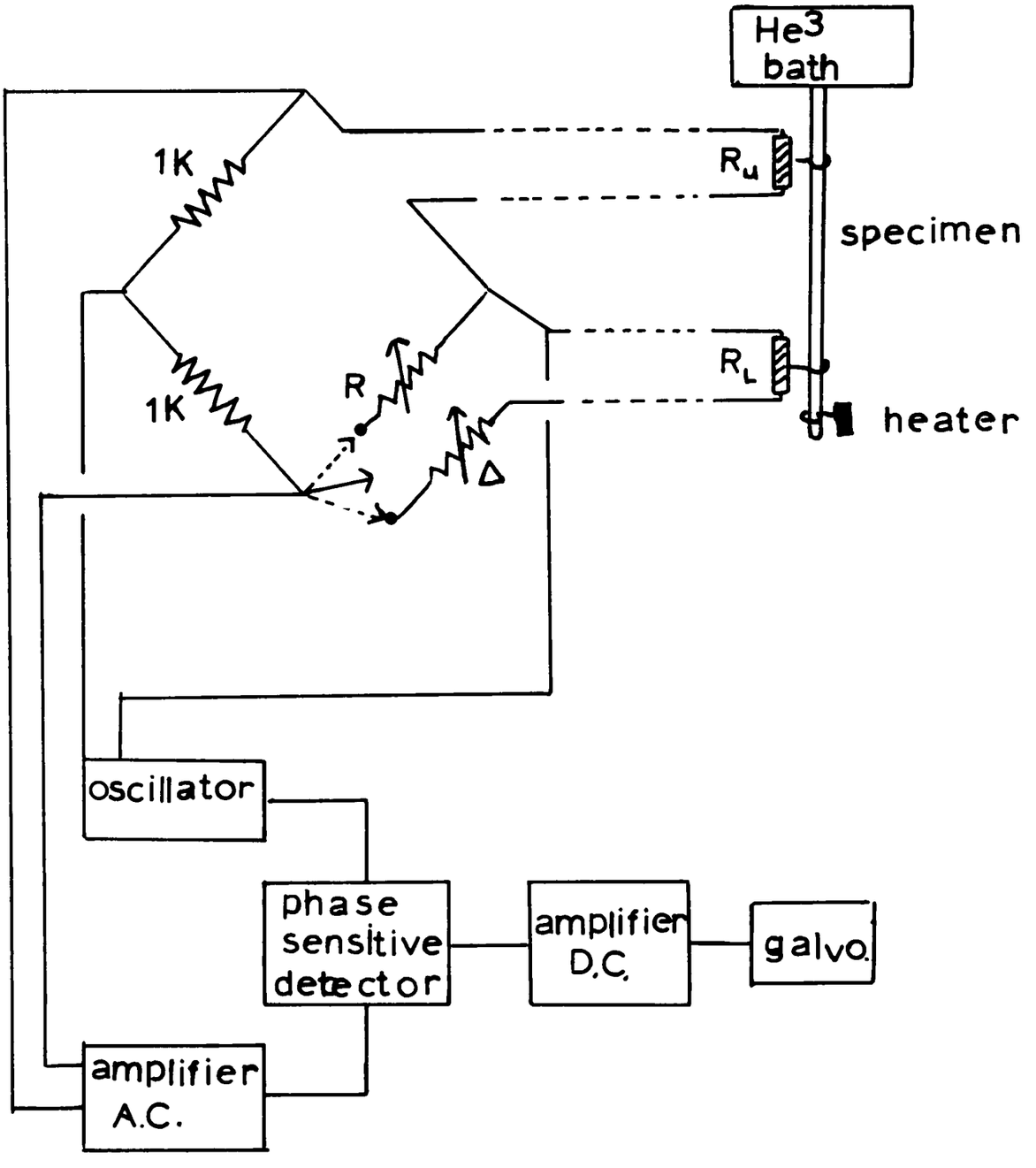


FIGURE 2.4

equation for R (resistance) as a function of T (temperature) are available. This problem is eased by choosing very closely matched thermometers but as such 'matched' pairs are difficult and time consuming to find, and frequently the match deteriorates with successive thermal cycling, our method is accurate and does not put any restrictions on the choice of thermometers.

The resistance of the carbon resistors was measured using a carefully shielded A.C. Wheatstone Bridge, whose circuit is shown in figure 2.4. This bridge does not measure the D.C. resistance, but provided a suitable variable to calibrate against the absolute temperature. The decade boxes gave a resistance up to 11,000 ohms, so that at lower temperatures it was necessary to operate the bridge using an arm ratio of 10: 1. The bridge is arranged so that the resistance of one thermometer and the difference between thermometers can be measured simultaneously be balancing against two separate decade resistance boxes R and Δ . Small drifts in the mean temperature are by this means rendered much less important. The inclusion of a dummy lead enabled the lead resistance to be determined and allowed for. The sensitivity of the arrangement is of the order 0.2 ohms at 1.1^{o}K and 5 ohms at 0.6^{o}K, which corresponds to errors of 0.1 and 0.06 milledegrees respectively.

The power dissipated in the thermometers was in the region of 10^{-9} watts, which was far less than that in measuring the conductivity of any of our specimens.

The carbon resistance thermometers were calibrated against the absolute temperature obtained from the vapour pressure of the helium three (see section 2C-2). To obtain a particular calibration point, the pumping speed was carefully adjusted by means of the needle valve to obtain the approximate temperature required and the electronic regulator was switched on. About 30 calibration points in the range 1.4^{o} - 0.4^{o}K were normally taken. The thermometers are fitted to a formula

$$\frac{1}{T^*} = a_0 + a_1(\ln R) + \cdots + a_n(\ln R)^n \qquad (2.1)$$

with three arbitrary constants $a_n (n=2)$. The use of a computer fit enabled a high-accuracy calibration to be drawn. The procedure was as follows; first the constants (a_n) are determined for each thermometers by a least squares fit. Formula (2.1) is used to calculate empirical temperatures T_A^* and T_B^* corresponding to the resistance of the upper and lower thermometers at each calibration point. The deviations

$$\varepsilon_A = T_A^* - T_A \quad \text{and} \quad \varepsilon_B = T_B^* - T_B$$

which are very small (less than 1.5 mdeg.) are printed out. Second, for each pair (j) of resistance values corresponding

to a measurement of thermal conductivity, the computer determines the corresponding empirical temperatures $T_A^*(j)$ and $T_B^*(j)$ and calculates the empirical thermal conductivities $K^*(j)$

$$K^*(j) = \text{constant} \times \frac{1}{T_B^*(j) - T_A^*(j)} \qquad (2.2)$$

The empirical thermal conductivites show systematic errors of about 1% due to the disparity between the empirical and the true temperatures. These errors may be eliminated to a large extent by making a small correction to K^* with the help of the relations between T^* and T for each thermometer.(1)

(2) Vapour Pressure Thermometry

As the carbon thermometers were used to determine ΔT in our measurement and were to be calibrated against the cryostat temperature, considerable care was taken in designing the vapour pressure thermometry. Cryogenic liquids have vapour pressures that vary rapidly with temperature and this forms a convenient secondary thermometer. As their vapour pressures have been measured and tabulated as a function of absolute thermodynamic temperature, they form a sufficiently reliable series of primary scales of temperature for many low temperature experiments.

The vapour pressure of helium^3 is quite small at and below 1°K to be measured accurately by mercury and oil

manometers (He^3 is absorbed by the oil - Apiezon A[3]). The vapour pressure at 1°K is about 8.6 mm. Hg.; at 0.7°K it is 1.3 mm. Hg.; 0.55°K it is 0.28 mm.Hg. and by 0.3°K it falls down to 1.9 microns. We used Mcleod gauges for the measurement of pressure. We have designed two Mcleod gauges, one to measure the pressure below 1.4°K and the other below 0.8°K and this meant we were able to measure from 14 mm. Hg. to 10^{-3} mm.Hg. quite accurately.

Two methods are commonly employed for obtaining the temperature at the same point beneath the surface of a liquid helium bath by vapour pressure measurements: measuring the vapour pressure at the surface of the bath and correcting this pressure with the hydrostatic pressure of the column liquid to the point in question below the surface; or measuring the vapour pressure of helium condensed into vapour pressure thermometer bulbs at the point in question. In our system we determined the vapour pressure of helium^3 condensed into a vapour pressure thermometer bulb in the copper pot via a 'static' 3 mm. german silver tube (see diagram 2.1).

The first method suffers from the disadvantage that the temperature within a liquid is not necessarily the same as that at its surface and this temperature inhomgenities may make the recorded vapour pressure a

poor indication of the true temperature within the liquid. This is taken care of, if the bath is stirred all the time (by heater)[4]. In any case the correction is negligible if the surface area of the helium evaporator (copper container) is quite comparable to the depth of the liquid.

(3) Thermomolecular Pressure Correction

There is a difference in temperature at the two ends of the pressure sensing tube, as one end is at room temperature and the other at temperatures of $1^{o}K$ and below. This temperature gradient along the length of the tube gives rise to a thermal creep (tagential stream) in the gas. The pressure measured on the Mcleod gauges at room temperature will be greater than the pressure over the cold liquid. This difference in pressure at the two ends of the tube becomes all the more important if the pressures to be measured are lower and if the mean free path of the gas molecules become comparable to the diameter of the tubes. This thermomolecular pressure effect becomes significant below $1^{o}K$.

Roberts and Sydoriak (1956)[5] give a table to make corrections for this effect using the Weber - Schmidt formula. They have tabulated values of $\frac{Pc}{Pw}$ against radius of pressure sensing tube x pressure at warm end (R.Pw). They have measured the thermomolecular pressure ratio

of both He^3 and He^4. In our case the correction was negligible at 1°K but at 0.55°K the correction in pressure was about 10% and at about 0.4°K the correction was nearly as high as the measured pressure. To make corrections for this effect we drew graphs on semi-log papers to find Pc/Pw for (R.Pw) in the range 0-1°K.

Watkins et al (1967)[6] have made measurements that show that the correction using the Weber-Schmidt formula is not great enough and from their results they estimate an error of few millidegrees in the range $0.3 < T < 0.7$°K can be expected. We could also encounter slight error in the inaccuracy of the determination of the radius of the sensing tubes.

After the correction applied by us, the absolute temperature was obtained from the 1962 He^3 Scale of Temperature of Robert, Sherman and Sydoriak[2].

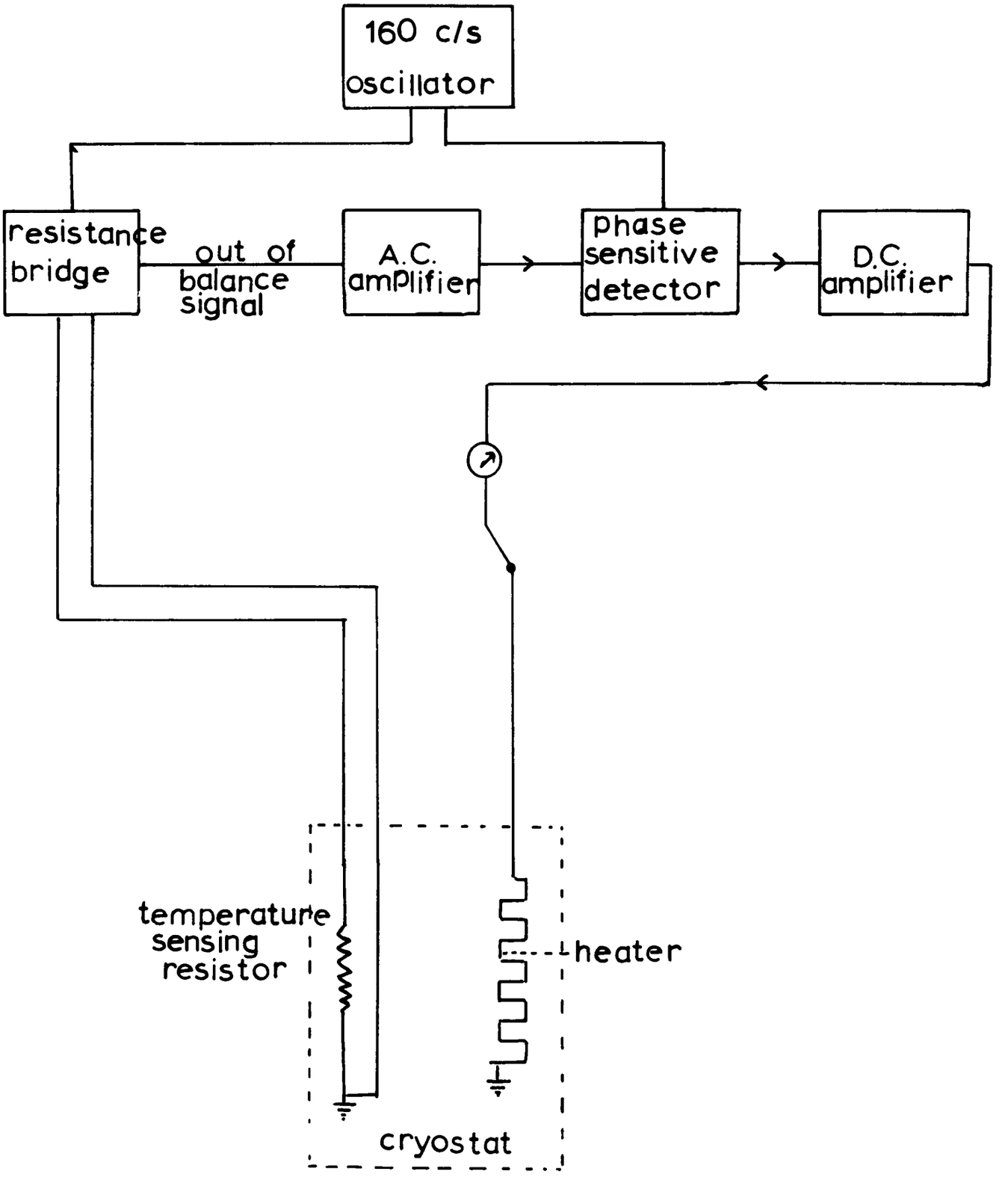
(4) Purity of He^3

The purity of the stored helium three gas as quoted by the manufacturers was 99.2%, the only impurity being 0.8% of He^4. The presence of a small amount of He^4 in liquid He^3 thermometers lowers the vapour pressure below that of pure He^3.

Robert, Sherman and Sydoriak (1964[7] have calculated the correction to a temperature measurement made with He^3, the sample containing 0.1% of He^4 in the liquid phase.

The correction for their He^3 sample according to them, would range from 0.02 millidegrees at 0.4°K to 0.71 millidegrees at 3.2°K. They have given their correction in the form of a plot in which $T_{62} - T_u$ is plotted against temperature for varying concentrations of He^4 in He^3 ranging from 0.01% to 0.1%. The correction was calculated from a smoothed curve obtained from the data of Sydoriak and Roberts (1960)(8) and Esel'son and Berezniak (1956)(9) for 90 per cent He^3 solutions. The liquid phase diagram of the above workers indicates that $\left(\frac{dP_x}{dx}\right)_T$ is probably constant for $x \geqslant 0.9$, where Px is the observed vapour pressure for mole fraction of x of He^3 and so according to the workers(7) the same curve can be used for ten times the indicated percent of He^4 in the liquid. So, the correction in our case, due to the effect of 0.8% He^4 being present in He^3, would be 0.2 millidegrees at 0.4°K and 2.8 millidegrees at 1.4°K. The correction curve as we see it is linear and it may be able to affect the absolute value of the measured temperatures. However, for thermal conductivity measurements it is ΔT (the temperature difference between the two thermometers) which is important. The value of ΔT in our case varies from 40 to 100 millidegrees. An error of maximum value, 0.2 millidegree, is estimated when ΔT is 100 millidegrees and this would not show in our measurements on the thermal conductivity.

FIGURE 2.5



TEMPERATURE REGULATOR

(5) The Temperature Regulator

An electronic regulator, which was similar to that of Brown and Boyle (1954)[10], was used to control the temperature of the helium^3 bath. A carbon resistance in thermal contact with the helium^3 bath was the temperature sensor and this resistance is incorporated as one arm of an A.C. Wheatstone bridge. At the temperature which is required, the bridge is arranged to be balanced but any change in the temperature then unbalances the bridge and the off balance voltage is amplified and then rectified by the phase sensitive detector so that the output is positive for an increase in thermal resistance or decrease in temperature and negative for the reverse situation. This rectified output is added to a constant D.C. bias and applied to a heater in the bath. In this way an increase in bath temperature is counterbalanced by a decrease in power dissipated in the heater. The temperature of the helium^3 bath was kept constant at the time of calibration of carbon resistors (attached to the specimen) to better than 10^{-4} degrees. The block circuit diagram is shown in figure 2.5.

Section 2D:

EXPERIMENTAL PROCEDURE

(1) Pre-cooling. The pre-cooling procedure was as follows:

(1) The H.V.J. and the He^3 system were pumped out in order to test for leaks after the cryostat had been dismantled to mount a specimen.

(2) The H.V.J. was filled with helium^4 exchange gas at a pressure of about few mm. of Hg.

(3) After the 'liquid helium^4 space' was filled with exchange gas (He^4) liquid nitrogen was introduced into the nitrogen jackets of the outer dewar. Liquid nitrogen was then siphoned into the 'helium^4 space'.

(4) When the cryostat had cooled down to nitrogen temperatures, we got rid of the remaining liquid nitrogen in the 'helium^4 space'. This was done by siphoning out most of the nitrogen and boiling off the remainder by a heater, which was wound around a Spears carbon resistor, which lay at the bottom of the dewar. When the temperature of the carbon resistor suddenly increased, we knew that all the liquid nitrogen in the 'space' had boiled off.

(5) Two and a half litres of liquid helium^4 was then transferred into the dewar by the usual method. To cool the cryostat to helium temperatures from nitrogen temperatures, we used about 300 c.c. of liquid helium^4.

(6) After the necessary amount of helium^4 had been collected in the dewar we pumped out the exchange gas in the H.V.J. Now the helium^4 bath was pumped by a rotary pump I.S.C. 450B to a temperature of 1.3^{o}K.

(7) When this minimum temperature of the helium^4 bath was attained by our pumps, we checked the He^3 systems again for leaks after which we admitted He^3 into the cryostat and proceeded with our experiments. The He^3 thus condensed would last for about 6 to 7 hours. After this it had to be recondensed. A useful running time of 15 hours could be obtained with one transfer of liquid helium^4.

(2) Electrical Resistivity Measurements

The electrical resistance was determined by adopting the four probe method. The current carrying leads were copper wire and were soldered, one at the contact at the base of the specimen at which the specimen heater is soldered and the other at the contact, which is used to attach the specimen to the specimen holder. The potential across two points was also measured by means another two copper wires, which were soldered at the same contacts used for temperature gradient measurements in determining thermal conductivity. This avoided any error to the form-factor in the calculation of the Lorentz number. We made observations with the

electric current flowing successively in opposite directions.

The measurement was by a null method and the system comprised a Tinsely type 5214 photo-cell galvanometer amplifier and a sensitive galvanometer (type 4500 E.M.S.2). The balancing voltage is obtained from Tinsely potentiometer type 3387B to an accuracy of about 1 to 2%.

Section2E:

(1) Errors

The thermal conductivity is calculated from the relation

$$K = \frac{\dot{Q} \times f}{\Delta T}$$

where ΔT is the temperature gradient, $\dot{Q}$ the heat input and f the form factor.

(a) The major source of error which affects K is due to the measurement of the form factor. In our case it was known with an accuracy of the order of 2% but this would vary from sample to sample and this error would affect all experimental points in the same proportion.

(b) Another source of error is from the estimation of $\dot{Q}$, the percentage of the total heat generated that travels along the specimen and other heat losses. The thermal conductivity of rare earths is small compared to non rare earth metals and this makes small heat losses important.

In the helium^4 range of temperature, the heater power for the rare earth metals was usually between 1×10^{-5} 4×10^{-5} watts while at temperatures below $1^{\circ}K$ the minimum heat input was of the order of 1×10^{-6} watts. The maximum heat generated in the carbon thermometers was $\sim 10^{-9}$ watts, very small when compared to the calculated $\dot{Q}$.

It has been shown that half the heat generated in the heater leads can be considered to flow to the heater, and

we have taken this into account by adding half the resistance of the leads to the resistance of the heater. We find this correction slightly less than 1% of the heater resistance. The heater resistance was measured to be a constant throughout the temperature range.

Heat flow through the leads was calculated to be 0.4% of the main power of the heater and heat losses by radiation were extremely small.

(c) The accuracy of ΔT depends on the accuracy with which the absolute temperature can be determined and also on the accuracy to which the temperature can be derived from the secondary thermometers. Temperature differences ranging from 40 millidegrees to 120 millidegrees were measured. The resistance could be measured accurate to $10^{-4}{}^{o}K$. In the calibration curve, the deviations were less than 1.5 millidegree (Section 2C - 2). Errors in the actual temperature were small and since our carbon thermometers had similar characteristics, the errors almost cancelled in the difference ΔT.

(d) The use of a finite temperature gradient along the sample introduces a systematic error. Calculations show that the experimental value K_E can be corrected according to the relation

$$K = K_E - \frac{1}{24} \frac{d^2 K_\epsilon}{dT^2} (\Delta T)^2$$

For the rare earth metals we have studied, K_E is almost linear with a small T^2 term noticeable in the higher temperature region of our range of study and the correction can be neglected.

Performance of the He^3 cryostat

Before measuring the thermal conductivity of the rare earths below 1.3°K in the newly constructed He^3 apparatus, we did measurements on two niobium samples in the superconducting (pure and mixed) state. These experiments were done mainly to acquaint the author with the performance and reliability of the apparatus. The results obtained were in qualitative agreement with the earlier measurements. We present the results of our measurement in Appendix A.

References to Chapter Two

1. Soursa, J.B. (1968) D. Phil. Thesis, Oxford University.

2. Roberts, T.R., Sherman, R.H., and Sydoriak, S.G. (1964). J.Resch, NBSA, (Phys. & Chem.) 68A, 579.

3. Davey, G. (1965) D.Phil. Thesis Oxford University.

4. Corak et al (1955) Phys. Rev. 98, 1699.

5. Roberts, T.R., and Sydoriak, S.G. (1956) Phys. Rev. 102, 304.

6. Watkins et al (1967) J. Chem. and Phys. 46, 1007.

7. Roberts, T.R., Sherman, R.H., and Sydoriak, S.G. (1964) J.Resch.NBSA (Phys. and Chem). 68A, 567.

8. Sydoriak, S.G., and Roberts, T.R. (1960) Phys. Rev. 118, 901.

9. Esel'son and Berezniak (1956) Soviet Phys., JETP, 3,568.

10. Brown,J.B., and Boyle, W.S. (1954) Rev. Sci. Instrum. 25, 359.

CHAPTER THREE

RESULTS AND DISCUSSIONS

Introduction

The transport properties of the heavy rare earth elements exhibit many interesting features because of the various magnetic structures found in these elements. The little data available on the thermal conductivity of the heavy rare earths cover mostly the high temperature range, especially around the magnetic transition temperatures. The Lorenz number calculated from their measurements at the lower end of their temperature range (around $5^{o}K$) give an anomalously high number (they vary from 3 to 12 x 10^{-8} watts - ohms- $^{o}K^{-2}$ - theoretical value 2.45 x 10^{-8}) and they assume that phonons and/or magnons contribute significantly to the heat conduction in addition to the usual electronic conduction.

The present work is a systematic thermal conductivity study of the heavy rare earths in the temperature range 0.4 to $4.2^{o}K$ covered by two different cryostats - a He^{3} and a He^{4} cryostat. The measurement and techniques used have been very accurate and the study was undertaken, that at sufficiently low temperatures a predominantly electronic thermal conductivity obeying Wiedemann-Franz law would emerge and if possible to separate the various carriers of heat.

The results that have been obtained by us show no anomaly and are very consistent. The measured thermal conductivity can be separated quite accurately into a linear and a quadratic term in temperature. The linear term, when related to the residual electrical resistivity, give Lorenz numbers, which are remarkably close to the theoretical value.

In this chapter, we shall first of all describe the experimental results of the specimens we have measured - gadolinium (2 samples), dysprosium (2 samples), holmium (2 samples), erbium (2 samples) terbium (1 sample) and a specimen of ytterbium. The results of each element are given in a separate section and comparison is made with other experimental results of the elements.

A detail analysis of the results is attempted in a later section. As we were able to separate the thermal conductivity into components of different temperature variation, we have, in the absence of a theory applicable to the rare earth metals, given explanations for the various temperature terms, remembering that we have to take into consideration the magnetic energy for these metals. Finally with the help of electrical resistivity data, and ideas already recognised on the thermal conductivity of ordinary metals, possible general conclusions on the rare earth ferromagnets are given.

Section 3A:

SPECIMENS

The specimens were used as they were received from the various sources. In Tables 3.1 and 3.2 we give the various information that was available to us about the specimens.

Table 3.1

Specimen	Physical State	Form Factor $f^* = l/a$	Diameter
1. Gadolinium (1)	polycrystalline wire	302.5	1.248 mm.
2. Gadolinium (2)	Polycrystal thin slab	52.9	1.57 x 2.95 mm. (cross-section)
3. Dysprosium (1)	Bi-crystal rod	44.3	4.89 mm.
4. Dysprosium (2)	Polycrystalline wire	200.8	1.50 mm.
5. Holmium (1)	Polycrystalline wire	282.3	1.37 mm.
6. Holmium (2)	Single crystal rod	31.1	3.04 mm.
7. Erbium (1)	Polycrystal thin slab	26.4	2.75 x 3.98 mm (cross-section)
8. Erbium (2)	Polycrystalline wire	235.3	1.51 mm.
9. Ytterbium (1)	Polycrystalline wire	245.0	1.50 mm.
10. Terbium (1)	Polycrystalline wire	157.1	1.48 mm.

$$f^* = \frac{l}{a} = \frac{\text{length of the specimen between two thermometers}}{\text{cross-sectional area}}$$

Table 3.2

Specimens	Source	Quoted Impurities
1. Gadolinium (1)	Johnson Matthey & Co.Ltd.,	other rare earth metals 0.1% tantalum content 0.1% other base metals 0.02%
2. Gadolinium (2)	Mr. J. Rolf	Unknown
3. Dysprosium (1)	Dr. D.M.S.Bagguley	Unknown
4. Dysprosium (2)	Johnson Matthey & Co.Ltd.,	other rare earth metals 0.1% other base metals 0.02% tantalum not detectable by spec. methods
5. Holmium (1)	Johnson Matthey & Co.Ltd.,	dysprosium approx. 800 ppm. thulium " 200 ppm. silicon 5 ppm. iron 3 ppm. magnesium less than 1 ppm.
6. Holmium (2)	Dr. D.M.S.Bagguley	unknown
7. Erbium (1)	Mr. J. Rolf	unknown
8. Erbium (2)	Johnson Matthey & Co.Ltd.,	other rare earth metals 0.1% other base metals 0.02% tantalum content not detectable by spec. methods
9. Ytterbium (1)	Johnson Matthey & Co.Ltd.	other rare earth metals 0.1% other base metals 0.02% tantalum content not detectable
10. Terbium (1)	Johnson Matthey & Co.Ltd.	other rare earth metals 0.1% other base metals 0.02%

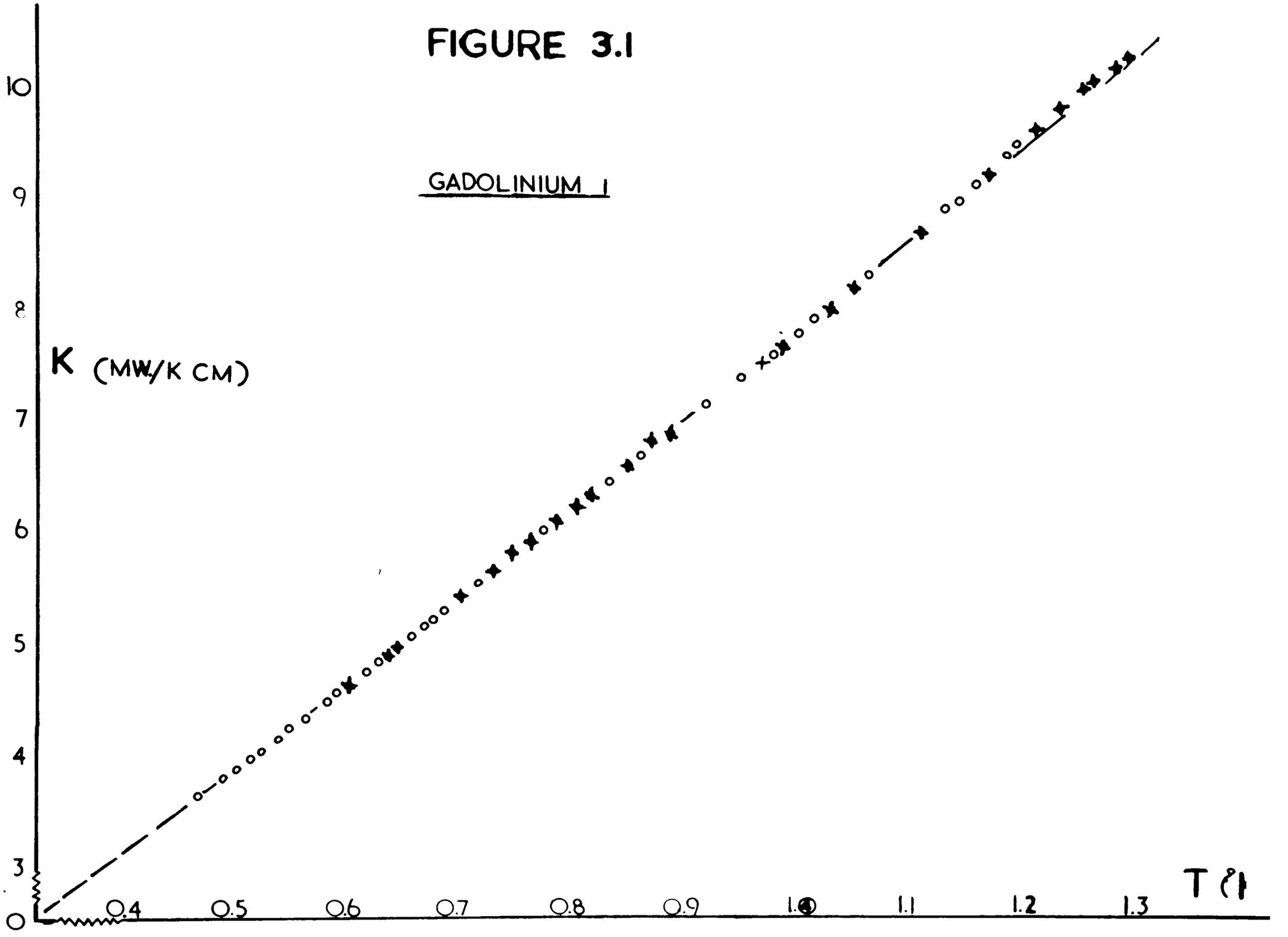
Section 3B:

GADOLINIUM

The thermal conductivity of gadolinium has been measured in recent years by several investigators. Arjas and Colvin (1964)[1] and Aliev et al (1965)[2] have measured over the ranges 5 - 300°K and 2 - 100°K respectively. At low temperatures ($T \ll \Theta_{Debye}$) the thermal conductivity (K) was found to decrease linearly with T and this was attributed to the usual predominance of the electronic component, limited by impurity scattering. The ratio between K/T and the electrical conductivity is then expected to be a universal constant $L = 2.45 \times 10^{-8}$ watts- ohms-$^{o}K^{-2}$ (Lorenz number)[3]. However, the experimental values for L were anomalously high (7×10^{-8} watts-ohms $^{o}K^{-2}$) and these authors concluded that other mechanisms of heat conduction must also be present.

As these authors and others[4][5] were primarily concerned with a wide range of temperature (and high temperature anomalies - especially at transition temperatures and high temperature anistropy), and because the Wiedemann-Franz law (L) is only strictly valid at very low (or very high) temperatures[3], it is desirable to investigate in detail the thermal conductivity at very low temperatures.

FIGURE 3.1



Rao et al [6] measured recently the thermal conductivity (K) between 1 and 4°K and found a very anomalous behaviour. Their results did not extrapolate to the origin and the thermal conductivity K, rises anomalously fast with T near 4°K, where the Lorenz number largely exceeds the theoretical value. This again, was attributed to additional contribution besides electrons. These discrepancies and the hope that at sufficiently low temperatures a predominantly electronic thermal conductivity obeying Wiedemann-Franz law would emerge were good reasons for a detailed investigation down to a lower limit of temperature.

The results presented here were obtained on two different polycrystal samples (see Tables 3.1 and 3.2 for details of specimen) and over the whole range of temperature, 0.4 to 4.2°K covered by a He^3 and a He^4 cryostat. (Sample gadolinium 1 was the same one used by Rao et al[6]).

Figures 3.1 and 3.2 show the temperature dependence of the thermal conductivity, K versus T, measured from 0.4 to 1.4°K in the He^3 cryostat of gadolinium 1 and gadolinium 2 respectively. The results are of several different runs. Long waiting periods ($\sim$ 5 minutes) were adopted before each thermal conductivity measurement, so that thermal equilibrium was fully ensured. The scatter is less than 1%. In the figures we have used different symbols to denote the results from different runs.

FIGURE 3.2

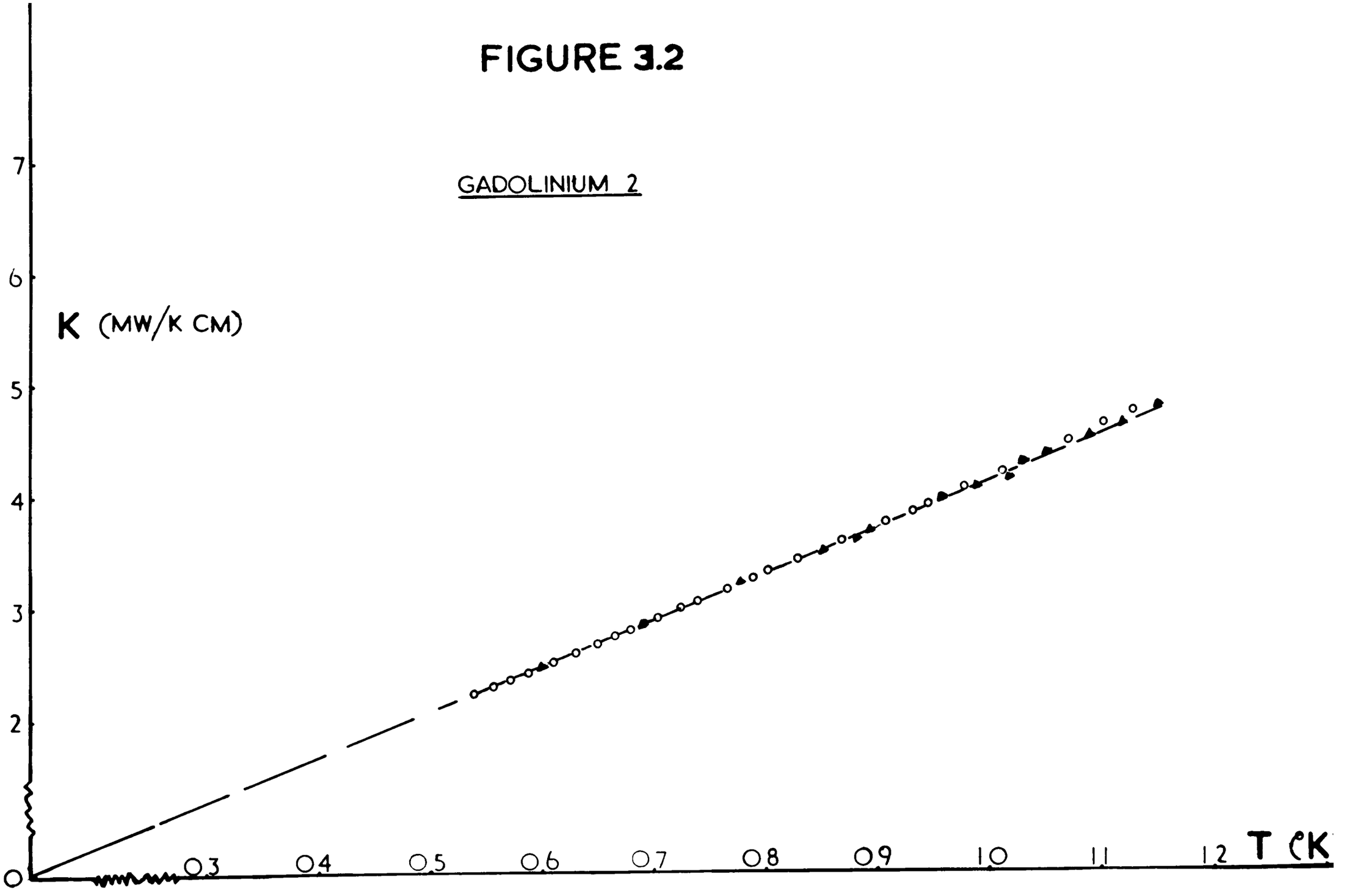


Figure 3.3 shows K versus T of both samples measured from 0.4 to 4.2°K in both the cryostats. (Here results from different cryostats are marked differently). There is very good agreement between the results from the two different cryostats. Our results can be accurately described by an expression of the form

$$K = aT + bT^2$$

as shown by a plot of K/T versus T (figure 3.4). Expressing K in milliwatts /°K cm., we can give for our two specimens

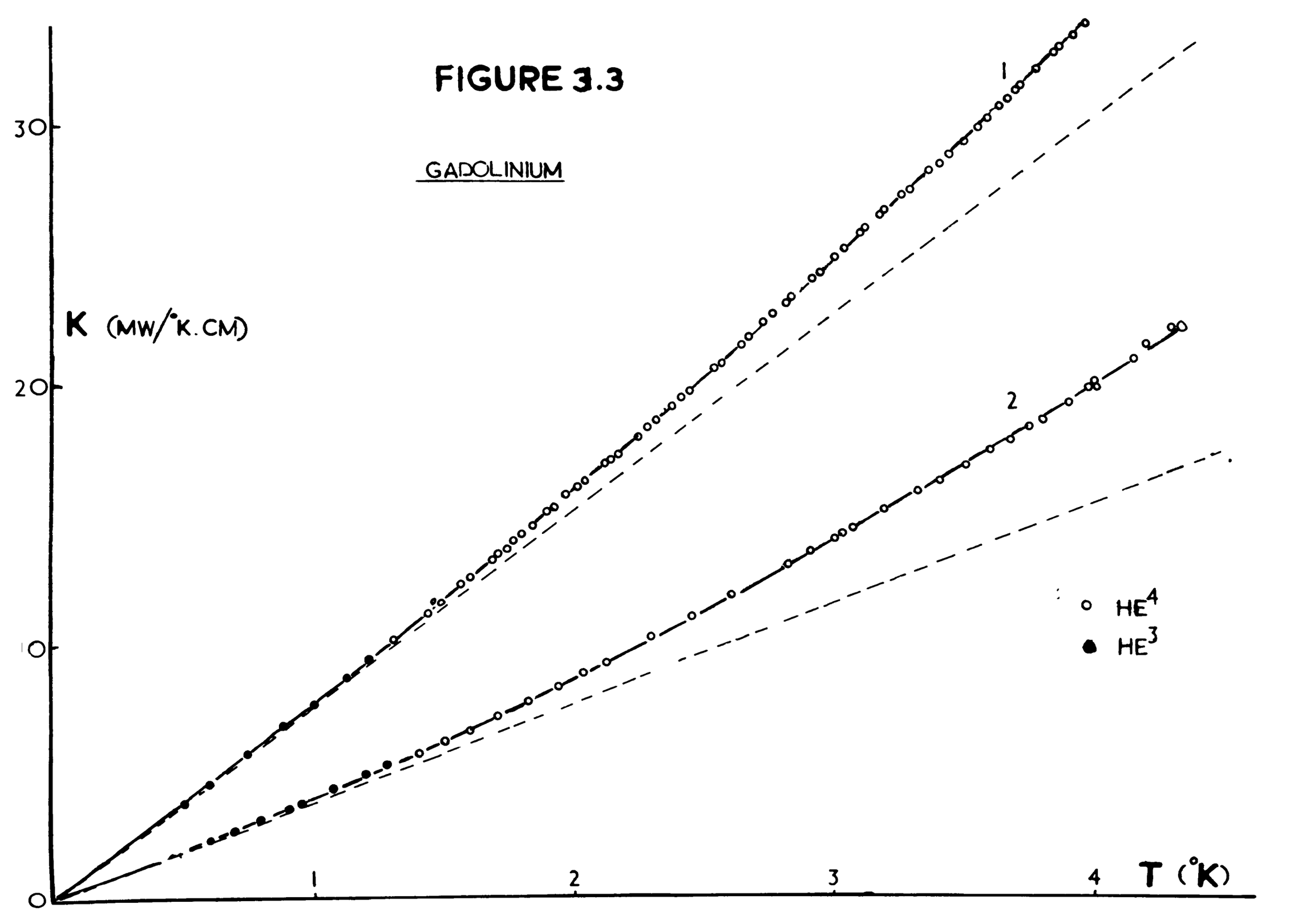
$$K = 7.51T + 0.257\ T^2 \quad \text{(gadolinium 1)}$$

$$K = 3.75T + 0.307\ T^2 \quad \text{(gadolinium 2)}$$

In order to investigate the origin of the linear term contribution (possibly electronic), we measured the electrical resistivity at 4.2°K. For one of the specimens, gadolinium 2, we also measured the electrical resistivity at different temperatures from 4.2°K to 2.5°K and found the values to be constant (figure 3.5). (Measurement of electrical resistivity of gadolinium by other investigators [4][7] show that their specimens are at their residual values in our range of temperature. The residual resistivity of their specimens were very similar to ours).

If the measured electrical resistivity are related to the linear term of the thermal conductivity (aT) using Wiedemann-Franz law, we obtain Lorenz numbers, which are remarkably close to the theoretical value (2.45×10^{-8} watts- ohms- K^{-2}).

FIGURE 3.3



We have tabulated the results below

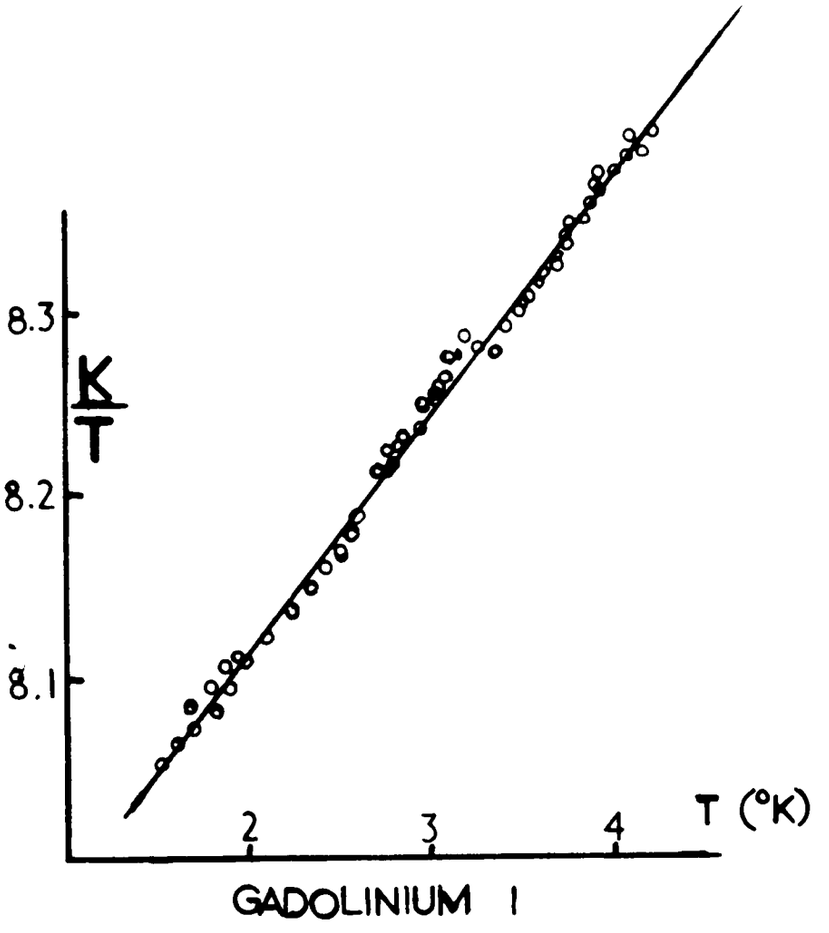
	ρ_0 $\mu\Omega$ cm.	ρ_{295}/ρ_0	a mw/K²cm.	b mw/K³cm.	L×10⁸ wΩ/K²
gadolinium 1	3.37	44.3	7.51	0.257	2.53
gadolinium 2	6.44	22.3	3.75	0.302	2.47

We therefore can say that the linear term represents an electronic contribution, with the electron mean free path limited by 'impurity' scattering. (We have used the word 'impurity' scattering to denote scattering by all static defects. These defects include chemical impurities, vacancies dislocations etc.) Using the kinetic theory formulation, we can estimate an order of magnitude of this mean free path ($K = \frac{1}{3}C_E v l$). Using C_E = 10.5T milli joules/mole (the electronic contribution to specific heat[8]) and v as the Fermi velocity we find the mean free path l is of the orderof 10^{-7} cm.

The magnitude of the quadratic contribution (bT^2) for both the specimens is quite similar, though in gadolinium 1 (the purer of the two) the linear turn is twice the value of the corresponding term for gadolinium 2. At 4^oK the quadratic term for gadolinium 1 is about 12% of the total conductivity while at 1^oK it is about 3.3%.

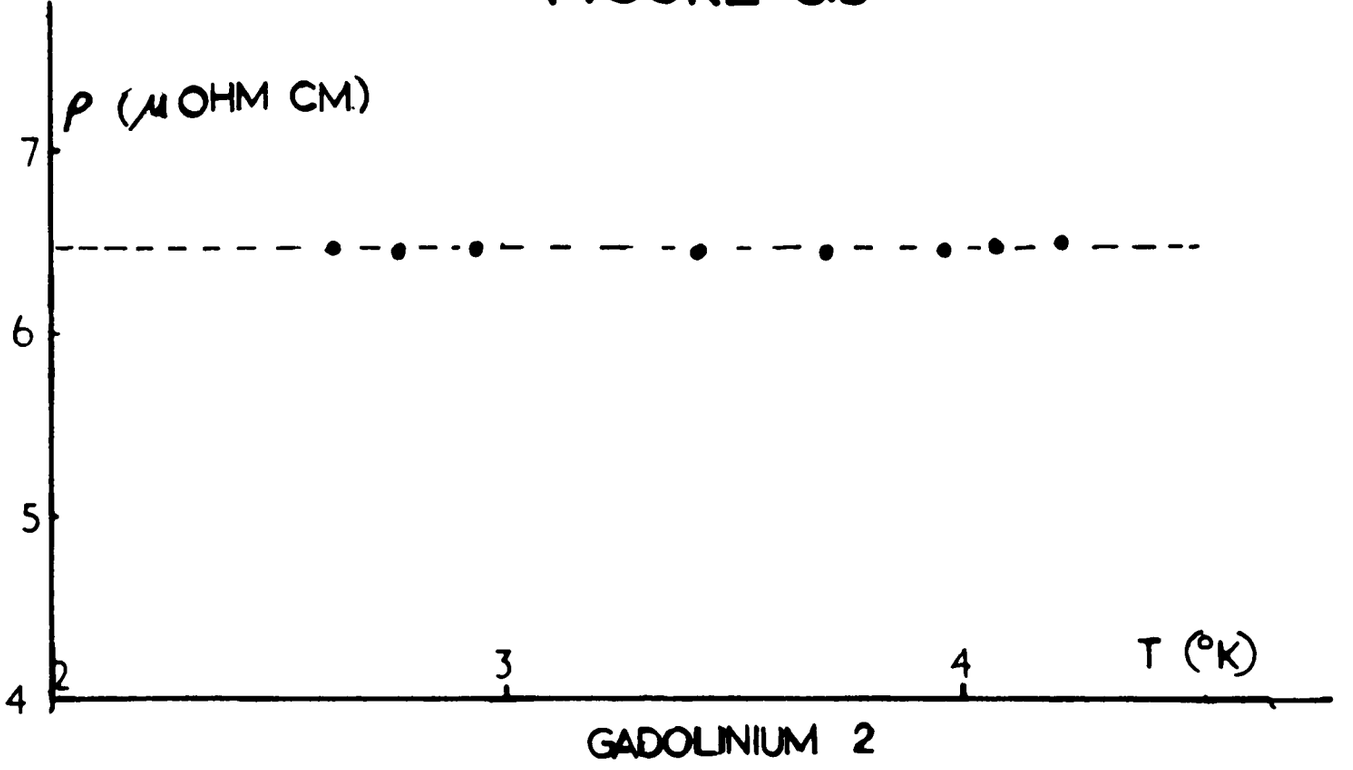
To understand this quadratic contribution, we can in principle invoke other transport mechanisms - phonons and

FIGURE 3.4



GADOLINIUM 1

FIGURE 3.5



GADOLINIUM 2

magnons. The specific heat measurements of gadolinium[8] give at 5°K, the magnetic contribution to be 39%. of the total specific heat, the electronic term 31% and the contribution due to phonons being 30% of the total. We shall be in a better position to explain the T^2 contribution after we have measured the thermal conductivity of other rare earth ferromagnets of different magnetic structures, especially those that have no spin waves at low temperatures (due to the energy gap in the spin wave spectrum) and non-magnetic rare earths. Hence we have discussed the T^2 term in a later section under general analysis, though we can say that gadolinium, which is a typical Heisenberg ferromagnet[9] has this T^2 term in the measured thermal conductivity.

The sample gadolinium 2 was measured again after being cold worked to see if there were any effects on the T^2 term. The results are presented and discussed later in Section (3H).

Finally, we point out that the anomalies previously reported[6] for gadolinium have not been observed in our observations; also our results do not confirm the anomalously high Lorenz numbers previously referred to in the literature[1-2].

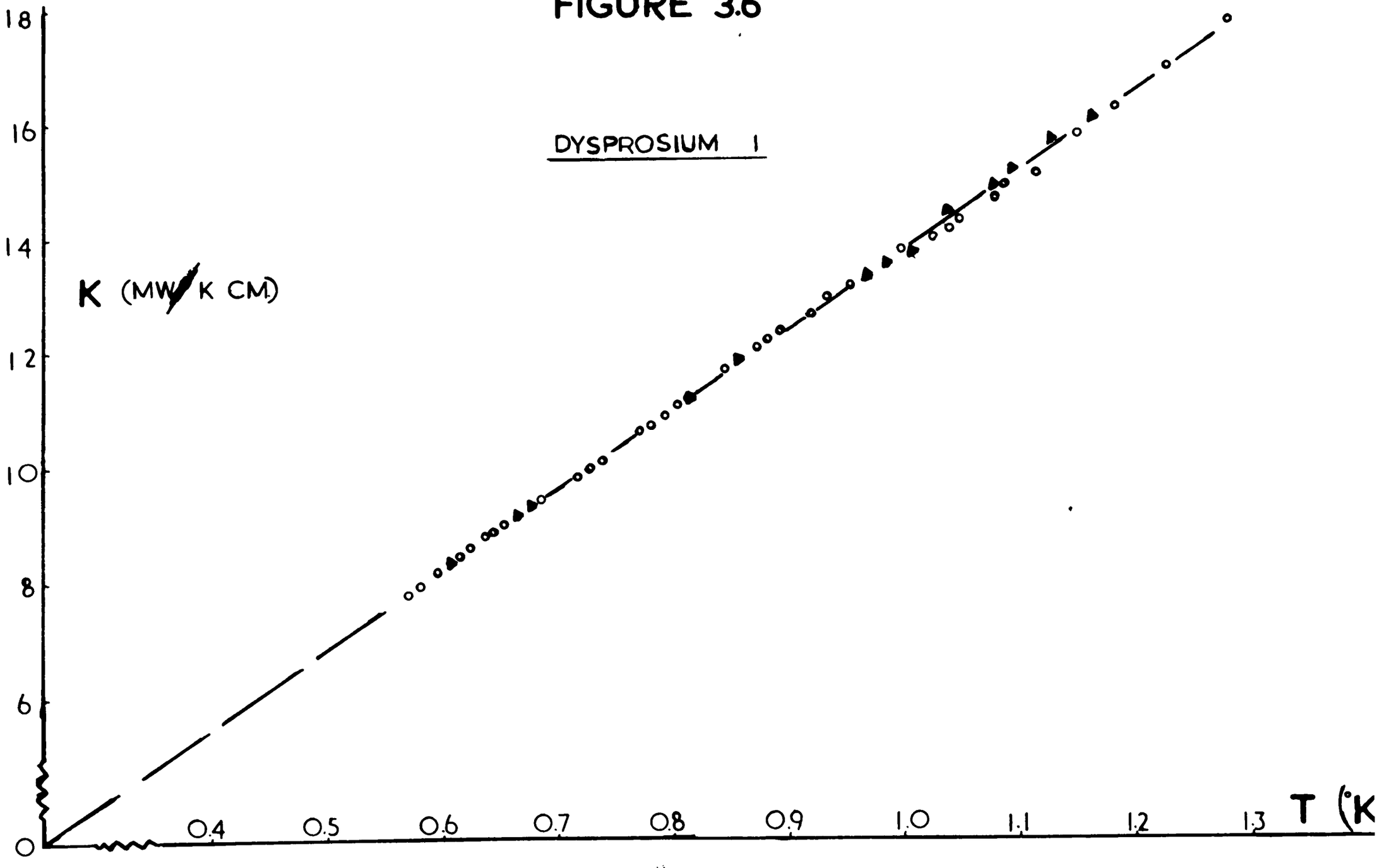
Section 3C:

DYSPROSIUM

Dysprosium in the ferromagnetic region ($T_c \simeq 85^oK$) has its magnetic moments lying in the basal plane, parallel to one another (i.e. basal anistropy). The preference for spin allignment in the basal plane as opposed to being along the c-axis is thought to be due to the combined effects of crystal field anistropy and spin orbit coupling. Niira (1960)[10] has shown that these effects can produce energy gaps in the spin wave spectrum requiring thereby a finite amount of energy to excite even a long wavelength spin wave. The sphysical origin of the energy gap (30^oK for Dy.) lies in the fact that it always takes a finite energy to turn a spin against the anistropy field. (Niira's model applies also to terbium). Specific heat measurements of dysprosium[11] show that the magnetic contribution is negligible below 4^oK and the result can be understood in terms of non-excitation of spin waves at low temperatures.

This element would therefore be the right choice to measure the thermal conductivity after the gadolinium specimens, which had appreciable magnetic contribution to specific heat at 4^oK [8]. We managed to obtain two dysprosium specimens, one a bi-crystal and the other in the form of a polycrystalline wire (see tables 3.1 and 3.2 for details of the specimens).

FIGURE 3.6

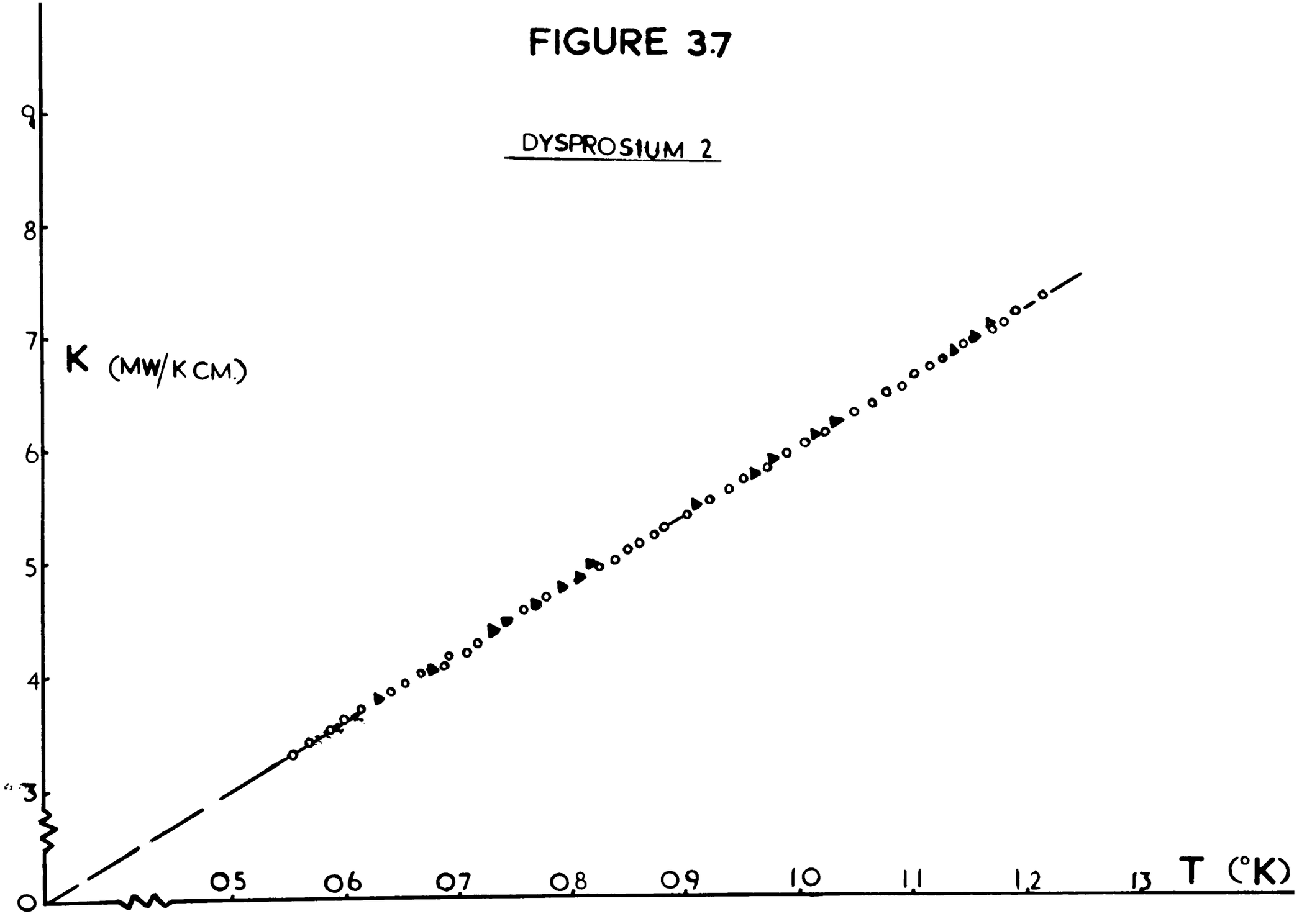

DYSPROSIUM 1
K (MW/K CM)
18
16
14
12
10
8
6
0
0.4
0.5
0.6
0.7
0.8
0.9
1.0
1.1
1.2
1.3
T (°K

We present in figures 3.6 and 3.7 the measured thermal conductivity (K) of the bi-crystal (dysprosium 1) and the polycrystalline wire (dysprosium 2) respectively. These figures show the measurement in the He^3 cryostat and in this range of temperature (below 1.3°K) the graphs are very much linear and extrapolate to zero at 0°K (like the other specimens in this range). (In the figures different runs are denoted by different symbols). The scatter is less than 1%. In figure 3.8 we give the observed temperature dependence of the thermal conductivity of both the specimens in the range 0.5° to 4.2°K measured in the He^3 and He^4 cryostats. The results of the He^3 cryostat are in complete agreement with the measurement of the He^4 cryostat. From figure 3.8 we see that dysprosium 1 (bi-crystal) has the higher value of thermal conductivity of the two specimens and can be accurately described by the expression (from a plot of K/T vs.T)

$$K = 12.75\ T + 0.422T^2 \qquad \text{(dysprosium 1)}$$

K is expressed in milliwatts/°K cm. Like the two gadolinium samples in the last section (3B) this specimen had a term in T and a term in T^2. At 4°K this quadratic term in temperature is 11.6% of the total conductivity and at 1°K is 3.1%.. The sample dysprosium 2 (polycrystal) was linear with temperature in the whole temperature range and can be given by

FIGURE 3.7



$K = 6.01\ T$ (dysprosium 2)

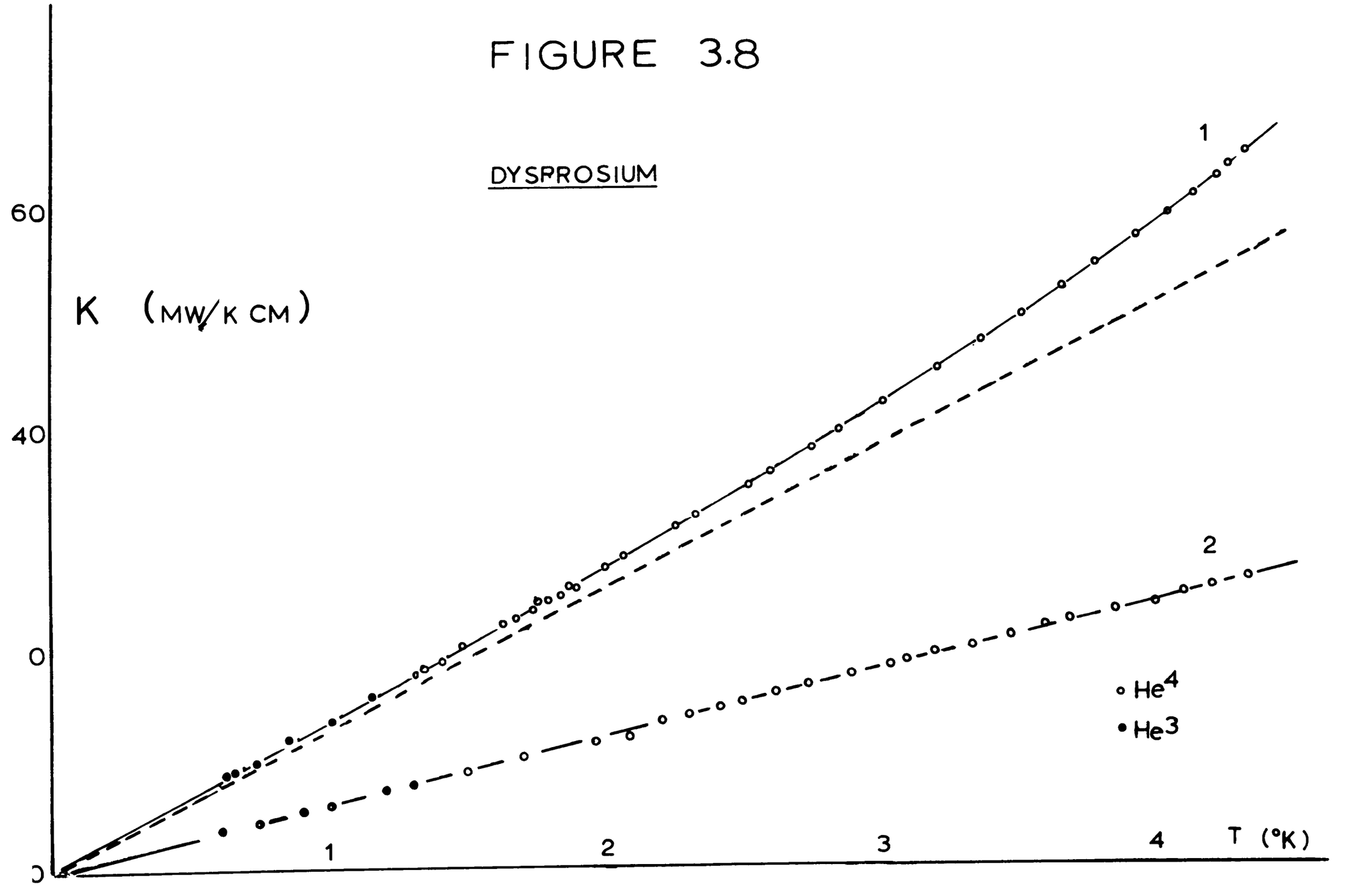
We measured the electrical resistivity of both samples at 4.2°K. (Boys et al (1968)[12], Colvin et al (1960)[7] have measured electrical resistivity of dysprosium and they reached constant values below 10°K for their samples. Our specimens had similar values for the residual resistivity as theirs). To understand the linear term in temperature of the conductivity, we related them with the residual electrical resistivity and obtained Lorenz numbers (L), which are given below

	ρ_0 $\mu\Omega$.cm.	ρ_{295}/ρ_0	a mw/K²cm.	b mw/K³cm.	$L \times 10^8$ w-Ω/K²
dysprosium 1	2.02	31.3	12.75	0.422	2.59
dysprosium 2	4.05	24.2	6.01	-	2.43

The L obtained are in good agreement with the theoretical value of 2.45×10^{-8} watts- ohms/K^2.

The data available on the thermal conductivity of dysprosium are mainly in the high temperature range. Boys et al (1968)[12] have measured from 5° - 300°K. They were not able to separate the various contributions at their lower range of temperature but their calculated Lorenz functions exceeded the value expected for pure electron heat conduction and they indicated that other carriers must contribute significantly to the heat conduction (their L 6×10^{-8} WΩ/K^2). At high temperatures the thermal conductivity was separated into suggested electron and

FIGURE 3.8



phonon contributions. The magnetic transitions in dysprosium produced an anistropic effect on the thermal conductivity, which they interpreted on the basis of magnetic superzones. The high temperature anistropy was explained by the anistropic shape of the Fermi surface. Colwin and Arjas (1964)[13] measured dysprosium in the temperature range 5 to 300°K and they obtained an L ~ 10×10^{-8} watts- ohms/$^{o}K^{-2}$. for their sample.

Our specimens gave good Lorenz numbers for the linear term in temperature of thermal conductivity and we can interpret this term as electronic contribution to heat conduction and the scattering mechanism of the electrons being 'impurities'.

Our results are accurate and we are able to see another term to the heat conductivity for dysprosium 1. This T^2 contribution will be explained in a later section under general analysis after presenting the results of all the other specimens, but we can say that this quadratic term in temperature is also observed for specimens that had significant magnetic contribution to specific heat (gadolinium) and now for this dysprosium 1, which should have no spin waves excited at these low temperatures. Dysprosium 2 had no T^2 contribution or at least too small to be observed. This specimen was measured again after

annealing it and we did observe a T^2 contribution of similar magnitude like the other specimens. Again these results are presented and discussed later in section 3H.

Section 3D:

HOLMIUM

From the specific heat data on holmium at low temperatures[14-15] we note that there is a large contribution to the total specific heat from the nuclear term. In most rare earths this term is effective only below 1°K but in holmium it is considerable up to 10°K. The nuclear term is due to splitting of the nuclear spin states by the interaction with the 4f electrons; by far the largest contribution is from the magnetic field produced at the nucleus by the orbital angular momentum of the 4f electrons. From the specific heat measurements of Lounasmaa[14] it is found that at 5°K the nuclear specific heat contribution for holmium is 33% while the magnetic term is 49%, electronic 11% and the lattice contribution 7%.

The thermal conductivity of holmium has been previously investigated in the liquid helium[4] and higher range of temperature[4,16,17]. From the measurements of Nellis et al[4] the conductivity has a maximum at 20°K (T_c), a slope change at 132°K(T_N) and a positive slope above the ordering temperature. This behaviour at higher temperatures is similar to the measurements of other rare earth ferromagnets.

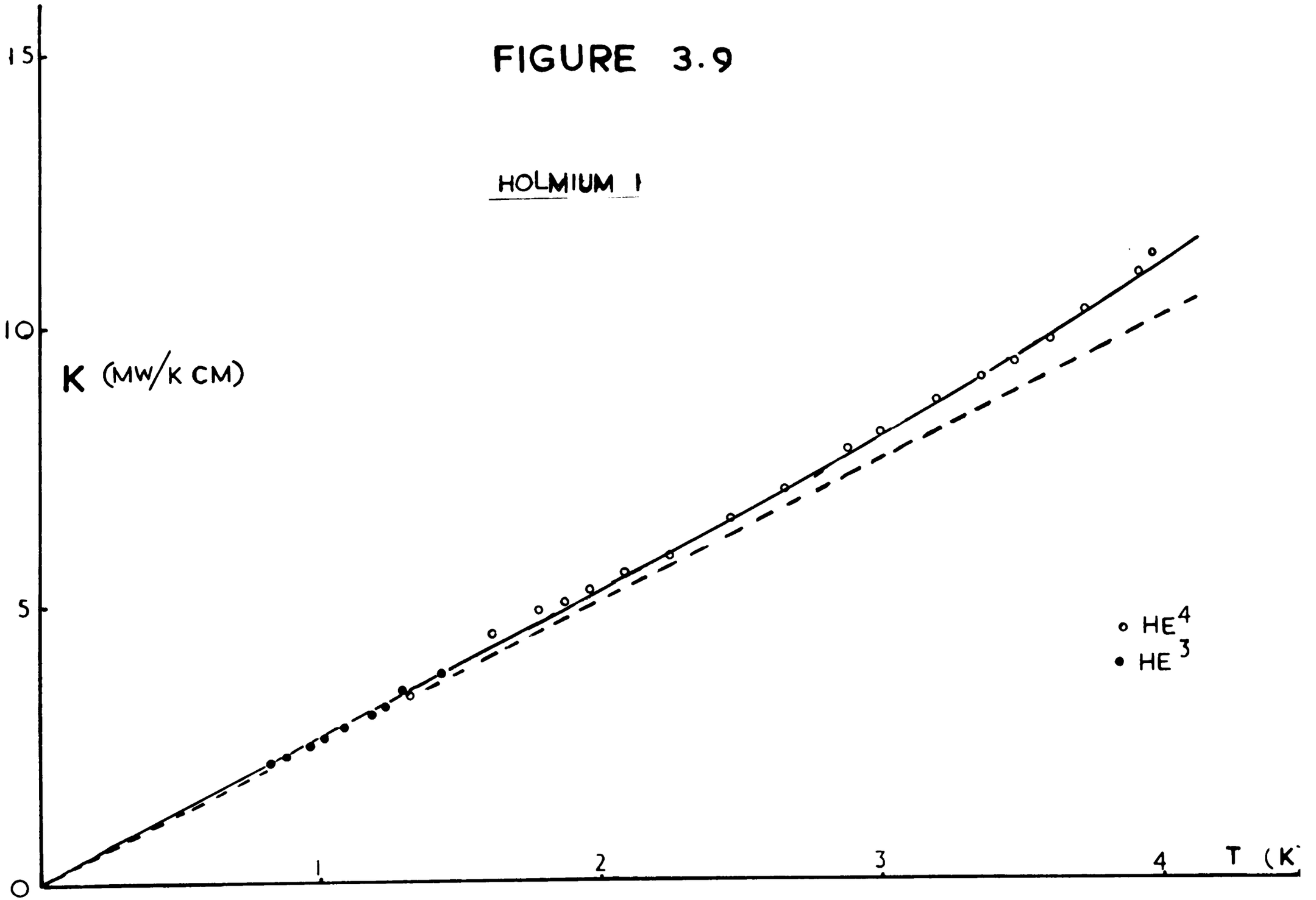
The measured value of thermal conductivity of holmium by these authors largely exceeds the value derived from the electrical resistivity via the Wiedemann-Franz law.

Nellis et al obtained for their two single crystal specimens values of 7.65×10^{-8} watts-ohms-$^{o}K^{-2}$ and 3.96×10^{-8} watts-ohms-$^{o}K^{-2}$ for L at $5^{o}K$, while Aliev and Volkenshtein[16] got 9.1×10^{-8} watts-ohms-$^{o}K^{-2}$ for their polycrystalline sample. The only other data available below $4^{o}K$ are those of Rao[17] and here the conductivity drops almost linearly between $4.2^{o}K$ and $3.4^{o}K$ from where the curve gradually decreases with superimposed hump on it around 2.8 K. The trend in the curve below 1.8 K is not obvious but it definitely does not appear to pass through the origin. The L obtained here was 12×10^{-8} watts- ohms- $^{o}K^{-2}$.

The high temperature anomalies (at transition temperatures) are probably due to the appearance of the magnetic supper lattice energy gaps (Section 1D-5) though the influence of the various magnetic states on thermal conductivity has yet to be explained theoretically, but the low temperature anomalies were not explained.

More recently another anomaly has been reported by Rao (1969)[18] for holmium at very low temperatures (below $1.3^{o}K$), where the thermal conductivity suddenly begins to rise and passes through a maximum around $1^{o}K$. Since holmium at these temperatures has a very high nuclear specific heat, it has been suggested that this might provide an extra contribution to the thermal conductivity via a Rudermann-

FIGURE 3.9



Kittel-Kasuya-Yosida type interaction between the nuclei, 4f electrons and conduction electrons. There has been no calculations so far to show that the nuclear spin contributes significantly to the transport properties by means of this indirect exchange interaction (Section 1D-4).

In view of these anomalies, we have measured the temperature dependence of the thermal conductivity (K) of a polycrystal and a single crystal holmium. The polycrystalline specimen wire was of average diameter 1.37 mm. and of length 5 cms. The quoted impurities were other rare earths, iron, silicon and magnesium and the total impurities were about 0.1%. The single crystal was in the form of a rod of length 4.5 cms. and diameter about 5 mm. The temperature gradient was measured across a section 3.5 cms. at about the middle of the sample.

Figures 3.9 and 3.10 show a plot of K vs.T for our specimens, the polycrystal and single crystal respectively. Both curves can be accurately described by (from a plot of K/T vs T)

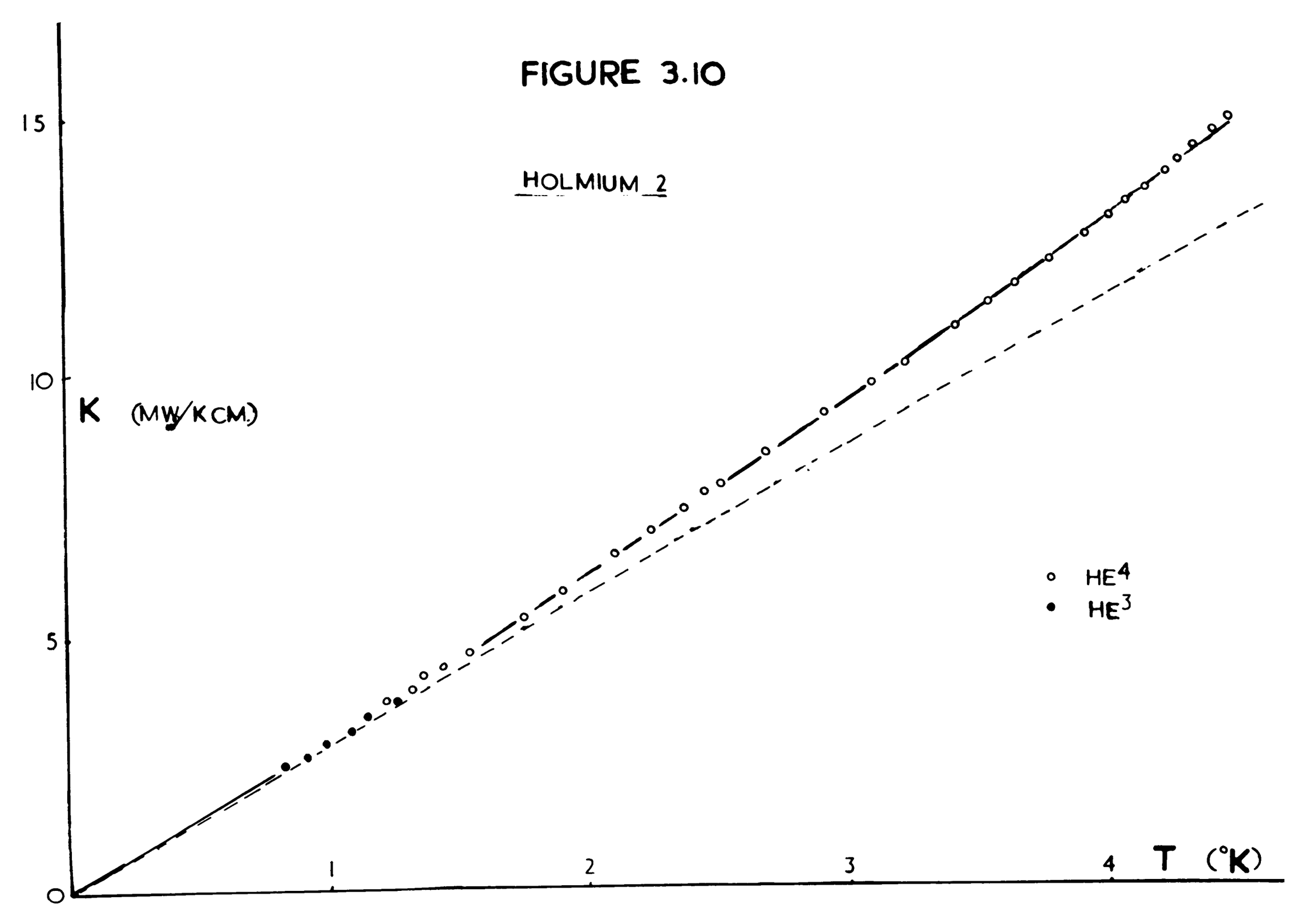
(holmium 1) $K = 2.55T + 0.053T^2$ (milliwatts/^{o}Kcm.)

(holmium 2) $K = 2.85T + 0.087T^2$ (milliwatts/^{o}Kcm.)

The above expression for K is similar to that found for most of the other specimens we have reported so far.

Like the others, these specimens were measured in

FIGURE 3.10



a He^4 cryostat and a helium^3 cryostat, but here measurements were done only down to 0.8°K. We have presented the measurements done in both cryostats in one graph. (In the graphs different symbols denote the measurements in different cryostats). The results presented are of few different runs and the reproducibility is very good. The scatter in the high temperature region is small, almost like the other specimens measured so far, but below 1.5°K the scatter was slightly greater than for the others (about 1.5%). In holmium the time taken to reach the steady state before measuring the temperature gradient was very much larger than for the other rare earths. This 'equilibrium time' was found to increase with lowering of temperature. The fact that at lower temperatures the specific heat is already very large, and combined with rather low thermal conductivity causes a long relaxation time (2 hours at 0.8°K in our case - compared to few minutes in *Gd*) and this makes it extremely difficult to extend the measurements to lower temperatures. This long relaxation time also affects the accuracy in calibration of the thermometers and the measurement of ΔT (the temperature difference between the two thermometers) in determining the thermal conductivity (we have discussed this in more detail later).

Looking at our experimental results obtained and assuming the linear term in temperature is due to electrons, with

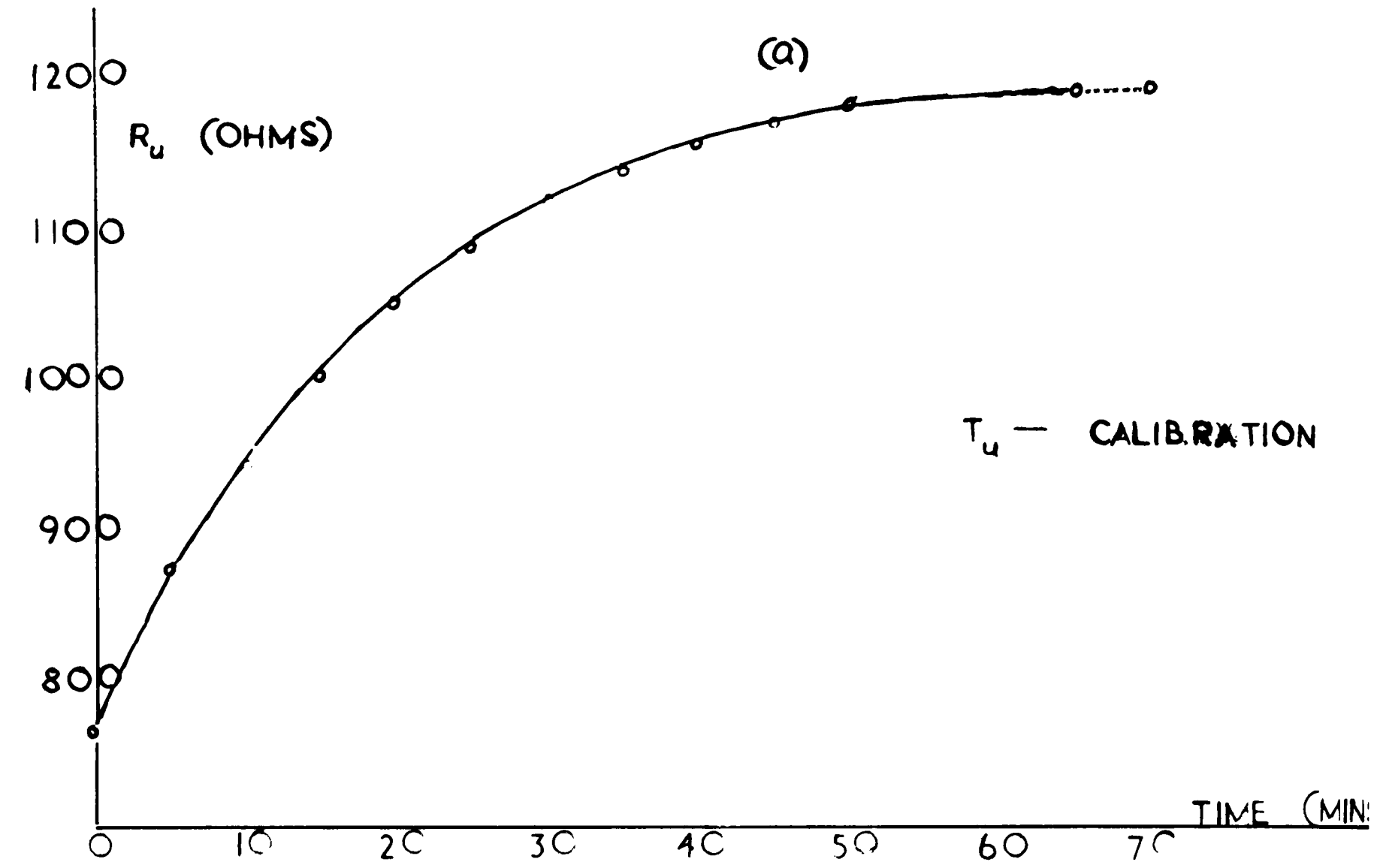
mean free path limited by impurity scattering, we find using electrical resistivity measurements of our samples (measured at 4.2°K - measurement of electrical resistivity of holmium by Colvis et al[7] show that their sample was in constant residual state below 10°K - their $\rho_0 \sim 7 \mu\Omega$cm.), the values of the calculated Lorenz number (L) reasonably close to the theoretical value (see Table below).

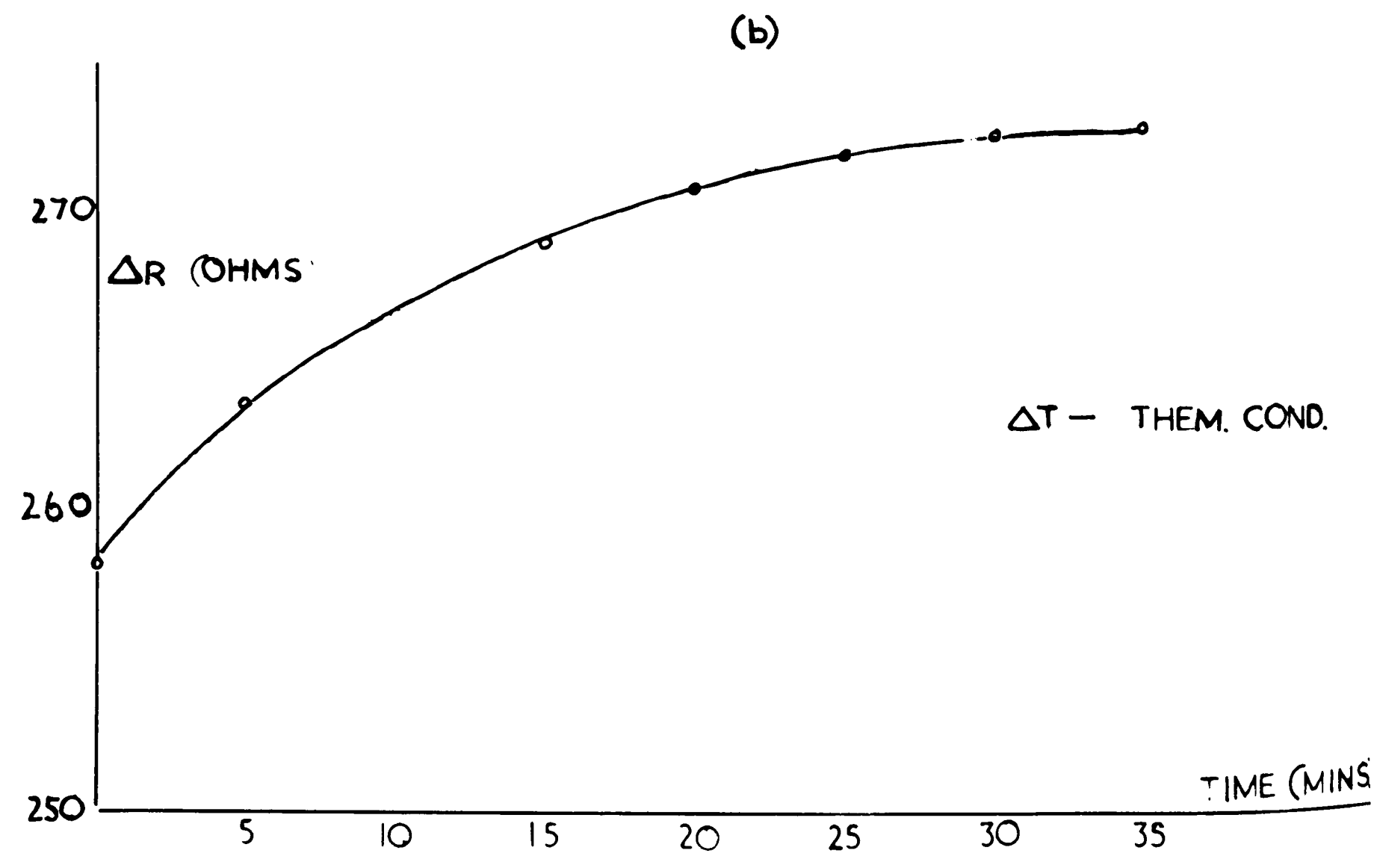
	ρ_0 $\mu\Omega$ cm.	ρ_{295}/ρ_0	a mw/K²cm	b mw/K³cm.	L x 10⁸ WΩ/K²
holmium 1	9.95	9.33	2.55	0.053	2.38
holmium 2	7.25	9.73	2.85	0.087	2.76

We shall discuss the origin of the small T^2 contribution in a later section of general analysis, although we can say it is also present in other rare earth metals investigated, even on those which do not have any appreciable nuclear contribution to the specific heat at the temperatures considered. At 4°K, we find the T^2 contribution is about 7.7% of the total heat conductivity and at 1°K it is about 2% for the polycrystal specimen. The magnitude of this T^2 term of both specimens is quite similar.

We must emphasise the difficulty in measuring the thermal conductivity of holmium at very low temperatures. As we had mentioned earlier that it had an exceptionally long relaxation time for thermal equilibrium (this time increasing with lowering of temperature), any measurement

FIGURE 3.20


(a)
1200
1100
1000
900
800
R_u (OHMS)
T_u — CALIBRATION
TIME (MIN
0
10
20
30
40
50
60
70


(b)
270
260
250
ΔR (OHMS
ΔT — THEM. COND.
TIME (MINS
5
10
15
20
25
30
35

of ΔT (the temperature difference between the two thermometers), say after a fixed interval of time, during which the heater was on, would mean determining a smaller ΔT than the actual value. If this was the case then the calculated thermal conductivity would be rising with lowering of temperature. (Figure 3.20(a) gives an idea of the time involved to attain steady conditions for calibration ($T \sim 0.96^{o}K$). Figure 3.20(b) shows the value of ΔR (corresponding to ΔT) in the case of thermal conductivity measurement). One has to ensure that steady state or nearly steady state conditions are reached. In our case this was done by observing T (the temperature of the upper thermometer) and ΔT with time until T and ΔT were constant with time within the experimental accuracy (changes in $T \sim 1$ mdeg. in five minutes).

In conclusion we can say that the thermal conductivity of the holmium samples investigated is essentially due to electrons with mean free path $l \sim 10^{-7}$cm. and there is no evidence of any anomaly down to $0.8^{o}K$, where the nuclear contribution to the specific heat is very large.

Section 3E:

ERBIUM

The erbium specimens we investigated were polycrystal samples. One of the specimen, erbium 1, was in the form of a rectangular parallelepiped. The sample cross section was about 2.75 x 3.98 mm. and the length was about 32 mm. The other specimen, erbium 2, was in the form of a polycrystalline wire about 5 cms. long and average diameter 1.5 mm.

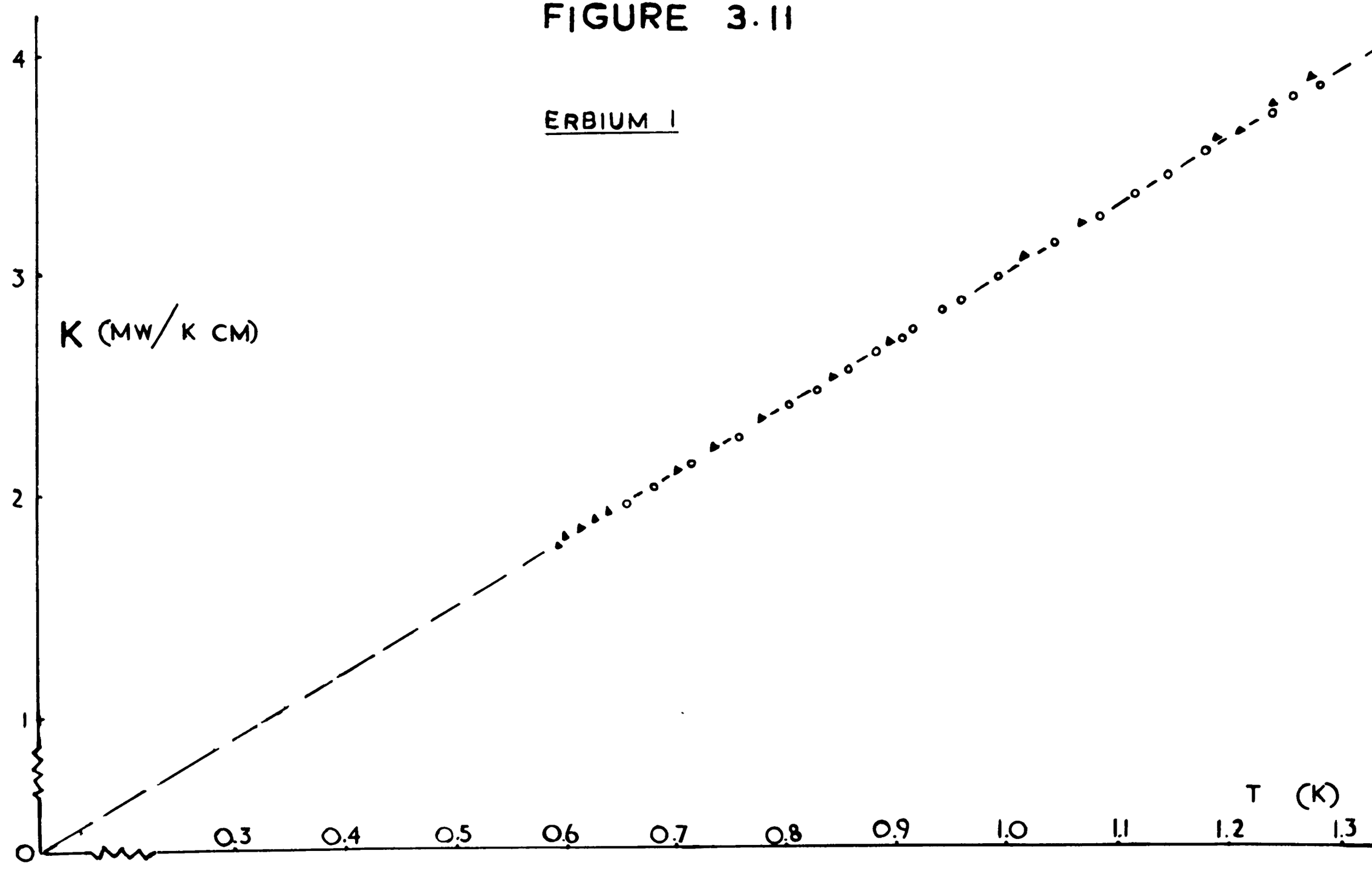
The observed values of the thermal conductivity (K) of erbium 1 and erbium 2 have been plotted as a function of temperature (T), measured in the temperature range covered by the He^3 cryostat in figures 3.11 and 3.12 respectively. The results appear quite linear in temperature in this range and extrapolates to zero at 0^oK. (Different symbols are used in the figures to denote different runs). Figure 3.13 gives the value for K in the temperature range 0.5 to 4.2^oK and shows both the specimens plotted on the same graph. The results are from two different cryostats and different symbols are used in the figure to denote them. For both the specimens, we can give quite accurately

$$K = aT + bT^2$$

from a plot K/T vs. T (see table below for values of a and b).

We measured the electrical resistivity of the specimens at 4.2^oK and related this value to the linear term in

FIGURE 3.11



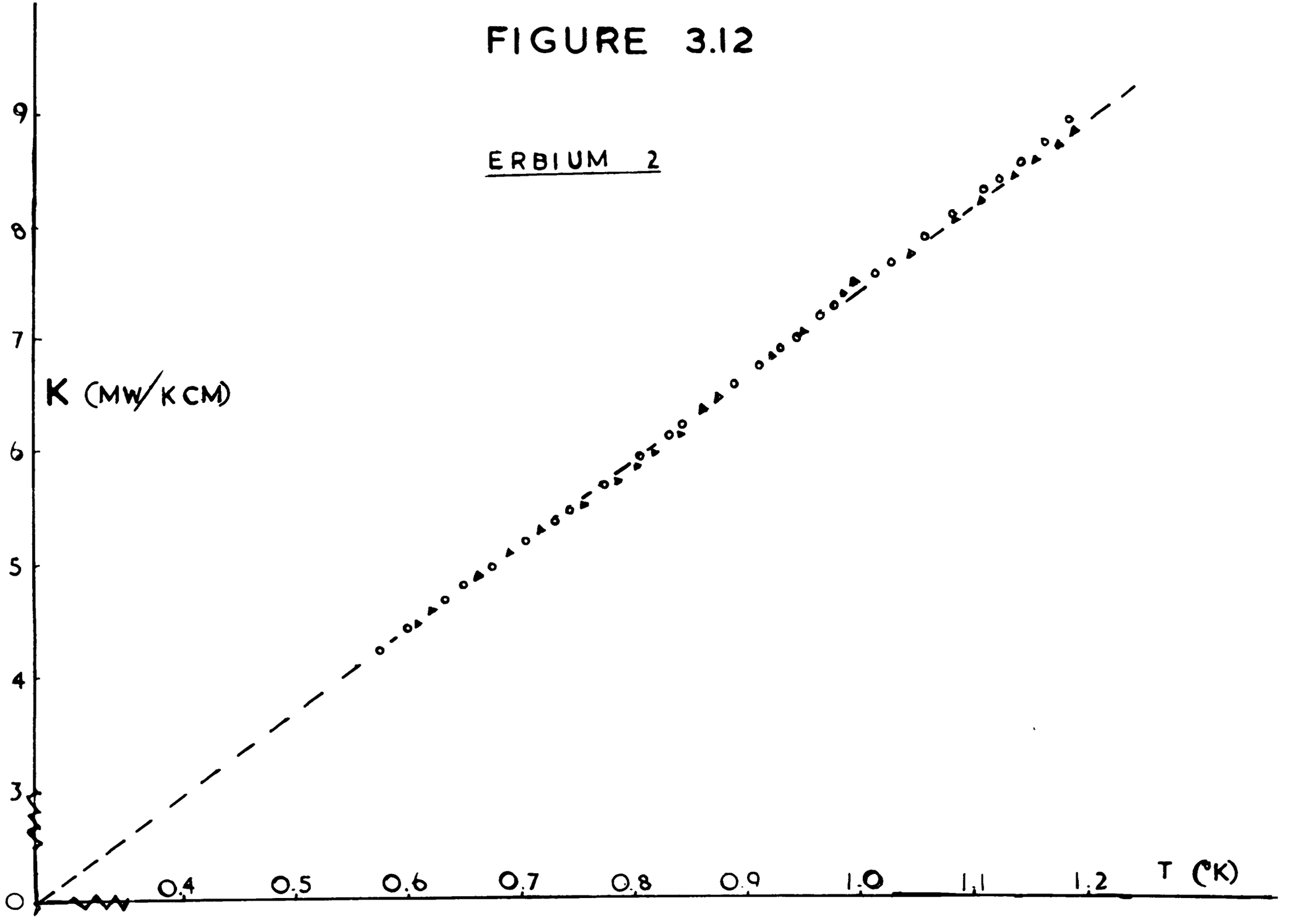
temperature of the thermal conductivity via the Wiedemann-Franz law and again obtained very good Lorenz numbers (see Table below). (Electrical resistivity measurements of erbium by Arajs and Dunmyre (1965)[19] show that their specimen (ρ_0 = 3.79 $\mu\Omega$ cm.) is at the residual value below 15°K).

	ρ_0 $\mu\Omega$ cm	ρ_{295}/ρ_0	a mW/°K²cm	b mW/°K³cm.	L x 10⁸ WΩ/°K²
Erbium 1	8.60	10.7	2.82	0.155	2.40
Erbium 2	3.32	25.1	7.26	0.132	2.41

The temperature variation of the thermal conductivity of our erbium specimens are very similar to the other elements of the heavy rare earth metals we have measured so far. Here again we can say that the linear term (aT) of the conductivity is due to electrons whose mean free path is determined from 'impurity' scattering.

Erbium 2, which is more pure than erbium 1 has the higher values of thermal conductivity. For the linear term, erbium 2 is about 2.6 times greater than erbium 1. For the quadratic term in temperature (bT^2) of the conductivity, we see that both specimens have this term quite similar in magnitude. (For sample erbium 2, the quadratic term is about 6.5% of the total conductivity at 4°K and about 1.8% at 1°K). We shall try to account for this quadratic term along with the results of the other specimens in a later section.

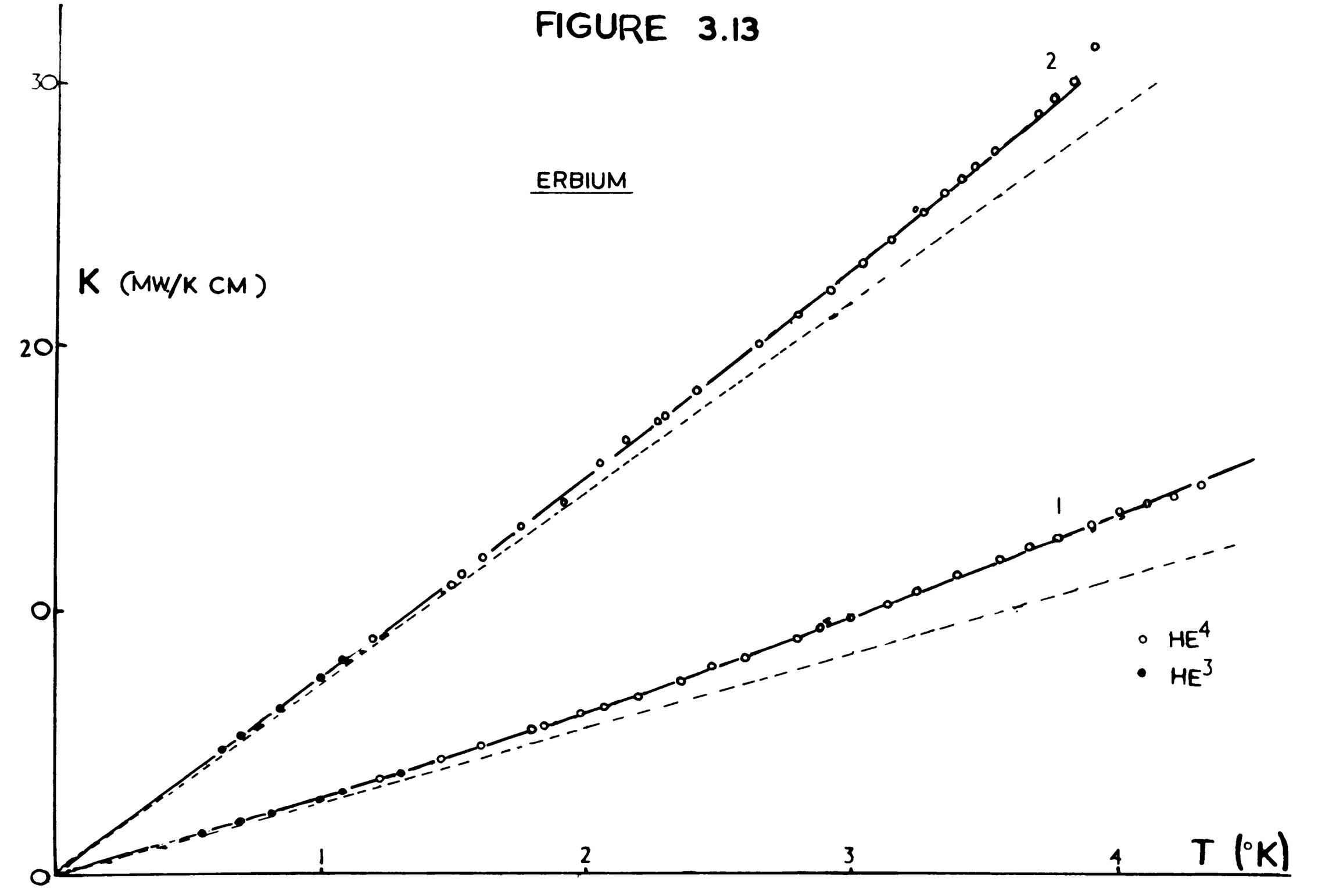
FIGURE 3.12



Arajs and Dunmyre (1965)[19] have reported the measurement of thermal conductivity of erbium between 5 - 300°K. They obtained a Lorenz number of 5×10^{-8} watts-ohms- K^{-2} for their sample at 5°K using the total thermal conductivity. Aliev and Volkenshtein (1966)[16] reported getting a number 9 for their specimen. They have interpreted in terms of other carriers than the electrons. Measurements on single crystal erbium have been reported in the high temperature range[12]. Anistropy was evident in their samples. In the paramagnetic temperature region (above 86°K), the c-axis thermal conductivity always exceeds the basal plane conductivity and the reason for this was suggested as due to the anistropic shape of the Fermi surface. A second type of anistropy was observed due to the magnetic ordering. The c-axis thermal conductivity dropped sharply as the temperature was increased through the ferro-magnetic-antiferromagnetic transition temperature (T_c = 20°K). As the Neel temperature T_N (86°K) was approached, the c-axis thermal conductivity began to rise rapidly and underwent a change in slope near T_N. Only slight effects were seen in the basal plane results.

There does not appear to be any specific heat data on erbium below 4°K, Since on dimensional considerations the heat conductivity is proportional to the specific heat, any data on specific heat helps to a better understanding of the

FIGURE 3.13



thermal conductivity results.

In concluding this section, we report that the thermal conductivity of our erbium samples did not show any anomaly. The Lorenz numbers obtained were close to the theoretical value and like the other specimens we measured, the erbium samples had a quadratic term (bT^2) in addition to the dominant linear term (aT).

Section 3F:

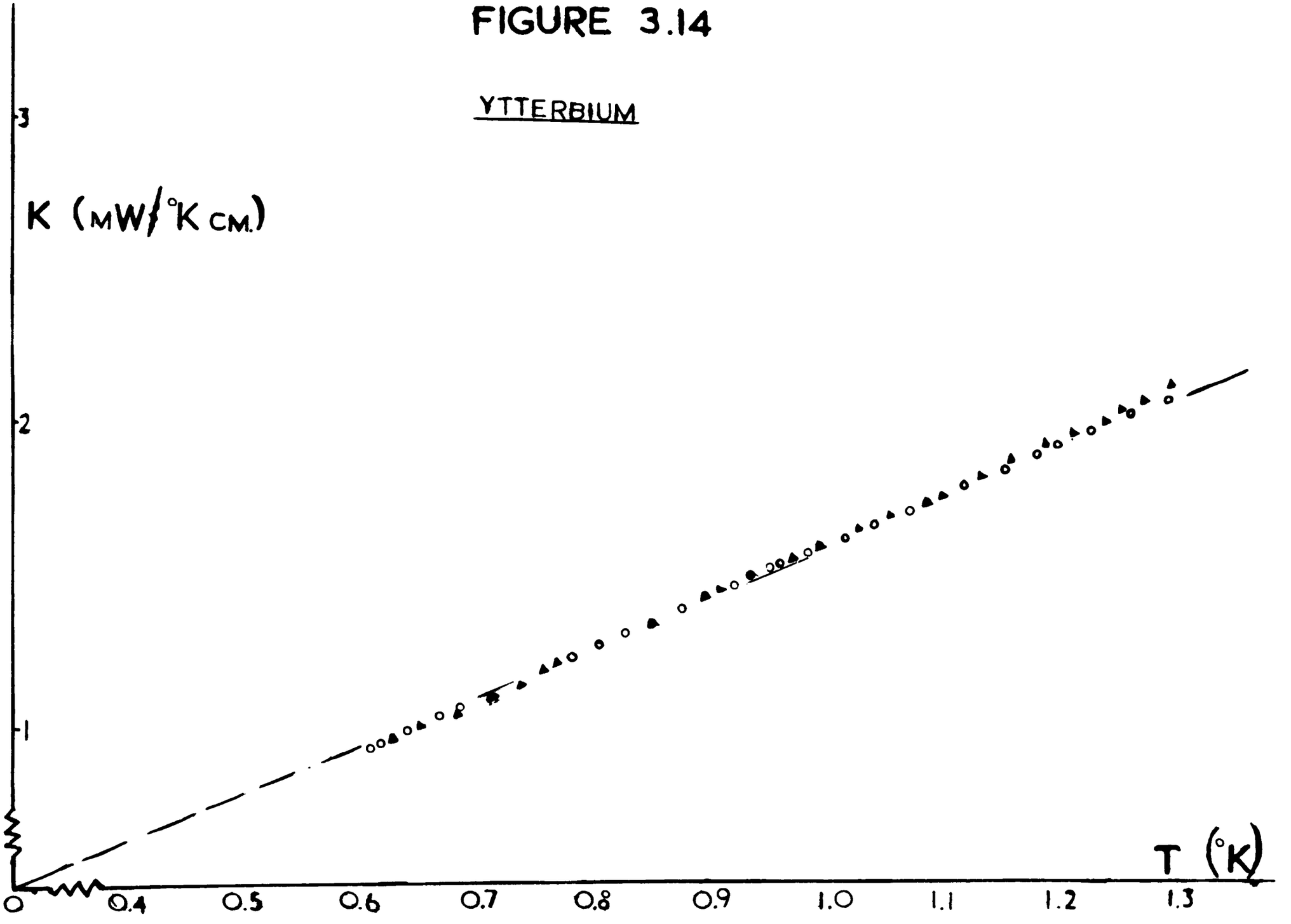
YTTERBIUM

In our measurement of the rare earth ferromagnets so far, we have observed a linear and a quadratic term in temperature for the total thermal conductivity. The linear term agrees well with the Wiedemann-Franz law, but in explaining the T^2 term we have to look for other excitations, namely phonons and magnons.

In a rare earth metal having a closed 4f shell and no magnetic moment, the magnon thermal conductivity should be absent. Ytterbium and lutetium in the heavy rare earth series are non-magnetic. Ytterbium in tripositive form has a $4f^{13}$ configuration, gains the extra correlation energy of a completed shell from the 5d electron and so takes the divalent form with $4f^{14}$ configuration. It crystallizes in the face centred cubic rather than the hexagonal close packed structure of the others, and also some of its physical properties are different in that it is soft, having a density of 7.0gm/cm^3 (the others around 8.0gm/cm^3) and a larger atomic volume. Lutetium has a completed 4f shell ($4f^{14}$) and has identical crystal symmetry, valency and nearly similar Debye temperature to the other heavy rare earth metals.

A study of these metals can be useful in the general study of the series and it is possible to get an idea of the lattice

FIGURE 3.14

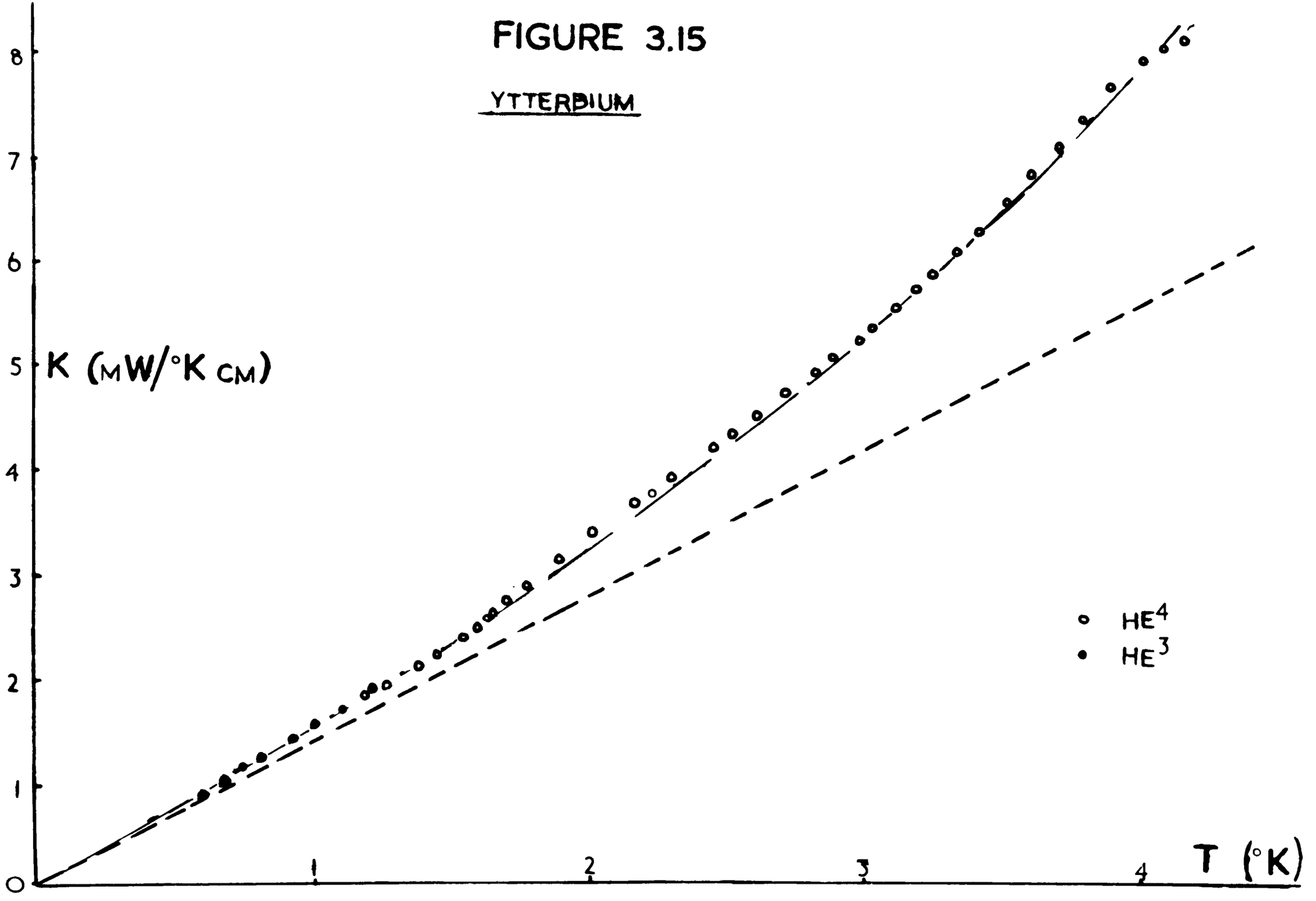


term of the other heavy rare earths from the measurement of lutetium. As lutetium was not available, we measured on an ytterbium specimen. The co-ordination number is the same for both hexagonal close packed (h.c.p.) and face centred cubic structures (f.c.c.). Therefore, if the binding energy depended only on the number of nearest neighbour bonds, there would be no difference between h.c.p. and f.c.c. structures.

The sample measured was polycrystalline in the form of a drawn out wire (for details see Tables 3.1 and 3.2). We present in figure 3.14 the thermal conductivity of ytterbium as a function of temperature (below 1.3°K) measured in the He^3 cryostat. The results are of two different runs and we can see that the conductivity is almost linear in this range of temperature and extrapolates to zero at 0°K. The reproducibility of our results in different runs is evident from the graph (different runs are denoted by different symbols in the figure).

In figure 3.15 we present the results obtained in the He^4 and He^3 cryostats (below 4.2°K) and again the measured absolute values of both cryostats agreed very well. Like the other specimens measured so far, we are able to separate a T (temperature) and a T^2 term for K (conductivity) and can accurately represent

FIGURE 3.15



$$K = 1.46T + 0.138T^2 \ (mw/^oKcm.)$$

The residual resistivity (measured at 4.2°K) was 15.76 $\mu\Omega$/cm. and this when related with the T term via Wiedemann-Franz law gave a Lorenz number L = 2.3 x 10^{-8} watts- ohms-$^oK^{-2}$, which was in fair agreement with the theoretical value. The overall value of the conductivity is much lower than in the other rare-earth metals we have measured. Lounsamaa (1963)[8] observed, in his measurement of the specific heat of ytterbium between 0.4 and 4°K, the electronic specific heat (C_E = 2.90 T milli joules/mole) is also smaller than the usual value (C_E = 10.0T milli joule/mole) of the other rare earths and the lattice specific heat corresponds to a Debye Θ = 118.1°K, which is lower than the value $\Theta \sim 180^oK$ observed for the others. In the non-magnetic ytterbium the 5d electron normally in the conduction band is added to the 4f shell and this reduces the density of states at the Fermi level.

In the measurement of Aliev and Volkenshtein (1966)[20] of ytterbium between 2 - 100°K, the curve had the form typical of the thermal conductivity of pure metals: the conductivity increases sharply with temperature at low temperatures, passes through a maximum near T = $\Theta/10$ and decreases rapidly at higher temperatures, becoming finally almost independent of temperatures.

In analysing the results obtained for ytterbium we can say that the term linear in temperature is due to electrons linuted by 'impurity' scattering.

Specific heat studies of ytterbium[8] show no magnetic contribution, and it should be mentioned that the magnon component should appear only in metals having a magnetically ordered state. The T^2 term in the measured conductivity has the 'right' temperature dependence for phonon conduction (resistance caused by scattering of phonons by electrons and dislocations). We shall analyse this T^2 term in more detail in a later section of general analysis, though we can say that this term is also present in the other heavy rare earth metals as well as non-magnetic ytterbium.

Section 3G:

TERBIUM

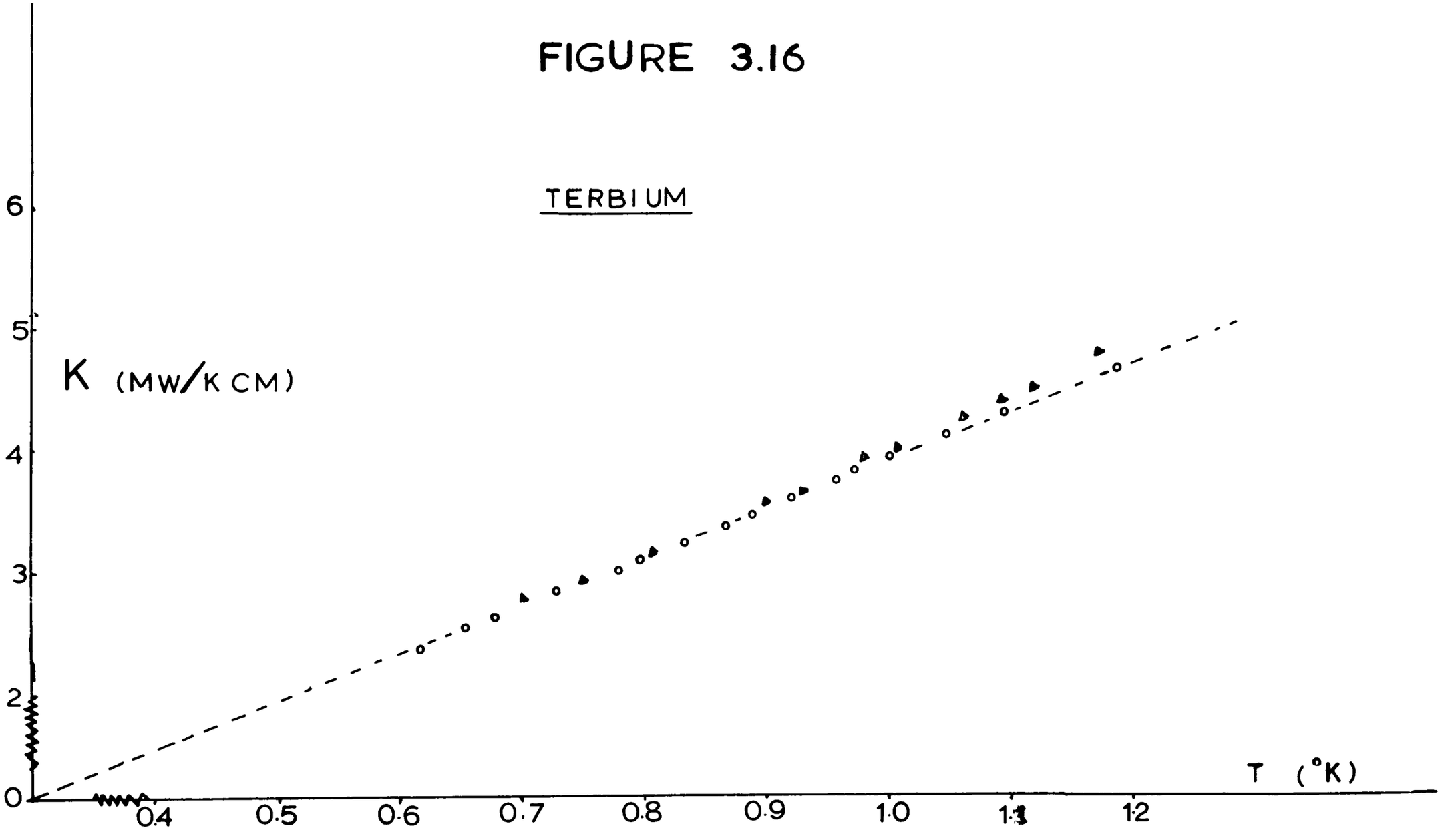
Terbium in the ferromagnetic region (T_c = 218°K) has a similar structure to dysprosium. The magnetic moments lie in the basal plane and are parallel to one another (figure 1.2(a)). It has similar basal anistropy although the direction of easy magnetization in the basal plane is different. The energy gap, Δ, which represents the minimum energy required to excite a spin wave is about 30°K[29] (similar in magnitude to that in dysprosium). The energy gap should manifest itself at low temperatures in all properties, which depend on the magnetic specific heat. In an anistropic material we expect the low temperature specific heat to have the form

$$C_M = B T^{3/2} e^{-\Delta/k_0 T}$$

Lounasmaa and Roach (1962)[30] show that the magnetic contribution in terbium is negligible below 4°K (these results can be understood in terms of non-excitation of spin waves at low temperatures).

The specimen we measured was a polycrystalline wire of length 3.4 cms. and of average diameter 1.48 mm. The observed variation of thermal conductivity of terbium, plotted as a function of temperature is given in figures 3.16 and 3.17. Figure 3.16 represents the results measured in the He^3

FIGURE 3.16



cryostat (below 1.2°K). In this temperature region the conductivity is very much linear and extrapolates to the origin at 0°K. In figure 3.17 we have the results in the temperature range below 4.2°K (He^3 and He^4 cryostats) and from a plot of K/T vs T we can separate the conductivity into

$$K = 3.64\ T + 0.203\ T^2$$

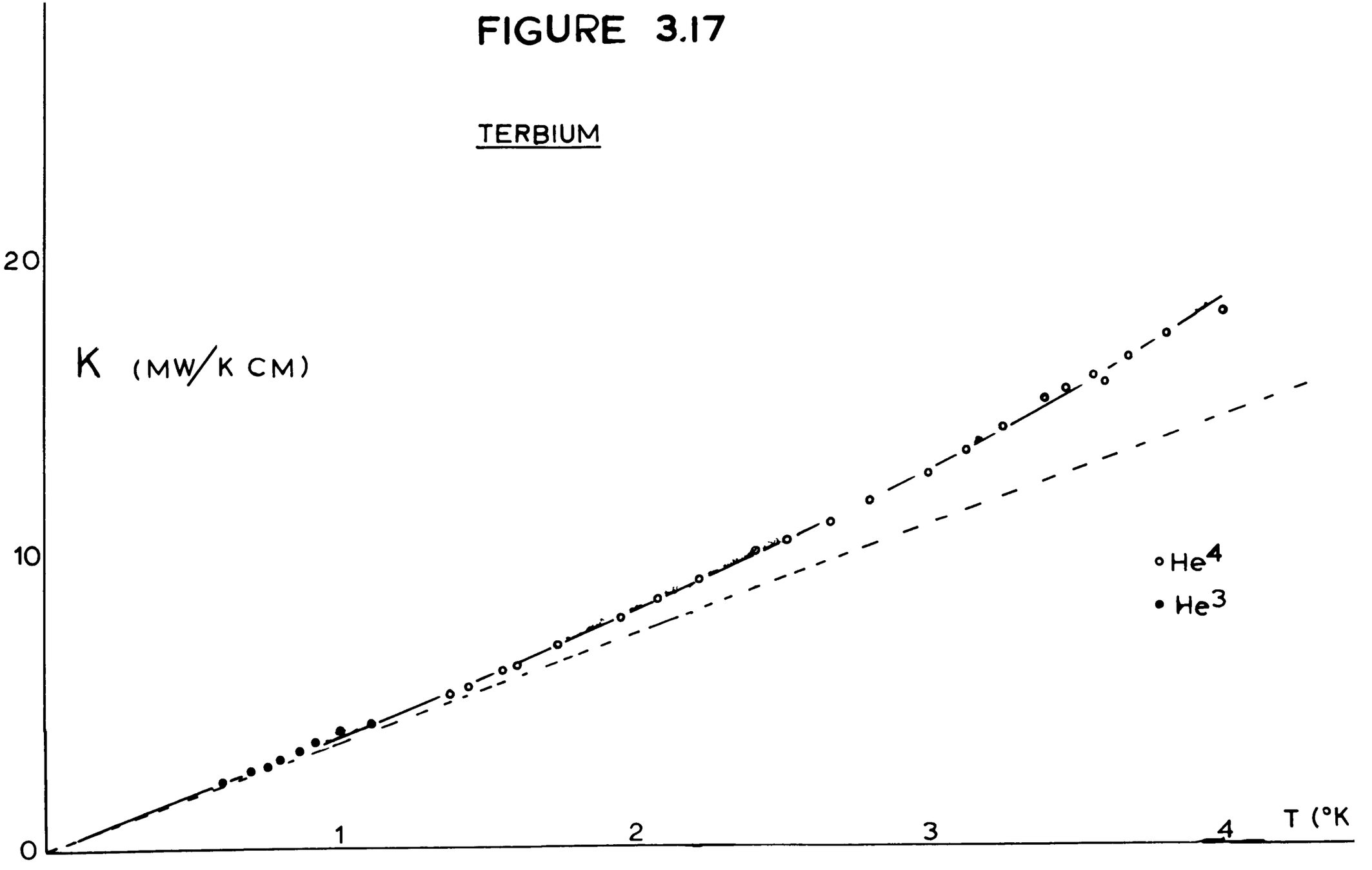
This result, again like the others, has a linear and a quadratic term in temperature. The electrical resistivity ρ_o was measured at 4.2°K. (Electrical resistivity at low temperatures of terbium by other investigators[4][7] show no anomalous behaviour and all their samples reached the residual value below 10°K. Colvin et al[7] had $\rho_o = 3.5\ \mu\Omega$cm. for their sample). The linear term in temperature of the thermal conductivity, when related to the residual electrical resistivity gave a Lorenz number very close to the theoretical value (see below).

	ρ_o $\mu\Omega$ cm.	ρ_{295}/ρ_o	a mw/°K²cm	b mw/°K³cm	$L \times 10^8$ $W\Omega/°K^2$
terbium 1	6.61	20.9	3.64	0.203	2.41

We therefore can say that the linear term represents an electronic contribution, with the electron mean free path limited by 'impurity' scattering.

From specific heat results[3], we can take it as if there are practically no spin waves at low temperatures

FIGURE 3.17



and so to account for the quadratic term (bT^2) in conductivity we turn towards the other carriers present namely phonons. However, we shall discuss this term later in detail. There is appreciable nuclear specific heat in terbium at low temperatures. At 4^oK we find from specific heat measurements that the nuclear contribution to specific heat is about 17% of the total, while the electronic term is 43% and that due to the lattice about 40%. The nuclear term appears in the specific heat as a term inversely proportional to powers of temperature and is responsible for the sharp rise to the total specific heat below 1.5^oK. (In holmium the nuclear magnetic energy was as high as 33% of the total at 5^oK). At low temperatures the equilibrium time for the terbium sample was longer than the other specimens (except for the holmium samples which were much longer). At about 0.65^oK the equilibrium time was as long as 20 minutes. The reason is that at low temperatures (especially below 1^oK) the specific heat is already very large and this coupled with a low thermal conductivity causes a long relaxation time. This fact would make it difficult for accurate determination of the conductivity at still lower temperatures.

The data available on the thermal conductivity of terbium are mainly in the high temperature range[4][5]. Arajs and Colvin (1964)[33] have measured terbium between $5-300^oK$.

The antiferromagnetic-paramagnetic transition causes an anomaly in the thermal conductivity at about 225°K. The ferro-antiferromagnetic transition, because of the narrow antiferromagnetic region was not observable. At low temperatures their Lorenz number was high (7×10^{-8} $W\Omega/K^2$). Gallo[5] finds in his results that below 100°K, the additional contribution to the thermal conductivity (the difference between the measured and the ordinary electronic thermal conductivity calculated from the Wiedemann-Franz law) has a temperature dependence, which is characteristic of the lattice thermal conductivity.

In concluding this section we can say that the linear term like the other specimens represents electronic conduction limited by 'impurity' scattering. The quadratic term observed in terbium was also observed in other rare earths which had appreciable magnetic specific heat in the temperature range of our measurement.

Section 3H:

GENERAL ANALYSIS

This thesis presents a systematic study of the thermal conductivity of the heavy rare earth metals in the temperature range 0.4 to 4.2°K. The specimens studied were gadolinium (2 samples), dysprosium (2 samples), holmium (2 samples), erbium (2 samples), terbium (1 sample) and ytterbium (1 sample). Most of them were polycrystals (some in the form of drawn out wire) but measurements were also made on a single crystal of holmium and a bi-crystal of dysprosium. (Various particulars about the specimens that were available to us are given in tables 3.1 and 3.2). These elements display most of the various types of magnetic ordering (see table 1.1) found in the rare earth ferromagnets. Ytterbium is non-magnetic.

From our measurement of the thermal conductivity (K), we are able to separate quite accurately the conductivity into a linear term and a quadratic term in temperature (T) from a plot of K/T vs. T and we can express K as

$$K = aT + bT^2 \qquad (3.1)$$

(One of the specimen, dysprosium 2, had only a linear term in temperature). Table 3.3 gives the values of a and b for all the specimens we have measured. Also given in the table are the electrical resistivities of the

Table 3.3

Sample	a mw. deg K^{-2} cm^{-1}	b mw. deg. K^{-3} cm^{-1}	ρ_0 $\mu\Omega cm^{-1}$	ρ_{295} $\mu\Omega cm^{-1}$	ρ_{295}/ρ_0	$L \times 10^8$ $W\Omega K^{-2}$
Gadolinium 1	7.51±0.01	0.257±0.003	3.37	147.9	44.3	2.53
Gadolinium 2	3.75±0.02	0.307±0.008	6.44	143.4	22.3	2.44
Gadolinium 2 (cold worked)	3.46±0.02	0.270±0.011	7.31	144.7	19.8	2.53
Gadolinium 2 (further cold worked)	2.56±0.01	0.152±0.004	9.79	147.8	15.1	2.51
Dysprosium 1	12.75±0.02	0.422±0.005	2.02	64	31.3	2.59
Dysprosium 2	6.01±0.02	0.01	4.05	108.0	24.2	2.43
Dysprosium 2 (annealed)	4.75±0.03	0.268±0.013	5.39	109.8	20.4	2.56
Holmium 1	2.55±0.01	0.053±0.006	10.6	92.83	10.6	2.38
Holmium 2	2.85±0.02	0.087±0.007	9.73	70.35	7.23	2.76
Erbium 1	2.82±0.01	0.155±0.008	8.6	92.34	10.7	2.40
Erbium 2	7.26±0.02	0.132±0.010	3.32	83.36	25.11	2.41
Ytterbium 1	1.46±0.02	0.138±0.007	15.76	35.1	2.23	2.30
Terbium 1	3.64±0.02	0.203±0.011	6.61	138.45	20.9	2.41

specimens measured at 4.2°K (ρ_o - the residual resistivity) and the Lorenz number L calculated from a and ρ_o . The calculated Lorenz numbers are remarkably close to the theoretical value (2.45×10^{-8} watts-ohms-K^{-2}). Our measured conductivities of the rare earths are small compared to non-rare earth metals (in agreement with previous authors). Ytterbium had the lowest conductivity compared to the other rare earths in our observations (we have discussed in section 3F the possible reasons for this). Our results showed no anomalous humps or deviations but showed smooth temperature variation and extrapolated to the origin (unlike those reported by Rao[17], even though some of our specimens were the same as those used by him).

Having summaried the observed experimental results above, we now attempt to analyse these results.

In a normal metal two parallel mechanisms of thermal conduction have to be considered, that of the electrons (contributing an electronic thermal conduction Ke) and that of the phonons (contributing a phonon thermal conduction Kg). It is customary to assume that the processes are independent of each other i.e.

$$K = Ke + Kg \qquad (3.2)$$

It is generally accepted, that in almost pure metals all the heat is conducted by electrons and at low temperatures

$$\frac{1}{K_e} = W_e = W_i + W_o = \alpha T^2 + \beta/T \qquad (3.3)$$

where α and β are due to lattice and impurity scattering and β is given by $\rho_o T/L$.

In impure metals and relatively poor conductors, measurements of heat conductivity show the presence of an appreciable lattice conductivity[21]. In a metal the scattering of phonons by electrons dominates the other scattering mechanisms. The thermal conductivity can be written as

$$K = Ke + Kg = AT + BT^2 \qquad (3.4)$$

(if $W_o \gg W_i$ in equation (3.3)). The conductivity is divided into electronic (Ke) and phonons (Kg) contributions, limited by impurity (AT) and electron scattering (BT^2), respectively. A plot of K/T against T will therefore give a straight line provided the above mentioned assumptions are correct.

In order to investigate the origin of the contribution to the conductivity of our specimens, which is linear with temperature, we related this term with ρ_o of the corresponding specimens, using the Wiedemann-Franz law and obtained the corresponding Lorenz numbers in good agreement with the theory. We therefore conclude that the linear term represents an electronic contribution, with the electron mean free path

limited by 'impurity' scattering. To give us an idea of the order of magnitude of the electron mean free path, we invoke the kinetic theory result

$$K = \tfrac{1}{3} C_E v_F l \qquad (3.5)$$

where C_E is the electronic contribution to the specific heat and is obtained from experimental results[22]. C_E is approximately 10.5 T mJoules/mole, except for ytterbium[8], where it is low and approximately 2.9T mJoules/mole (we observed a correspondingly low thermal conductivity for ytterbium). We take v_F as the Fermi velocity and obtain a value for l of $\sim 10^{-7}$ cm.

To understand the quadratic contribution (bT^2) that is shown in our experiments, we turn towards other excitations, which are present in the heavy rare earths, that can transport heat at temperatures below 4.2°K. The transport of heat by phonons in solids is well known and well studied. Magnons are also present in most of the heavy rare earths at low temperatures. Specific heat studies of these metals at low temperatures show that magnons can contribute significantly to the total specific heat and correspondingly it would not be improbable that magnons should carry a significant amount of heat.

For qualitative purposes using the kinetic theory result and assuming a phonon contribution (Kg) mainly limited by electron scattering, as usually happens with metals at low temperatures, the mean free path of the phonons, l, will

be proportional to the number of electrons with which it can interact. The only electrons with which this is possible are those whose energy lies within $k_o T$ of the Fermi Energy E_F and the proportion of these electrons will be of the order $k_o T/E_F$. Hence the number of electrons available for scattering will be proportional to T and therefore l will vary as T^{-1}. Since v is constant and we are in the realm of the T^3 law for lattice specific heat, we obtain from equation (3.5) the right temperature dependence for this contribution (T^2). The actual value of this contribution depends on the magnitude of the phonon-electron interaction.

From table 3.3 we see that the quadratic terms (bT^2) for the specimens we measured are nearly all of the same magnitude. All the elements in our measurement have very similar crystalline structure, nearly the same lattice constants and the same number of valence electrons. Klemens (1954) [23] has worked out the order of magnitude for phonon conductivity limited by electron scattering. To overcome the uncertainty in the value of the interaction constant between the electrons and phonons, he used the low temperature electronic thermal resistivity W_i (see equation (3.3)) as the experimental quantity, which contains the interaction constant. His expression was

$$\frac{1}{K_{ge}} = W_{ge} = 3.2 \times 10^{-3} \alpha \Theta^4 n_o^{4/3} T^{-2} \qquad (3.6)$$

where α is defined by $W_i = \alpha T^2$, Θ, the Debye temperature and n_o the number of free electrons per atom. It would be interesting to compare our results for the quadratic term in temperature of the conductivity with those calculated by Klemens' formula for thermal conduction by phonons scattered by electrons. Klemens uses the experimental value W_i (equation 3.3)), but clearly W_i cannot be obtained on the same specimen, since the effects of Wge $\left(\frac{1}{K_{ge}}\right)$ would make it difficult to determine Wi and some assumption about Wi must be made. Klemens suggests in the measurement of alloys that Wi is the same as for the parent metal in the pure state (low W_o), where a direct measurement is possible, however he mentions that Wi is not independent of W_o. To estimate the order of magnitude, we have used $\alpha = 10^{-4}$ (this is the value given by Rosenberg (1955)[24] for some transition metals), $n_o = 3$ and the Debye temperature $\Theta = 180^{\circ}K$ and we see that our experimental results are of the same order of magnitude as the calculated value. This is fair agreement provided we are correct in our substitution in the formula and the assumption that the carriers are phonons, which are scattered by electrons.

The value calculated from Makinson's formula (1938)[25] (equation 1.44)), for phonon conductivity limited by electron scattering is in bad agreement with the experimental results (ours is two orders of magnitude greater). His formula

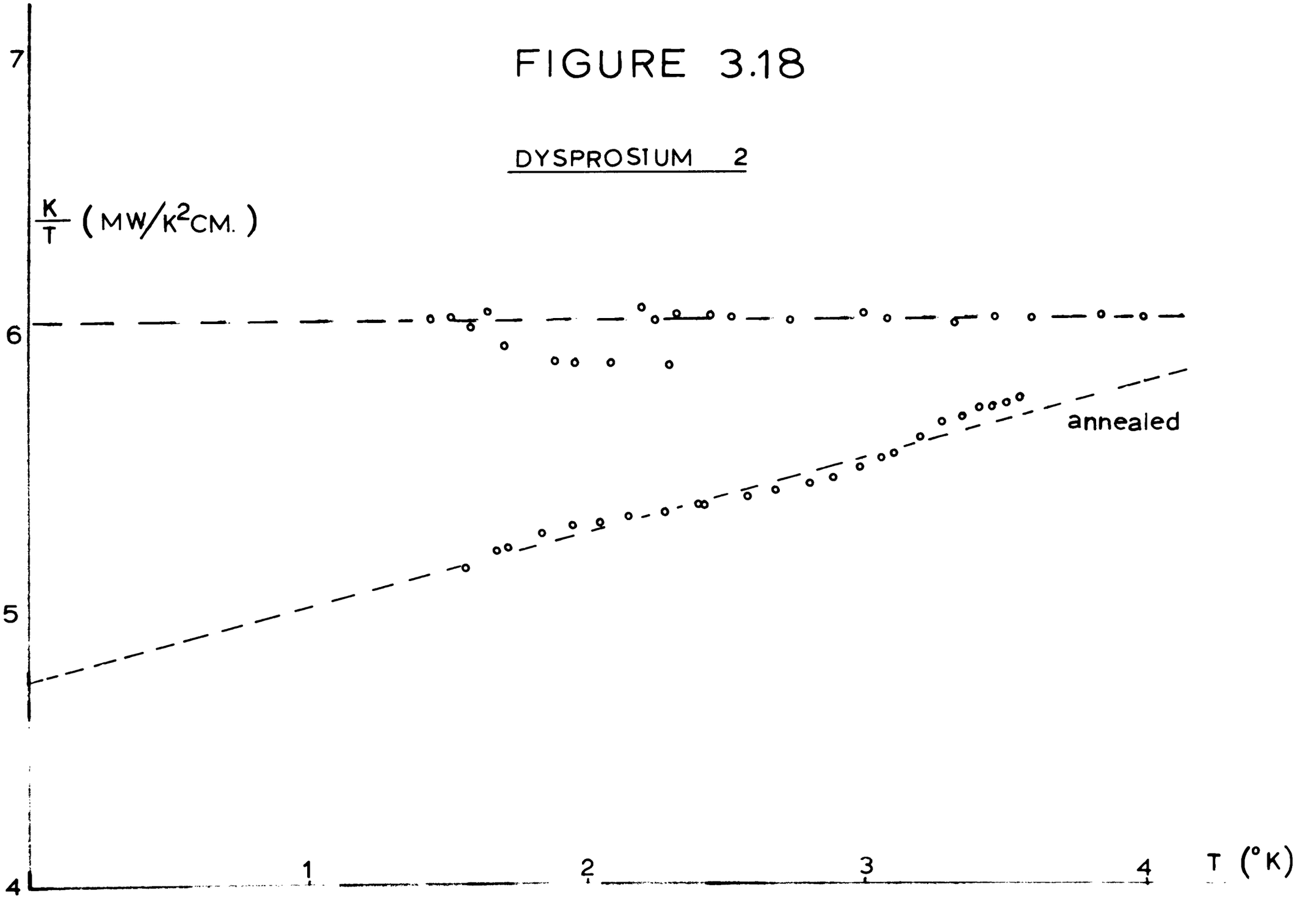
contains $K_{e\infty}$, the high temperature limiting electronic heat conductivity (this is calculated from ρ_{295}, the electrical resistivity at room temperatures, using the Wiedemann-Franz law) to substitute for the electron-phonon interaction constant. This may lead to error, since at high temperatures it includes Umklapp-processes, which are almost negligible at low temperatures. Also the Debye temperature of the longitudinal branch θ_L should be used instead of θ . The calculation of $K_{e\infty}$ from the electrical resistivity is made uncertain, as at room temperatures for the rare earths

$$\rho = aT + \rho_0 + \rho_s \qquad (3.7)$$

where ρ_s is a temperature independent spin disorder scattering[26] which can be quite large in comparison with ρ_0 and also high temperature thermal conductivity measurements of rare earths[4][5], show them to be rising with increasing temperatures (around room temperature) and are far from their limiting value.

The specimen dysprosium 2 did not have a quadratic term in temperature, in addition to the dominant linear term in thermal conductivity. All the other specimens we measured had this term and these specimens included some of the elements that have appreciable magnetic specific heat and others which do not have at very low temperatures, either they are non-magnetic or have no excitation of spin waves at these temperatures.

FIGURE 3.18



The only other contribution to the phonon resistivity that can become important in metals (particularly those which have been cold worked) is that produced by dislocations. This resistivity is directly proportional to the dislocation density and has the same temperature dependence as Wge (phonons scattered by electrons). Thus a T^{-2} phonon resistivity might be due to the combined effect of both dislocations and electrons. Experiments have been done on alloys[31][32], where the phonon resistivity contribution is appreciable and these show that for annealed and cold worked specimens the phonon contribution to the thermal conductivity, Kg, is proportional to T^2 at low temperatures, though for the former the absolute value of Kg is appreciably higher.

In view of this, we annealed sample dysprosium 2 and measured its thermal conductivity again. Figure 3.18 gives a plot of K/T vs.T for this specimen before and after annealing. We find that the annealed specimen showed a T^2 contribution to heat conductivity of quite similar magnitude as the other heavy rare earth samples. This is what we expect. As the number of dislocations are reduced, the phonon resistivity due to dislocations should be reduced and the total phonon resistivity (phonons scattered by electrons and dislocations) is diminished. Hence the heat conductivity due to phonon conduction (bT^2) should increase and show in a

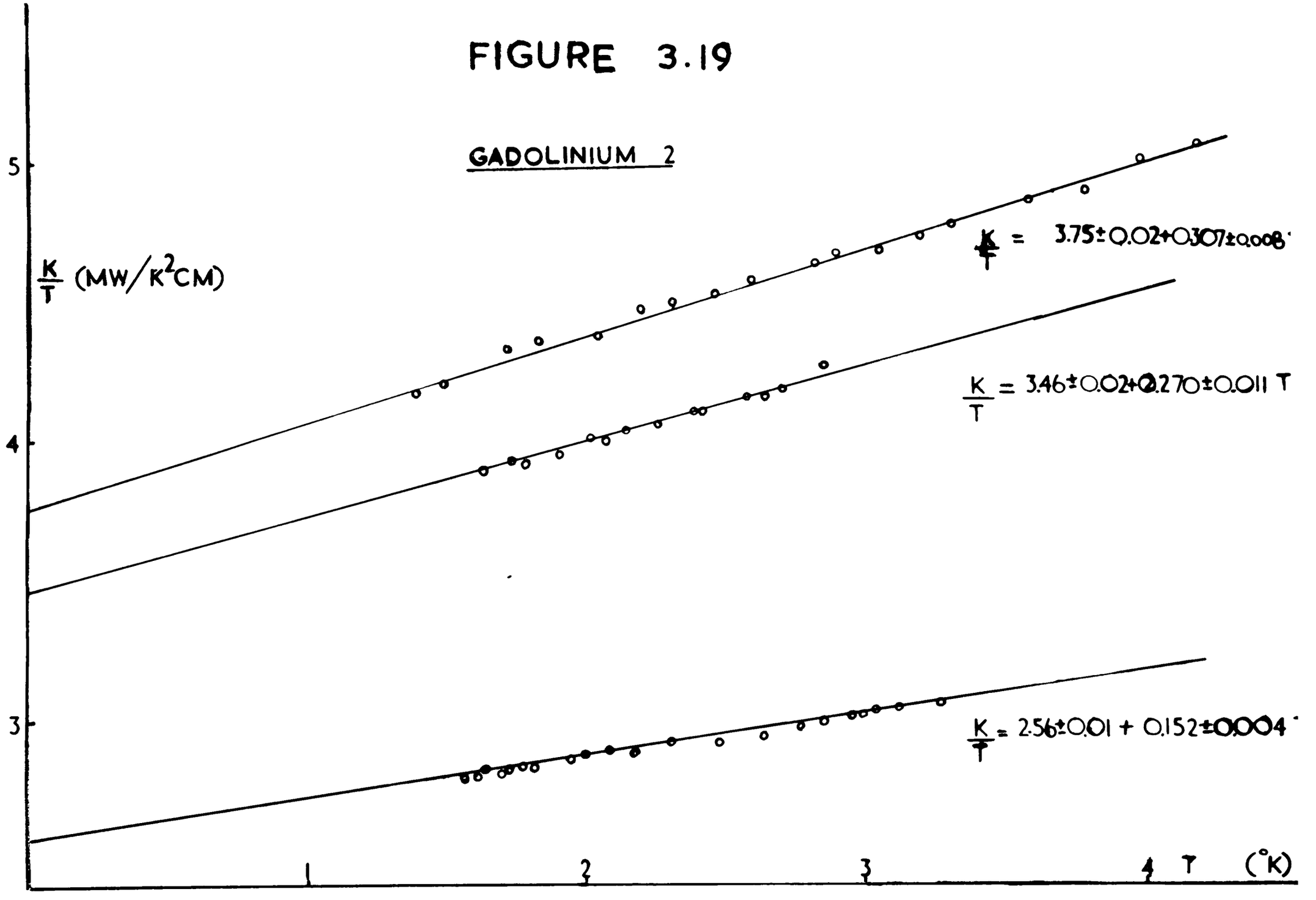
plot of K/T vs T.

The annealed specimen had a lower value for the linear term in temperature of the heat conductivity (aT) than prior to annealing (it had also a higher electrical residual resistivity). This is contrary to what we expect. As the dislocations are reduced, the total static defects (chemical impurities, physical imperfections etc.) in the sample are decreased and the linear term in the heat conduction (this term is due to electrons limited by 'impurity' (or defect scattering) should increase in magnitude. The only plausible explanation is that in the process of annealing (done at vacuum - 10^{-5} torr) chemical impurities may have been introduced and the effect of additional chemical impurities were greater than the reduction of dislocations on the electron conduction. Chemical impurities, which affect the electronic term had negligible effect on the phonon term of heat conductivity at low temperatures (due to the lengthening of the lattice waves).

The linear term (aT) of the heat conductivity of the annealed sample, when related to its residual resistivity using Wiedemann-Franz law, give a Lorenz number 2.56×10^{-8} watts- ohms-K^{-2}, which is again close to the theoretical value (see table 3.3 for details of the results).

One of the specimens, gadolinium 2, which had an appreciable T^2 contribution in comparison to the total conductivity, was cold worked and the conductivity measured

FIGURE 3.19


GADOLINIUM 2
5
4
3
$\frac{K}{T}$ (MW/K²CM)
$\frac{K}{T}$ = 3.75±0.02+0.307±0.008
$\frac{K}{T}$ = 3.46±0.02+0.270±0.011 T
$\frac{K}{T}$ = 2.56±0.01 + 0.152±0.004
1
2
3
4
T (°K)

again to see if the dislocations introduced had any effect on this term. The specimen, which was in the form of a rectangular slab, was strained and deformed in shape by using rollers. The form factor for thermal conductivity measurements were determined for the deformed sample in a similar manner used by others[32]. This was done by first determining the form factor F_A, in the usual manner, when the specimen was in a regular shape before straining and then the change in F due to deformation were calculated by electrical resistance measurements, determined at room temperatures r_T and helium temperatures r_o. Assuming Matthiessen's rule to hold

$$\frac{F\ (\text{strained})}{F_A} \qquad \frac{(r_T - r_o)\ \text{strained}}{(r_T - r_o)}$$

Figure 3.19 gives a plot of K/T vs T for the sample gadolinium 2 before and after being cold worked. First we find the linear term of the thermal conductivity (the intercept on the K/T axis) has decreased after cold working the sample (the residual electrical resistivity has increased as more dislocations are introduced). This linear term of the heat conductivity of the cold worked sample when related to its residual resistivity gave good Lorenz number (see table 3.3).

We find the small quadratic term in temperature of the heat conductivity has decreased after cold working the sample and decreased further with further cold

working on the sample. This change in the quadratic term is obtained from the change in the slope of the plot of K/T vs T and we find this change by almost half for the final cold worked sample and the original sample. This pattern of behaviour, the reduction of the T^2 term as dislocations are introduced, is similar to phonon conduction in a metal and this gives further evidence for the quadratic term obtained in our samples to be a phonon contribution,

Using equation (3.4) we can write the total thermal conductivity as

$$K = Ke + Kg$$

or in terms of thermal resistivity

$$\frac{1}{K} = W = We + W_g = AT^{-1} + BT^{-2}$$

When the samples are cold worked, i.e. the introduction of dislocations, the electronic thermal resistivity and phonon resistivity are increased and with further cold working the sample, the resistivities are increased further. We see from our results on the sample after cold working, the change in resistance of the electronic term of the final cold worked sample from the initial cold worked sample is about 4.6 times the change in resistance introduced when the sample was initially cold worked. The corresponding change in resistance of the phonon term is 6.4 times the initial change. We find, within our experimental accuracy,

the percentage change in thermal resistance of the electronic and phonon terms of the cold worked sample the same. We can understand this in terms of the change in resistance of both terms being proportional to the number of dislocations introduced.

When we calculate the resistance due to boundary scattering of phonons, W_B, using Casimir's formula (equation 1.21), we find the resistance is about 0.2% of the resistance due to phonons limited by electron scattering W_{ge} (the assumption here is that the quadratic form (bT^2) of the conductivity is due to phonons scattered by electrons and the boundary size is equal to the external dimension of the crystal).

We may have a clearer picture of the T^2 contribution in rare earths if we look at other possible sources of heat carriers and their effects. Sato (1955)[27] has shown that in ferromagnetic insulators at low temperatures, magnons (spin wave quanta) might be expected to make a substantial contribution to the thermal conductivity. The number of spin waves and phonons are few at low temperatures and in this case he shows the thermal conductivity of spin waves is proportional to T^2 and that of phonons to T^3 (mean free paths of both magnons and phonons limited by grain or specimen boundaries) and because of the different dependence upon T, it is possible for the magnon conductivity to exceed

the phonon conductivity in the region below 4°K. Experiments have been done that show heat transport by magnons limited by boundary in typical ferromagnetic crystals[28] and the result for this magnon conductivity can be expressed as

$$K = \frac{0.765\ ls\ k_o^3}{hC}\ T^2 \qquad (3.8)$$

where C is obtained from the magnon dispersion formula $\hbar\omega_q = Cq^2$ and ls is constant magnon free path and ko the Boltzmann constant.

The situation in a ferromagnetic metal is obviously more complicated and does not conform to the simple model mentioned. Here the thermal conductivity is essentially determined by the presence of free electrons. It has been reported[34] that Rezanor and Cherpanov have calculated the thermal conductivity of a ferromagnetic metal, treating the magnons present as Bose particles. The conductivity is found to be essentially electronic, the magnons serving primarily to scatter electrons, thus reducing the electronic conductivity in much the same way as do phonons. The isolation and identification of the magnon effect in this situation is difficult and has not been attempted.

As we have mentioned earlier, the elements of the rare earth ferromagnets we have measured display most of the various types of magnetic ordering in this series. After the

measurement of the gadolinium samples, which had a T^2 term in addition to the dominant linear term, we measured dysprosium and terbium. Dysprosium and terbium have energy gaps for their spin wave spectrum and it was shown that the magnetic specific heat can be given by[10]

$$C_M = e^{-\Delta E/k_0 T} D T^{3/2}$$

where D is a constant and for dysprosium and terbium an energy gap of $\Delta E/k_0 \approx 30^\circ K$ is given. Specific heat studies[11] show that no spin waves are excited at $4^\circ K$. Now our samples of dysprosium and terbium had a T^2 contribution. In holmium, the energy gap is very small[29] and both the holmium specimens had a T^2 contribution and so did both the erbium specimens. The ytterbium sample, which is non-magnetic had also this particular term (specific heat studies show no magnetic contribution[8]).

From our analysis it seems that the quadratic term (bT^2) in thermal conductivity is wholely or at least partly phonon conduction limited by electron scattering. We may have not reached the upper limit, for there may be a little additional scattering of the phonons due to dislocations, which has the same temperature dependence. (Gallo (1965)[5]) found, in his measurement of thermal conductivity of some heavy rare earths (5-300°K), that below 100°K the lattice thermal conductivity is the dominant cause of the deviation of $K\rho/T$ from the classical Lorenz number).

Without a complete theoretical knowledge of the part played by spin waves in heat conduction in metals, it is difficult to say whether they are significant at the temperatures of our measurement and what kind of temperature variation they would have. As all evidence points to a dominant phonon contribution in the quadratic term, we do not say that the contribution due to spin waves is totally absent below $4^{o}K$, but if present in specimens, which do have spin waves, they cannot be isolated within our experimental accuracy.

Conclusion

In conclusion we can say that the results obtained by us, for the heavy rare earth specimens in our possession, show no anomalous results in the temperature range 0.4 to 4.2°K. The thermal conductivity of all the specimens can be separated into a linear (T) and a quadratic (T^2) contribution. Furthermore, our results do not confirm the anomalously high Lorenz numbers previously referred to in the literature but when we relate the linear temperature dependence of the thermal conductivity to the residual electrical resistivity using the Wiedemann-Franz law we obtain, for all the specimens, Lorenz numbers which are remarkably close to the theoretical value. We therefore conclude that the linear term represents an electronic contribution, with the electron mean free path limited by 'impurity' scattering.

To account for the quadratic contribution we have invoked other carriers - phonons and magnons. We have observed this term in specimens, which have spin waves and also in those which have no spin waves below 4°K. From our analysis we say that the dominant part of this term is due to phonon conduction limited by electron scattering with possibly some resistance due to dislocation scattering. Dysprosium 2, which had no T^2 term in conductivity or at least too small to be observed possibly had the phonon

conductivity reduced very much, because of high dislocation density. It displayed the small quadratic contribution after being annealed. We also observed a reduction in this term in gadolinium 2 after it was cold-worked, showing that dislocations reduce this term.

With lack of a proper theory for the part played by spin waves in heat conduction in rare earths at low temperatures, we cannot isolate the magnon contribution in the specimens, which do have spin waves excited at low temperatures. But our experimental evidence seems to point that the part played by them is not very significant in our specimens.

For holmium there was no anomalous results down to $0.8^{\circ}K$, where the nuclear contribution to specific heat is already very large.

Reference to Chapter Three

1. Arajs, S., and Colvin, R.V. (1964) — J. App. Phys. 35, 1043.
2. Aliev, N.C., and Volkenshtein, N.V. (1966) — Soviet Phys. JETP, 22, 17.
3. Mendelssohm, K. and Rosenberg, H.M. (1961) — Solid State Phys., 12, 223. Acad. Press, New York.
4. Nellis, W.J., and Legvold, S. (1968) — Phys. Rev., 180, 581.
5. Gallo, C.F. (1965) — J. App. Phys. 36, 3410.
6. Karagyozyan, A.G., and Rao, K.V. (1967) — Phys. Letters, 25A, 235.
7. Colvin etal (1960) — Phys. Rev. 120, 741.
8. Lounasmaa, O.V. (1963) — Phys. Rev. 129, 2460.
9. Elliot, R.J. (1965) — Magnetism, Vol. 2A, 385. Academic Press, New York
10. Niira, K. (1960) — Phys. Rev. 117, 129.
11. Lounasmaa, U.V. and Guenther, R.A. (1962) — Phys. Rev. 126, 1357.
12. Boys et al (1968) — Phys. Rev. 174, No.2, 377.
13. Colvin, R.V. and Arajs, S. (1964) — Phys. Rev. 133, A1076
14. Lounasmaa, O.V. (1962) — Phys. Rev. 128, No.3, 1136.
15. Lounasmaa, O.V., and Sundstrom, L.J. (1966) — Phys. Rev. 150, 399.
16. Aliev, N.G., and Volkenshtein, N.V. (1966) — Soviet Phys. Solid State 7, 2068
17. Rao, K.V. (1967) — D. Phil. Thesis, Oxford University
18. Rao, K.V. (1969) — Phys. Rev. Letters, 22, 943.

19. Arajs, S. and Dunmyre, C.R. (1965) — Physica 31, 1466.

20. Aliev, N.G., and Volkenshtein,N.V.(1966) — Soviet Phys. JETP,22, 997.

21. White, G.K., and Woods, S.B.(1958) — Phil. Trans. 251,273.

22. Lounasmaa,O.V., and Sundstrom,L.J. (1966) — Phys. Rev. 150, 399.

23. Klemens, P.G. (1954) — Austral.J.Physics, 7, 54.

24. Rosenberg, H.M. (1955) — Phil. Trans.,247, 441.

25. Mackinson,R.E.C.(1938) — Proc.Camb.Phil.Soc.34,474.

26. Dekker, A.J. (1965) — J. App. Phys. 36, 906.

27. Sato, H. (1955) — Progr.Theor.Phys.Kyoto 13, 119.

28. Friedberg,S.A., and Harris, E.D. (1962) — Proc. Eighth Int.Conf. on Law Temp. Phys. (Lond.) 302.

29. Mackintosh,A.R.(1962) — Phys.Rev.Letters 9, 90.

30. Lounasmaa O.V. and Roach,P.R. (1962) — Phys. Rev. 128, 622.

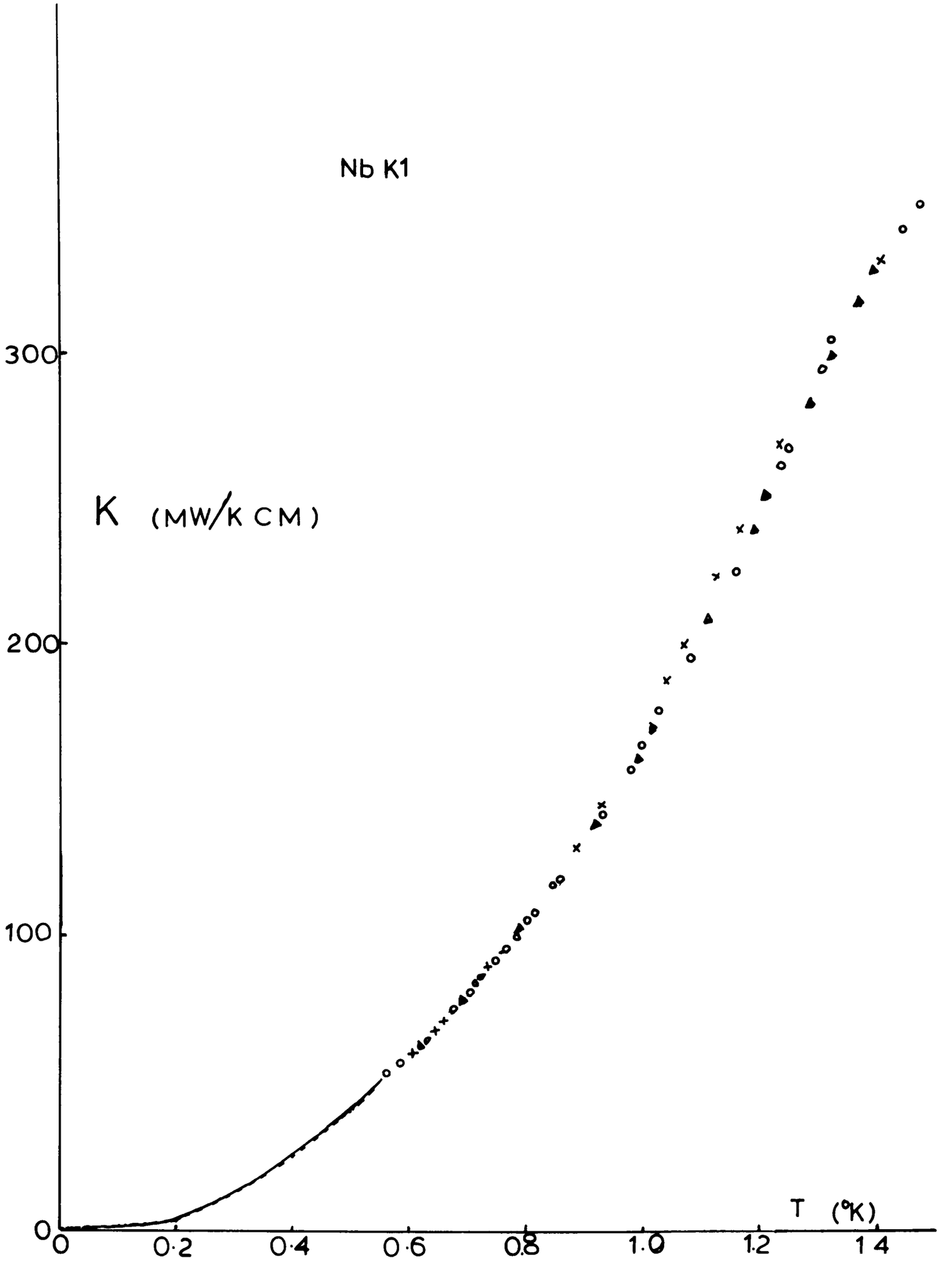
31. Kemp et al (1956) — Proc. Roy. Soc.,A233, 41.

32. Lomer, J.N., and Rosenberg, H.M. (1959) — Phil. Mag.,4, 467.

33. Arajs, S., and Colvin,R. (1964) — Phys. Rev. 136, A.439.

34. Douthett, D. and Friedberg, S.A.(1961) — Phys. Rev. 121, 1662.

FIGURE A 1

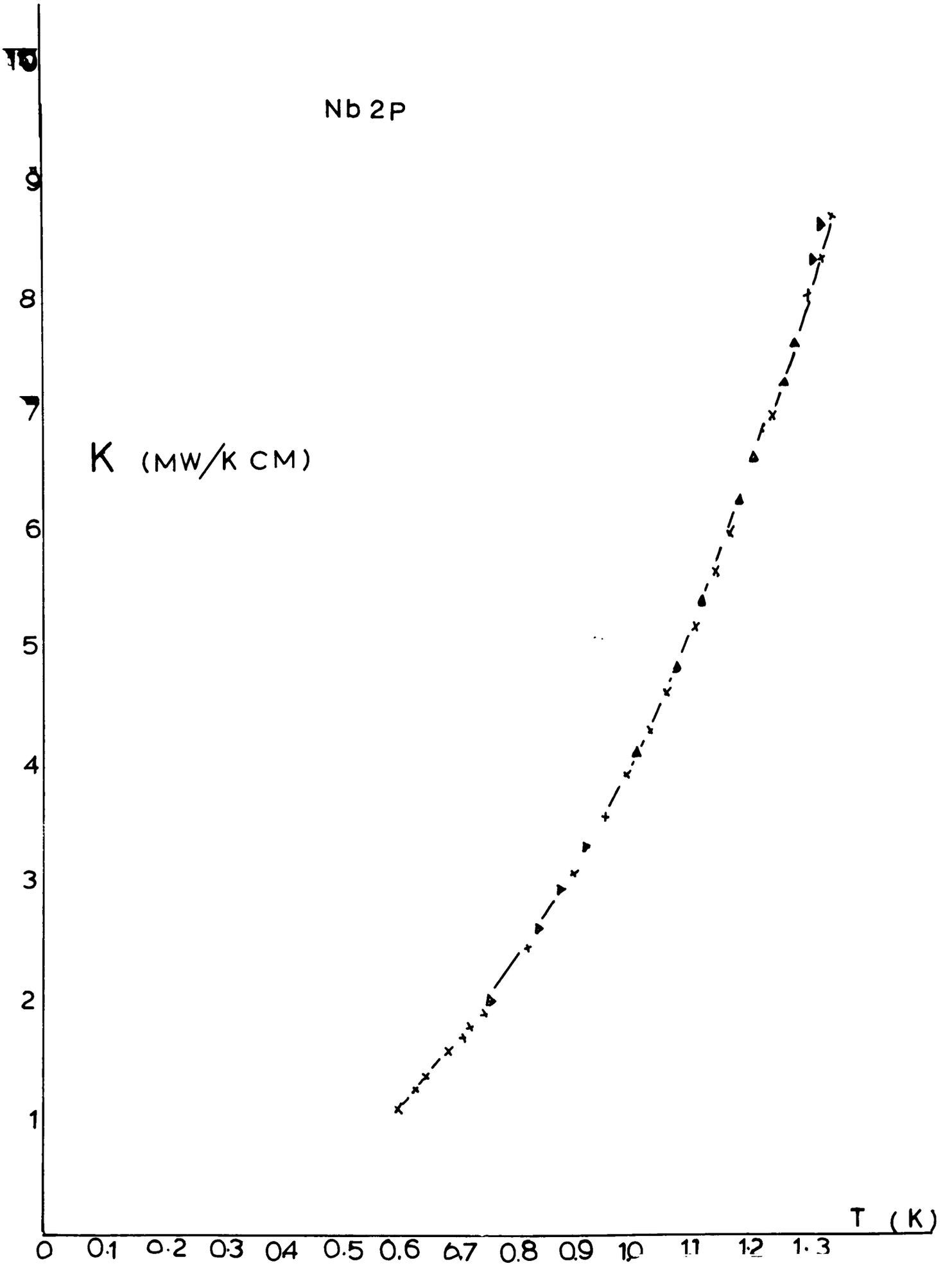


Appendix A.

Some preliminary measurements of thermal conductivity of niobium in the superconducting state were made in the He^3 cryostat constructed by the author. The results were in qualitative agreement with the earlier measurements.[1-2] We present below our results on niobium. As we have not pursued the study in detail no attempts are made to analyse the results quantitatively.

Figures A1 and A2 show a plot of K versus T for the two specimens in the superconducting state below 1.3°K. (Specimens: NbK1 - in the form of a rod, diameter 3.06mm., length 5 cm., Nb2p - in the form of a thin slab, cross-section 0.5 x 2.1 mm., length 2.3 cm.) The results are based on several runs and the reproducibility is good. The results extrapolated to the origin and did not show any unusual humps or deviations. Here we have two specimens whose absolute values of thermal conductivity are very different (NbK1 - 250 mW/°Kcm at 1.2°K to about 50 mW/°Kcm at 0.5°K; Nb2p - 6mW/°Kcm at 1.2°K to about 1 mW at 0.6°K), and hence during measurements very different heat energies have to be supplied to the specimens to get the appropriate temperature differences between the two thermometers (ΔT - we used similar values for both specimens). In the measurements we have used heat inputs ranging from 1×10^{-3} watts to 5×10^{-7} watts.

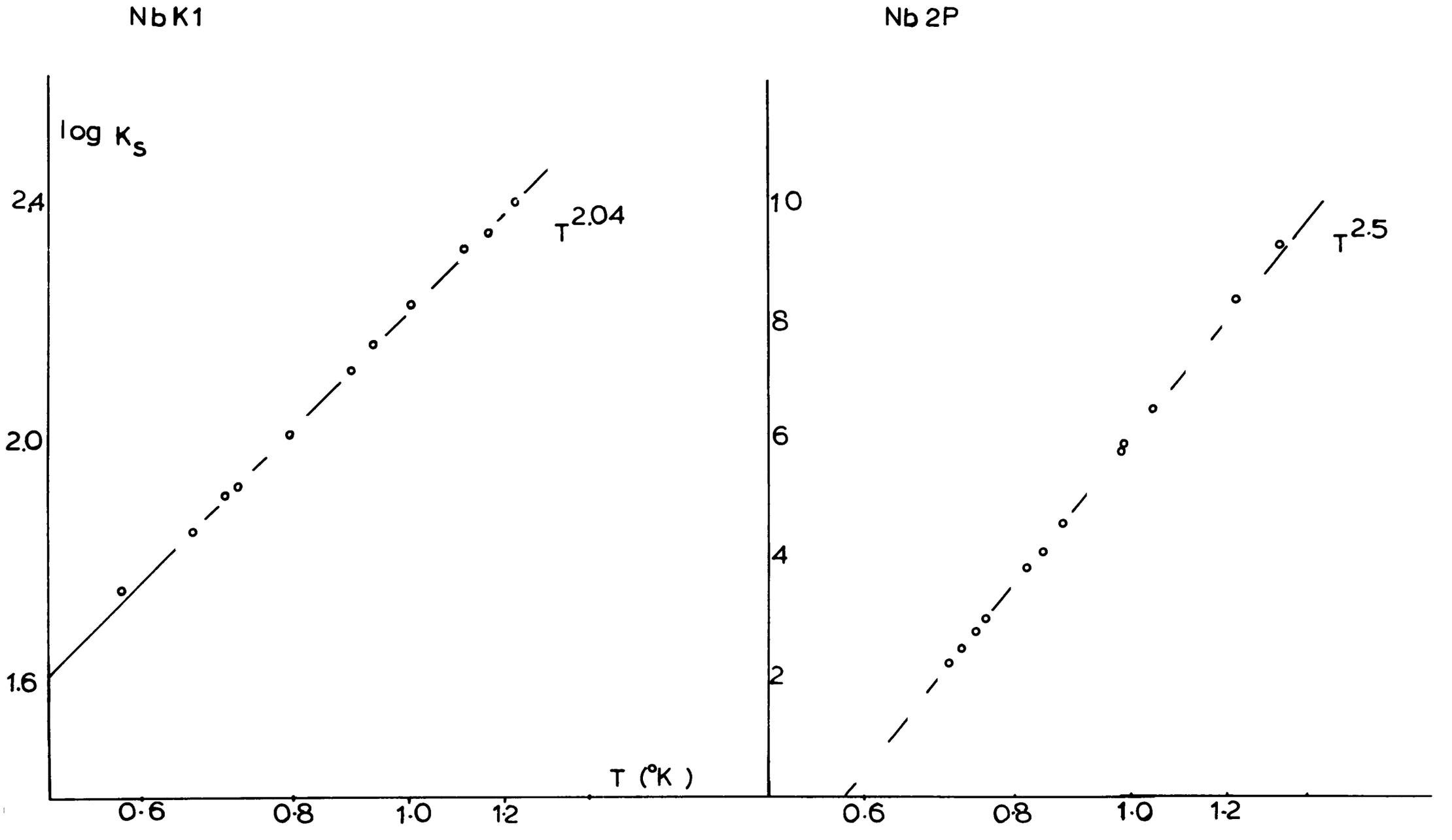
FIGURE A 2


Nb 2P
K (MW/K CM)
10
9
8
7
6
5
4
3
2
1
T (K)
0
0.1
0.2
0.3
0.4
0.5
0.6
0.7
0.8
0.9
1.0
1.1
1.2
1.3

For niobium (T_c = 9.1°K), at the temperatures of our measurement, the phonons are the main carriers of heat but in this range the phonon mean free path is limited by boundary scattering. This has been studied in niobium. Conolly and Mendelssohn[1] obtained a $T^{2.5}$ dependence for the conductivity in one sample and a T^3 dependence in another. Sousa[2] has obtained for his samples the conductivity proportional to T^n, where n varied between 2.6 and 2.8. This variation of the power of T depends on the sample surfaces and dimensions. Figure A3 shows a logarithamic plot of K vs. T of both our specimens. NbK1 shows a $T^{2.04}$ dependence while Nb2p had a $T^{2.5}$ dependence. Our results are in qualitative agreement with the theory and the temperature variation of the same order.

In figure A4, we present the thermal conductivity of NbK1 measured in the mixed state at three different temperatures. Plots of the measured conductivity (K) as a function of the magnetic field (H) are given. The field was perpendicular to the heat flow. The conductivity begins to decrease from its superconducting state and reaches a minimum at moderately low fields. With further increase in the field, K increases gradually towards its normal value, Kn, with the conductivity varying linearly with the field. This is the behaviour predicted by Caroli and Cyrot[3] for dirty superconductors. We observed however that our results suggest a linear

FIGURE A 3


Nb K1
log K_s
2.4
2.0
1.6
$T^{2.04}$
T (°K)
0·6
0·8
1·0
1·2
Nb 2P
10
8
6
4
2
$T^{2.5}$
0·6
0·8
1·0
1·2

dependence of K with H over a much wider range of fields (this has been generally observed experimentally[4]). Our results show that as the temperature is decreased the values of K/K_n are decreased and this is in qualitative agreement with the theory. Our results also show a smooth variation of K with H. We discuss below how the mixed state measurements were done.

Mixed State Measurements

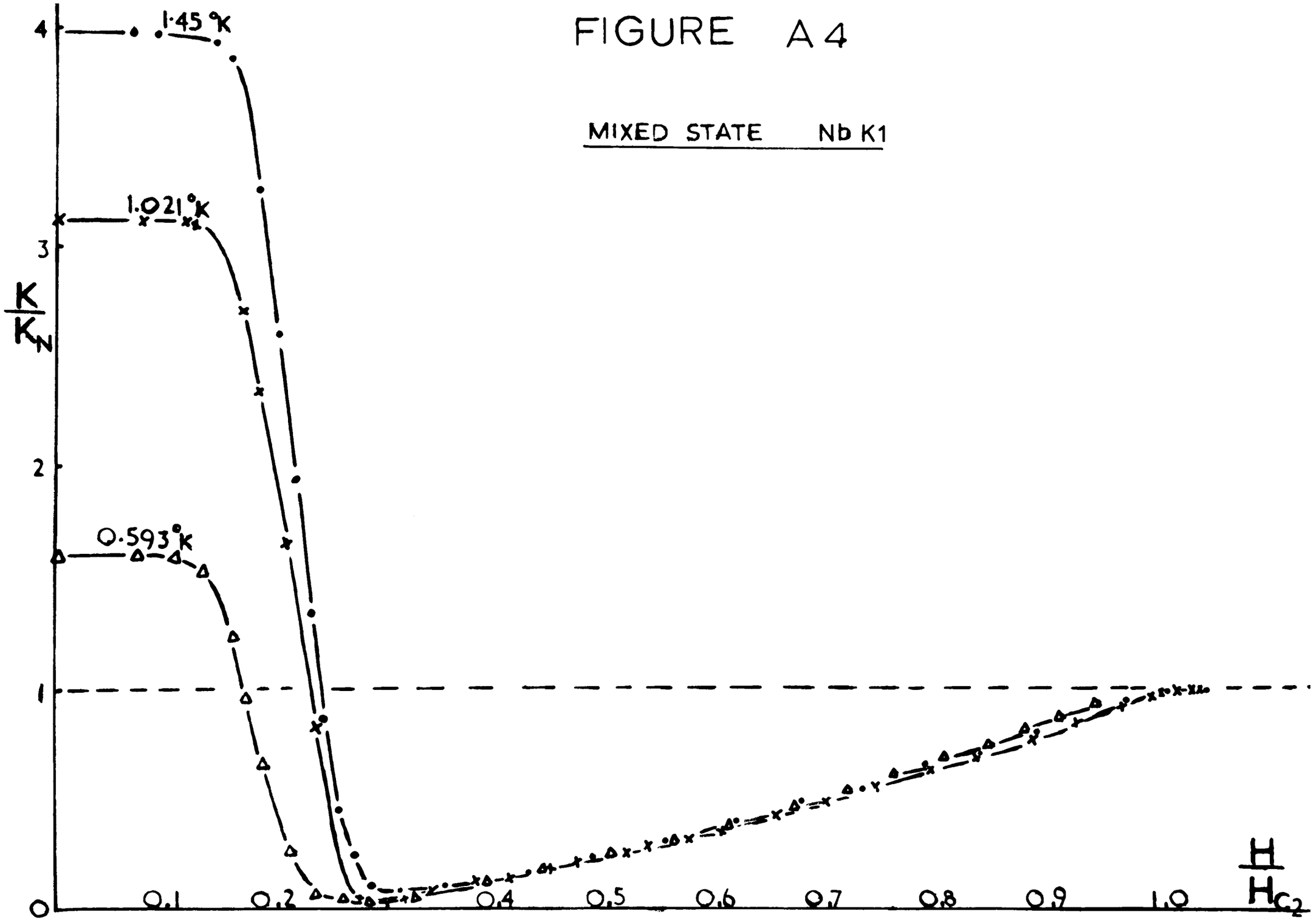
In the measurement of the field dependence of the thermal conductivity of niobium, which were performed at constant temperatures, errors due to calibration were avoided by keeping the same ΔT for each measurement. Measurements of the power $\dot{Q}$ required to keep ΔT constant enabled the relative values of the thermal conductivity to be accurately determined as a function of field H. Then

$$\frac{K(H)}{K_N} = \frac{\dot{Q}(H)}{\dot{Q}(H>H_{c_2})} \qquad K_N \equiv K(H>H_{c_2})$$

Helium^3 bath was first pumped so that a temperature below the temperature of interest was reached and during this procedure a set of calibration points (R_u, Δ, T) was taken. A few calibration points taken enabled the temperature to be determined to within a few millidegrees.

The specimen assembly was essentially the same as for the other conductivity measurements (i.e. in the superconducting state and normal measurements of rare earths) but there were two additional elements - heater H_u and a sensing carbon resistor R, which enabled the mean temperature of the sample

FIGURE A 4


MIXED STATE Nb K1
1.45 °K
1.021 °K
0.593 °K
K/K_N
H/H_C2
4
3
2
1
0
0.1
0.2
0.4
0.5
0.6
0.7
0.8
0.9
1.0

to be easily adjusted and accurately maintained (these additional elements were attached to the upper part of the specimen in the region between the upper thermometer and the sink).

In zero field and no power in the lower heater H, the mean temperature of the sample was roughly established by adjusting a D.C. current flowing through the upper heater H_u obtained from a dry cell driven circuit. A small current obtained from the off-balance of the regulating A.C. bridge (Figure 2.4 - described earlier, see section (2C-5)) was then superimposed on the constant current flowing through the heater H_u and with the carbon resistor R acting as the sensing element of the circuit and careful adjustment of the off-balance of this bridge enabled the required temperature to be established. This temperature could be determined from the value of R_u and using the corresponding calibration curve.

Power is now applied to the lower heater and the current adjusted so that a convenient difference of temperature (ΔT = 50 millidegrees) was established between the thermometers.

References to Appendix A.

1. Conolly, A., and Mendelssohn, K. (1962) — Proc. Roy. Soc., 266, 433.

2. Sousa, J.B. (1968) — D.Phil. Thesis, Oxford University.

3. Cyroli, C. and Cyrot, M. (1965) — Phys. Kondens.Mat. 4, 285.

4. Lowell, J., and Sousa, J.B. (1967) — Phys.Letters 25A, 469.

ACKNOWLEDGEMENTS

The author wishes to make grateful acknowledgement to the following:

Professor B. Bleaney, F.R.S., for granting me the use of the facilities of the Clarendon Laboratory.

Dr. K. Mendelssohm, F.R.S., for suggesting the problem, for very helpful criticism, advice and for his constant encouragement.

Dr. R. Berman for undertaking to supervise this thesis while Dr. K. Mendelssohn was away from Oxford. His interest, discussions and criticisms have been invaluable.

Dr. J.B. Sousa for helping to make measurements on some of the samples in the He^4 cryostat and also for many useful discussions.

Dr. D.M.S.Bagguley and Mr. J. Rolf for the loan of some of the samples.

Dr. S.T. Spence, Dr. A.R.Raychaudhuri, Professor K. Whitikar, Mr. D.J.Martin, Mr. A.A. Melo and Mr. C. Furtado with whom he had several useful discussions.

M/S 'Fred' Lanthall, R. Hewit and H. Lock for technical help with the apparatus.

Finally, to the Rhodes Trustees for the award of a scholarship for 1966-1969.